

Climatic Stress Events and Radial Growth Forecasting of *Acer saccharum*

Across New Brunswick and Central Nova Scotia, Canada

by

Benjamin E. Phillips



A thesis submitted to the Department of Geography and Environment,

in partial fulfillment of the requirements for the degree of

Master of Science in Environmental Science

July 2009

Table of Contents

Table of Contents	iii
List of Tables	vi
List of Figures	x
Abstract	xv
Preface.....	xvii
Acknowledgements	xviii
Dedication	xix
1. Establishing the Framework	1
1.1. Introduction.....	1
1.2. Hypothesis	3
2. Hypothesis Background.....	5
2.1. Sugar Maple Characteristics	5
2.1.1. <i>Range and Climate</i>	5
2.1.2. <i>Abundance</i>	5
2.1.3. <i>Habitat and Physiology</i>	8
2.1.4. <i>Foliar Phenology</i>	8
2.2. Dieback Phenomenon	9
2.2.1. <i>Dieback Definition</i>	9
2.2.2. <i>Dieback Research</i>	10
2.2.3. <i>Experimental Research</i>	11
2.2.4. <i>Potential Connections to Ocean Conditions</i>	12
3. Study Area	13
3.1. Study Sites	13
3.2. Climate.....	14
3.3. Biota.....	16
3.4. Ecological Site Classifications	17
4. Data Composition and Analysis Procedures	26

4.1. Instrumental Climate Data	26
4.2. Global Climate Model Data	27
4.3. Climate Change Scenarios	28
4.4. Global Climate Model Calibration	29
4.5. Climate Variables	30
4.6. Climate Model Summary.....	33
4.7. Global Coupled Ocean-atmosphere Interactions	34
4.8. Tree-ring Data.....	35
4.9. Tree-ring Analysis	36
4.10. Radial Growth-climate Analysis	37
5. Results and Model Outputs	41
5.1. Tree-ring Chronologies.....	41
5.2. Relationships to Ocean-atmosphere Interactions	44
5.3. Thaw/Refreeze Variables.....	46
5.4. Canadian Global Climate Model Third Generation Summary	46
5.5. Radial Growth Future Forecasts	48
5.6. Common Variable Aggregation and Verification.....	75
6. Discussion and Synthesis	78
6.1. Radial Growth Forecasts and Regional Climate Change	78
6.1.1. <i>Dendrochronological Insights</i>	76
6.1.2. <i>Stability of Radial Growth</i>	79
6.1.3. <i>Explained Variance</i>	79
6.1.4. <i>Verifying Climate Across Models</i>	81
6.1.5. <i>Common Model Variables</i>	82
6.1.5.1. Winter and the Transition to Spring	82
6.1.5.2. Spring.....	83
6.1.5.3. Summer and Fall	84
6.1.5.4. Regional and Subregional Summary	84
6.1.6. <i>Possible Future Climate in Relation to Model Forecasts</i>	85
6.1.7. <i>Daily Compiled Temperature Variables</i>	86

6.2. Model Limitations	89
6.2.1. <i>Uncertainty of Global Climate Models</i>	89
6.2.2. <i>Prospective Biological Thresholds</i>	90
6.2.3. <i>Nonclimatic Disturbance</i>	91
6.3. Hypotheses Insights	92
6.4. Atlantic Multidecadal Oscillation Influence	94
6.5. North Atlantic Oscillation Influence	96
6.6. Synthesis: Sugar Maple Climate Stress Potential	97
7. Closing Observations	103
7.1. Further Research.....	103
7.2. Conclusion	104
References	106

List of Tables

Table 3.1. Tree-ring sample sites including the site elevation, position, distance from the nearest climate station, and the elevational difference between the site and climate station for each of the ten sample sites.

Table 4.1. Environment Canada climate station information for the main station used for each sample site. Climate station identification including, the station ID number, the common interval of data covered by all data types, the approximate geographic position (latitude and longitude in degrees and minutes), and the elevation above sea level is provided for each climate site.

Table 4.2. Climate variables created for this study cover various months of the year and also include two previous years. Climate variable type, period length and annual occurrence are outlined. Months of the three-year time period covered are represented by only a first letter. Time periods included by each variable are marked in grey, the shortest of which only cover monthly intervals while other variables cover seasonal periods (black vertical lines separate monthly periods while seasonal periods are solid grey with no breaks between months). Variable names are Tmean = average monthly temperature, EvpStr = evapotranspirational stress, GDD = growing degree days, TRF Deep = thaw/refreeze deep, TRF S = thaw/refreeze surficial, RtFr = root freeze, Tprecip = total monthly precipitation, SD = snow depth, with expanded definitions below. Variable sets are separated by a bold horizontal black line and are described below.

Table 5.1. Statistics in this Table are calculated between individual tree ring indices produced for each sample site covering the common interval 1850-2006. Each site is represented by a minimum of 36 individual tree cores taken from a minimum of 17 trees. Intra-site correlations using Pearson's r-values illustrate the strength of relationships between sampled sugar maple trees at each site. Also presented are average mean sensitivity (AMS) values calculated using all trees at each site. Values for AMS are considered low from 0.1-0.19, intermediate from 0.2-0.29 and high from ≥ 0.3 (Grissino-Mayer 2001). * = ($p < 0.0001$).

Table 5.2. The comparative relationships between all sugar maple chronologies are illustrated in this inter-site correlation matrix with Pearson's r-values for the common period 1850-2006. Pearson's r-values are calculated between standardized tree-ring curves for each site. Cells in this Table are shaded depending on the strength of the r-value indicated; darker shading represents higher r-values while lighter shading indicates lower r-values.
* = ($p < 0.05$), ** = ($p < 0.01$).

Table 5.3. Pearson's r-values averaged for all ten sugar maple chronologies over 50-year periods lagged by 25-years are presented. This Table was derived from individual inter-site correlation

matrices calculated for each 50-year period. All five correlation values were composed of an average r-value computed between all sites in each individual matrix.

* = (p<0.05), ** = (p<0.01).

Table 5.4. Forecasted climatic changes expected by the end of the 21st century for the SRES A1b scenario produced by the CGCM3. T DJFM = winter temperature, RtFr = root freeze, GDD = growing degree days, EvpStr = evapotranspiration stress, T Apr = April temperature, P MAJ = spring precipitation and PJAS = summer precipitation.

Table 5.5. The regression model summary information for the AICc optimum variable subset. Model information including the variable type, period and length of model calibration, the number of included variables in each model and the amount of explained variance is presented. Explained variance is represented by an adjusted R² value for each model which is assessed for significance by an ANOVA. * = (p≤0.001)

Table 5.6. The regression model variables included in the AICc optimum variable subset for each site. The prefix denotes whether a variable is positive (+) or negative (-), as well as temperature (T) or precipitation (P). The root denotes the month or combination of months contributing to the variable, or a non-monthly associated variable such as snow depth, Thaw/Refreeze Deep (TRF), or Atlantic Multidecadal Oscillation (AMO). The suffix denotes the year of occurrence of the specific variable where “a” = current year, “b” = 1st lagged year, and “c” = 2nd lagged year.

Table 5.7. The regression model variables from the best subset model representing the Charlo climate data regressed against the Benjamin River sugar maple chronology are illustrated. The monthly variables used in this regression model are represented in the Table by: white = positive variable association, black = negative variable association, gray = variable not included in this model.

Table 5.8. The regression model variables from the best subset model representing the Edmunston climate data regressed against the Quisibis Mountain sugar maple chronology are illustrated. The monthly variables used in this regression model are represented in the Table by: white = positive variable association, black = negative variable association, gray = variable not included in this model.

Table 5.9. The regression model variables from the best subset model representing the Aroostook climate data regressed against the Kintore Ridge sugar maple chronology are illustrated. The monthly variables used in this regression model are represented in the Table by: white = positive variable association, black = negative variable association, gray = variable not included in this model.

Table 5.10. The regression model variables from the best subset model representing the Miramichi climate data regressed against the Horseshoe Ridge sugar maple chronology are illustrated. The monthly variables used in this regression model are represented in the Table by: white = positive variable association, black = negative variable association, gray = variable not included in this model.

Table 5.11. The regression model variables from the best subset model representing the Fredericton climate data regressed against the Odell Park sugar maple chronology are illustrated. The monthly variables used in this regression model are represented in the Table by: white = positive variable association, black = negative variable association, gray = variable not included in this model.

Table 5.12. The regression model variables from the best subset model representing the Gagetown climate data regressed against the Slipp Farm sugar maple chronology are illustrated. The monthly variables used in this regression model are represented in the Table by: white = positive variable association, black = negative variable association, gray = variable not included in this model.

Table 5.13. The regression model variables from the best subset model representing the Moncton climate data regressed against the Indian Mountain sugar maple chronology are illustrated. The monthly variables used in this regression model are represented in the Table by: white = positive variable association, black = negative variable association, gray = variable not included in this model.

Table 5.14. The regression model variables from the best subset model representing the Alma climate data regressed against the Fundy Park sugar maple chronology are illustrated. The monthly variables used in this regression model are represented in the Table by: white = positive variable association, black = negative variable association, gray = variable not included in this model.

Table 5.15. The regression model variables from the best subset model representing the Nappan climate data regressed against the Fenwick Ridge sugar maple chronology are illustrated. The monthly variables used in this regression model are represented in the Table by: white = positive variable association, black = negative variable association, gray = variable not included in this model.

Table 5.16. The regression model variables from the best subset model representing the Collegeville climate data regressed against the Keppoch Plateau sugar maple chronology are illustrated. The monthly variables used in this regression model are represented in the Table by:

white = positive variable association, black = negative variable association, gray = variable not included in this model.

Table 5.17. The regression model variables from the best subset model representing the Fredericton climate data regressed against the Odell Park sugar maple chronology are illustrated. The monthly variables used in this regression model are represented in the Table by: white = positive variable association, black = negative variable association, gray = variable not included in this model. The April temperature variable has been replaced in current year, 1st lagged year, and 2nd lagged year, with the TRF Deep variable symbolized as: * =TRF Deep.

Table 5.18. The regression model variables from the best subset model representing the Fredericton climate data regressed against the Odell Park sugar maple chronology are illustrated. The monthly variables used in this regression model are represented in the Table by: white = positive variable association, black = negative variable association, gray = variable not included in this model. This regression model is a supplementary model testing the TRF Deep variable and AMO index. The April temperature variable has been replaced in 1st lagged year, and 2nd lagged year with the TRF Deep variable symbolized as: * =TRF Deep. The AMO index (lagged three years) has also been added as another independent variable symbolized as: ω = AMO

Table 5.19. Aggregated variables from radial growth forecast models for verification of the most influential climate terms. Variables from the AICc selected model for each sample site are included in the Table. All variables including those from lagged years are displayed under the month of occurrence with indifference as to the number of years before radial growth. Temperature variables are arranged in the top half of the Table and precipitation variables are arranged in the bottom half of the Table. Black cells are negative associations to numerically high values of the variable and white cells are positive associations to numerically high values of the variable. Numbers in each cell represent the number of occurrences of a variable in a particular model (three is the maximum per model as no month can occur in more than the current year, 1st lagged year, and 2nd lagged year). DJFM/Snow Depth is the winter snow depth index, $\bar{\quad}$ = T ONDC, - = T JASc, $\underline{\quad}$ = P AMJc where the seasonal variable actually represents three months but the value is assigned to the first month in the season.

List of Figures

Figure 2.1. Sugar maple range map in eastern North America outlining the geographic range where the trees have been observed growing and reproducing.

Figure 3.1. Study site map with the geographical positions of the ten sugar maple sample sites and ten climate stations from New Brunswick and Nova Scotia used in this study. Base map © 2001. Her Majesty the Queen in Right of Canada, Natural Resources Canada.

Figure 4.1. The CGCM3 produces a set of forecast data that is homogenous across a $2.81^\circ \times 2.81^\circ$ grid square, and does so for a global grid. The CGCM3 output grid squares used in the study are illustrated over the Maritime provinces. Latitudinal and longitudinal boundaries for each grid square are also given. Base map © 2002. Her Majesty the Queen in Right of Canada, Natural Resources Canada.

Figure 5.1. All ten sugar maple chronologies representing the ten sample sites are depicted over the truncated common interval from 1850-2006. All chronologies are standardized using the program ARSTAN and indexed curves are presented. Each curve fluctuates around an average of one represented by the horizontal strike-through lines. Sample depth at each site has a minimum of thirty cores extending back in time 100 years and at least 10 cores extending back 150 years. Site names are presented adjacent to each radial growth curve.

Figure 5.2. The standardized index of the regional master sugar maple tree-ring chronology plotted against the AMO at a three year lag. The curves of both the annual variability and smoothed decadal variability (10 year moving average) data are plotted for visual comparison.

Figure 5.3. The standardized index of the regional master sugar maple tree-ring chronology plotted against the NAO at a three year lag. The curves of both the annual variability and smoothed decadal variability (10 year moving average) are plotted for visual comparison.

Figure 5.4. The Thaw/Refreeze Deep (TRF Deep) variable calculated using historical and forecast climate data for Fredericton is outlined. Noticeable is a large increase of occurrence in the data at the transition from historical to forecasted results around the year 2000.

Figure 5.5. The regression model defined in this Figure used climate data from Charlo and the sugar maple chronology from Benjamin River (BR). The black line illustrates the historic sugar maple radial growth curve for BR (Chronology MAD Lab code = 08ANLE00). The unbroken white line details the model calibration period. The broken white line estimates the future growth response of sugar maple using the SRES B1 scenario.

Figure 5.6. The regression model defined in this Figure used climate data from Charlo and the sugar maple chronology from Benjamin River (BR). The black line illustrates the historic sugar

maple radial growth curve for BR (Chronology MAD Lab code = 08ANLE00). The unbroken white line details the model calibration period. The broken white line estimates the future growth response of sugar maple using the SRES A1b scenario.

Figure 5.7. The regression model defined in this Figure used climate data from Edmunston and the sugar maple chronology from Quisibis Mountain. The black line illustrates the historic sugar maple radial growth curve for QM (Chronology MAD Lab code = 08AOLE00). The unbroken white line details the model calibration period. The broken white line estimates the future growth response of sugar maple using the SRES B1 scenario.

Figure 5.8. The regression model defined in this Figure used climate data from Edmunston and the sugar maple chronology from Quisibis Mountain. The black line illustrates the historic sugar maple radial growth curve for QM (Chronology MAD Lab code = 08AOLE00). The unbroken white line details the model calibration period. The broken white line estimates the future growth response of sugar maple using the SRES A1b scenario.

Figure 5.9. The regression model defined in this Figure used climate data from Aroostook and the sugar maple chronology from Kintore Ridge. The black line illustrates the historic sugar maple radial growth curve for KR (Chronology MAD Lab code = 08BFLE00). The unbroken white line details the model calibration period. The broken white line estimates the future growth response of sugar maple using the SRES B1 scenario.

Figure 5.10. The regression model defined in this Figure used climate data from Aroostook and the sugar maple chronology from Kintore Ridge. The black line illustrates the historic sugar maple radial growth curve for KR (Chronology MAD Lab code = 08BFLE00). The unbroken white line details the model calibration period. The broken white line estimates the future growth response of sugar maple using the SRES A1b scenario.

Figure 5.11. The regression model defined in this Figure used climate data from Miramichi and the sugar maple chronology from Horseshoe Ridge. The black line illustrates the historic sugar maple radial growth curve for HR (Chronology MAD Lab code = 08AMLE00). The unbroken white line details the model calibration period. The broken white line estimates the future growth response of sugar maple using the SRES B1 scenario.

Figure 5.12. The regression model defined in this Figure used climate data from Miramichi and the sugar maple chronology from Horseshoe Ridge. The black line illustrates the historic sugar maple radial growth curve for HR (Chronology MAD Lab code = 08AMLE00). The unbroken white line details the model calibration period. The broken white line estimates the future growth response of sugar maple using the SRES A1b scenario.

Figure 5.13. The regression model defined in this Figure used climate data from Fredericton and the sugar maple chronology from Odell Park. The black line illustrates the historic sugar maple radial growth curve for OP (Chronology MAD Lab code = 08XLE00). The unbroken white line details the model calibration period. The broken white line estimates the future growth response of sugar maple using the SRES B1 scenario.

Figure 5.14. The regression model defined in this Figure used climate data from Fredericton and the sugar maple chronology from Odell Park. The black line illustrates the historic sugar maple radial growth curve for OP (Chronology MAD Lab code = 08XLE00). The unbroken white line details the model calibration period. The broken white line estimates the future growth response of sugar maple using the SRES A1b scenario.

Figure 5.15. The regression model defined in this Figure used climate data from Gagetown and the sugar maple chronology from Slipp Farm. The black line illustrates the historic sugar maple radial growth curve for SF (Chronology MAD Lab code = 07CKLE00). The unbroken white line details the model calibration period. The broken white line estimates the future growth response of sugar maple using the SRES B1 scenario.

Figure 5.16. The regression model defined in this Figure used climate data from Gagetown and the sugar maple chronology from Slipp Farm. The black line illustrates the historic sugar maple radial growth curve for SF (Chronology MAD Lab code = 07CKLE00). The unbroken white line details the model calibration period. The broken white line estimates the future growth response of sugar maple using the SRES A1b scenario.

Figure 5.17. The regression model defined in this Figure used climate data from Moncton and the sugar maple chronology from Indian Mountain. The black line illustrates the historic sugar maple radial growth curve for IM (Chronology MAD Lab code = 07CTLE00). The unbroken white line details the model calibration period. The broken white line estimates the future growth response of sugar maple using the SRES B1 scenario.

Figure 5.18. The regression model defined in this Figure used climate data from Moncton and the sugar maple chronology from Indian Mountain. The black line illustrates the historic sugar maple radial growth curve for IM (Chronology MAD Lab code = 07CTLE00). The unbroken white line details the model calibration period. The broken white line estimates the future growth response of sugar maple using the SRES A1b scenario.

Figure 5.19. The regression model defined in this Figure used climate data from Alma and the sugar maple chronology from Fundy Park. The black line illustrates the historic sugar maple radial growth curve for FP (Chronology MAD Lab code = 07RLE00). The unbroken white line

details the model calibration period. The broken white line estimates the future growth response of sugar maple using the SRES B1 scenario.

Figure 5.20. The regression model defined in this Figure used climate data from Alma and the sugar maple chronology from Fundy Park. The black line illustrates the historic sugar maple radial growth curve for FP (Chronology MAD Lab code = 07RLE00). The unbroken white line details the model calibration period. The broken white line estimates the future growth response of sugar maple using the SRES A1b scenario.

Figure 5.21. The regression model defined in this Figure used climate data from Nappan and the sugar maple chronology from Fenwick Ridge. The black line illustrates the historic sugar maple radial growth curve for FR (Chronology MAD Lab code = 08ULE00). The unbroken white line details the model calibration period. The broken white line estimates the future growth response of sugar maple using the SRES B1 scenario.

Figure 5.22. The regression model defined in this Figure used climate data from Nappan and the sugar maple chronology from Fenwick Ridge. The black line illustrates the historic sugar maple radial growth curve for FR (Chronology MAD Lab code = 08ULE00). The unbroken white line details the model calibration period. The broken white line estimates the future growth response of sugar maple using the SRES A1b scenario.

Figure 5.23. The regression model defined in this Figure used climate data from Collegeville and the sugar maple chronology from Keppoch Plateau. The black line illustrates the historic sugar maple radial growth curve for KP (Chronology MAD Lab code = 08BILE00). The unbroken white line details the model calibration period. The broken white line estimates the future growth response of sugar maple using the SRES B1 scenario.

Figure 5.24. The regression model defined in this Figure used climate data from Collegeville and the sugar maple chronology from Keppoch Plateau. The black line illustrates the historic sugar maple radial growth curve for KP (Chronology MAD Lab code = 08BILE00). The unbroken white line details the model calibration period. The broken white line estimates the future growth response of sugar maple using the SRES A1b scenario.

Figure 5.25. The regression model defined in this Figure used climate data from Fredericton station and the sugar maple chronology from Odell Park. The black line illustrates the historic sugar maple radial growth curve for OP (Chronology MAD Lab code = 08XLE00). The unbroken white line details the model calibration period. The light grey bars indicated thaw/refreeze events defined by the TRF Deep variable. The thaw/refreeze component is only meant to position the events in time and does not detail severity of the event.

Figure 5.26. The regression model defined in this Figure used climate data from Fredericton and the sugar maple chronology from Odell Park. This regression model is a supplementary model testing the TRF Deep variable and AMO index (lagged three years). The black line illustrates the historic sugar maple radial growth curve for OP (Chronology MAD Lab code = 08XLE00). The unbroken white line details the model calibration period. The light grey bars indicated thaw/refreeze events defined by the TRF Deep variable. The thaw/refreeze component is only meant to position the events in time and does not detail the severity of the events.

Figure 6.1. A climatic induced stress map for sugar maple from 2010 – 2024 over the provinces of New Brunswick and Nova Scotia.

Figure 6.2. A climatic induced stress map for sugar maple from 2025 – 2050 over the provinces of New Brunswick and Nova Scotia.

Abstract

Sugar maple (*Acer saccharum* Marsh) trees near their northern range limit have been affected by stress episodes in the past impacting radial growth. This study examines the past occurrence and causes of short- and long-term radial growth suppression periods. Radial growth models using only climate variables are produced for sugar maple and future forecasts (2000 - 2100) are developed for New Brunswick and central Nova Scotia, Canada.

Improvements over past radial growth forecasting methodologies are sought to create more reliable future model projections. Tree-ring samples were collected from ten sugar maple stands in close proximity to long-term climate stations covering an area of climatic variability. A non-standard method was undertaken with the composition of climatic variables for application to the forecasting models by using daily climate records in an attempt to more effectively explain past short-term climatic events. Models were constructed using a stepwise regression analysis, employing both daily and monthly compiled variables for all ten sites. The model outputs were then cross-referenced to verify the important climate variables to sugar maple radial growth, and the landscape patterns of climatic responses were noted. Late winter thaw/refreeze events were examined for synchrony with sugar maple radial growth reduction periods, and Coupled Global Ocean-Atmosphere Interactions were evaluated for influence on sugar maple climatic responses.

Radial growth forecast model outputs illustrate a generally decreasing radial growth rate across all sites, and extreme radial growth reductions for the more southern sites. Coupled Global Ocean-Atmosphere Interaction correlation results indicate a strong positive relationship between sugar maple radial growth and long-term positive phases of the Atlantic Multidecadal

Oscillation index. Additionally, a strong negative relationship was discovered with positive multidecadal phases of the North Atlantic Oscillation winter index.

When all stressor information is synthesized, it appears that a period of favourable growing conditions may prevail until approximately 2025. After this time frame, climatic stress should increase, potentially leading to uneven effects across the landscape. This will cause growth reductions, crown dieback and limited mortality in sugar maple across the study area. Consequences of this outcome would be an expected impact to the volume of sugar maple sap for use in the production of maple syrup products, the aesthetics of fall foliage, the availability of maple wood products and the various ecological services that sugar maple trees provide to the Acadian Forest Region.

Preface

Today we no longer see the landscape as a static environment. Through many scientific processes we have created the capability to see far into the history of the planet and we have realized our world is an unstable place saturated with adaptive strategies. We have also seen that our actions are having a direct affect on the stability of the Earth's climate system. An awareness of the cumulative effects of humans on the environment has grown to become undeniable. This has helped conceive a vision of forthcoming ecologic transformation beyond the natural variability of the distant past. Now we are learning to anticipate the shifts in ecosystems that will define the planet's future.

The original research presented here represents a portion of a larger and ongoing body of work regarding radial growth response of Acadian Forest tree species to climate change. The questions pursued in this work developed from a curiosity concerning the viability of presently rooted trees. Our awareness of shifting climate conditions informs us about the potential for range migration of many species but how will those long-lived species with fixed addresses cope? An understanding of the future prosperity of established tree populations not only informs us of impending resource availability but advises us about potential shifts in biological interactions dependent upon the largest bio-structural component of forest ecosystems.

Anticipation of positive or negative reactions to climate induced changes in the forests offers the potential for mitigation and preparation. In this evaluation of sugar maple, the most geographically expansive attempt at radial growth forecasting is undertaken.

Acknowledgements

Credit for the completion of this thesis must be extended to many people and organizations. I would like to genuinely recognize the encouragement, confidence and contribution to my research over the past few years by Colin Laroque. Also I would like to thank Jennifer Baltzer for her advice and support.

I am grateful that the Fundy Model Forest has placed importance on this subject matter. Their vision and awareness will result in a better future for our forest community. They deserve recognition for their ongoing financial support of this research. Also the financial support of the Natural Sciences and Engineering Research Council (NSERC) funding to Colin Laroque has, in part, made this research possible.

Members of the MAD lab deserve particular praise for coring all those sugar maple trees in the field. Thanks to Nigel Selig, Lanna Campbell, Hannah MacDonald, Felicia Pickard, Mary MacQuaid, Nicole d'Entremont, Brian Crouse, Chris Kennedy and Carry White. Thanks to André Robichaud for lab work assistance. Thanks to the rest of the past and present lab members, including Hank, for all of the inspiring and unforgettable experiences.

Finally I cannot thank my family enough for supporting me through the long and meandering journey that has lead me to this achievement. You are the cornerstone of my success.

Dedication

This thesis is dedicated to my parents whose exceptional courage and determination in the face of adversity is an inspiration to all.

Chapter 1

1.0 Establishing the Framework

1.1 Introduction

Reactions to unprecedented climatic conditions are expected in forests around the world as they undergo compositional shifts to maintain climatic associations (IUFRO 2009). Tree species migration is often modeled when the long-term effects of climate change are contemplated (McKenney et al. 2007, Iverson et al. 2008), while the response of currently rooted trees to various forms of unusual disturbances and the new climate regimes is less quantifiable (IUFRO 2009). The considerably stressed ecosystems of the Acadian Forest Region of New Brunswick and Nova Scotia, Canada, are no different than any other forest in the world and much uncertainty exists concerning the future response of the tree species found within its reaches (Vasseur and Catto 2008).

Sugar maple (*Acer saccharum* Marsh) is of particular concern in the Acadian Forest Region. It has experienced periods of growth stress throughout its range, mainly in the latter half of the 20th century, which have been associated with freezing and drought related causes (Bauce and Allen 1991, Auclair et al. 1996, Robitaille et al. 1995, Payette et al. 1996, Auclair 2005). Other events such as nutrient limitation, insect outbreaks and pollution have also been implicated as sugar maple stressors (Pitelka and Raynal 1989, Hartmann and Messier 2008, St. Clair et al. 2008). Some combination of climatic triggering events (Bauce and Allen 1991, Payette et al. 1996), further exacerbated by local site factors (St. Clair et al. 2008) seem to have been the cause of sugar maple crown dieback and radial growth reductions in the past. Moreover, Auclair has linked ocean-atmosphere interactions, northern hemisphere temperatures and general climate

change to the occurrence of climatic triggering events (Auclair et al. 1996, Auclair 2005). Although the probable causes of the regional sugar maple stresses are diverse and complex, using a local example like an ice storm, it is relatively easy to imagine the cascading ecological effects on sugar maple trees that begin with a single climatic event (Smith and Shortle 2003).

A mix of continental and maritime air masses influence the climate over the Acadian Forest Region resulting in less drought (Phillips 1990, Payette et al. 1996) but more thaw/refreeze events than in other portions of the sugar maple range due to the closer proximity of oceanic influences (Phillips 1990). This difference in climate from other areas of the northeastern North American hardwood biome may predispose sugar maple in the Acadian Forest Region to more frequent freezing stressors. Analysis of the historic growth response of sugar maple trees to these types of stressors throughout the species' range has been performed routinely through tree-ring investigations in more continental regions (Bauce and Allen 1991, Lane et al. 1993, Yin and Arp 1994, Payette et al. 1996, Tardiff et al. 2001, Goldblum and Rigg 2005), but have never been attempted in a more maritime environment.

Dendroclimatological analysis is well suited to assess the past extent of sugar maple stress and evaluate the potential future success of the species. Long time periods can be examined for radial growth suppression through this technique, while models of future radial growth rates can be produced. Typically, monthly resolution climate data is regressed onto annual tree-ring measurement indices to estimate the extent and timing of climatic influence on radial growth (Payette et al. 1996, Tardiff et al. 2001, Goldblum and Rigg 2005, Phillips and Laroque 2008,). However, the ability of monthly climatic data to capture daily or weekly extreme events has been questioned by both Graumlich (1993) and Payette et al. (1996). It is therefore the objective of this study to attempt a reconstruction of potential stress events from the

instrumental daily climate record rather than using the more traditional monthly format.

Although freezing events have often been indicated as a trigger for sugar maple stress, never before has an attempt to model and forecast such conditions on a daily temporal scale been accomplished.

The production of radial growth forecasts for sugar maple under such a potentially complex series of influences is a formidable challenge. The uncertainty of Global Climate Model trajectories into the future further obscures the process being attempted here. But, keeping these challenges in mind, it is hoped that this more inclusive modeling process will result in a more persuasive forecast that will finally start to influence active management plans.

1.2 Hypothesis

Evidence is mounting in support of the theory that global change is causing stress on many forests (Auclair 2005, Beier et al. 2008, van Mantgem et al. 2009), and in particular, thaw-freeze cycles have been implicated as agents of stress in multiple species including sugar maple (Bauce and Allen 1991, Auclair et al. 1993a, Auclair et al. 1996, Robitaille et al. 1995, Payette et al. 1996, Auclair 2005, Beier et al. 2008). This evidence raises many new questions, such as how will thaw-freeze affect trees in the future, what maritime climate processes are causing it in the present, and has it affected them in the more distant past? How a radial growth analysis in the Maritime Provinces can help answer these questions is in part, the point of this study.

This research therefore tested the following two hypotheses:

- 1) Thaw/refreeze late winter conditions are injuring sugar maple trees and these events are occurring more frequently in the southern portions of New Brunswick and central areas of Nova Scotia than in more northern portions of the provinces, and;

- 2) Late winter thaw/refreeze events are likely to affect trees more often in northern areas of New Brunswick as future climatic changes advance, and more dominant influences of the adjacent oceans are felt.

Chapter 2

2.0 Hypotheses Background

2.1 Sugar Maple Characteristics

2.1.1 *Range and Climate*

Sugar maple range includes all of the Maritime Provinces of Canada but nears its northern latitudinal boundary in the northern reaches of New Brunswick (Fig. 2.1). Throughout the range, the average winter time low temperature varies between 10°C and -18°C depending on latitude and elevation, and the average summer high temperature varies between 16°C and 27°C (Burns et al. 1990). Precipitation averages vary between a low of 510 mm annually along the western edge of the range to a high of 2030 mm in the Southern Appalachian Mountains (Burns et al. 1990). These amounts put the Maritime average somewhere near the median range values of -4°C winters, 21.5°C summers and 1270mm of annual precipitation. Given that the Maritime range is currently near the northern boundary of the greater range and both the temperature and precipitation amounts experienced in the Maritimes are roughly equal to that of the intermediate values associated with the species, it is reasonable to expect that climate change and increasing temperatures will have little effect on the geographic distribution of trees in this area. In fact, climate envelop models running the high-medium SRES A2 climate change scenario only show slight sugar maple range contraction in Nova Scotia by 2100 AD (McKenney et al. 2007).

2.1.2 *Temporal Abundance*

Based mainly on pollen abundance in sediment cores taken from lakes in southwestern New Brunswick, it appears that maple (*Acer*) most likely first appeared on the landscape in the

Maritime Provinces sometime after 9500 years B.P. remaining relatively insignificant in a forest dominated by pine (*Pinus*). Around 6600 years B.P., maple populations increased along with other hardwood genera and hemlock (*Tsuga*). Population levels shifted again at approximately 5100 years B.P. when hemlock declined and beech (*Fagus*) numbers increased to dominate the forest along with maple, birch (*Betula*), ash (*Fraxinus*) and other hardwoods. Near 3000 years B.P., hemlock populations had rebounded and they dominated along with the hardwoods. About 1000 years B.P., hemlock declined and spruce (*Picea*) increased while the hardwoods, such as beech, maple and oak (*Quercus*), dominated but not to the same degree as in the previous 4000 years (Mott 1975). By the time European settlement started to influence the composition of regional forests (circa 1800), the maple genus accounted for 18.4% of trees, based on a witness tree study conducted in Kings County New Brunswick (Lutz 1997). Recent figures indicate the maple genus has realized a reduction of two percentage points dropping to about 16.4% of total trees in the same area. Of course this may vary across the landscape and tolerant sugar maple is likely to have experienced much larger declines while the more intolerant maple species, such as red maple (*Acer rubrum*), have likely increased in abundance (Woodley et al. 1998). This substitution in species would have made up much of the difference and maintained the maple genus population levels.

Palynological research has shown that maple trees have reached far greater abundance in past situations when the climate was much warmer than it is today in the Maritimes. Pollen analysis completed by Livingstone (1968) in eastern Canada shows that even though former time periods supported greater maple populations, the maple genus expanded and contracted greatly over time as past climates fluctuated. The human impact on maple populations is partially outlined by Loo and Ives (2003) where they describe the disturbances of agriculture clearing and

industrial forestry operations on diverse hardwood communities. These historical perspectives indicate that anthropogenic forces can greatly influence the abundance of sugar maple trees over long time periods and that large fluctuations in the sugar maple population should be expected with changing climates.

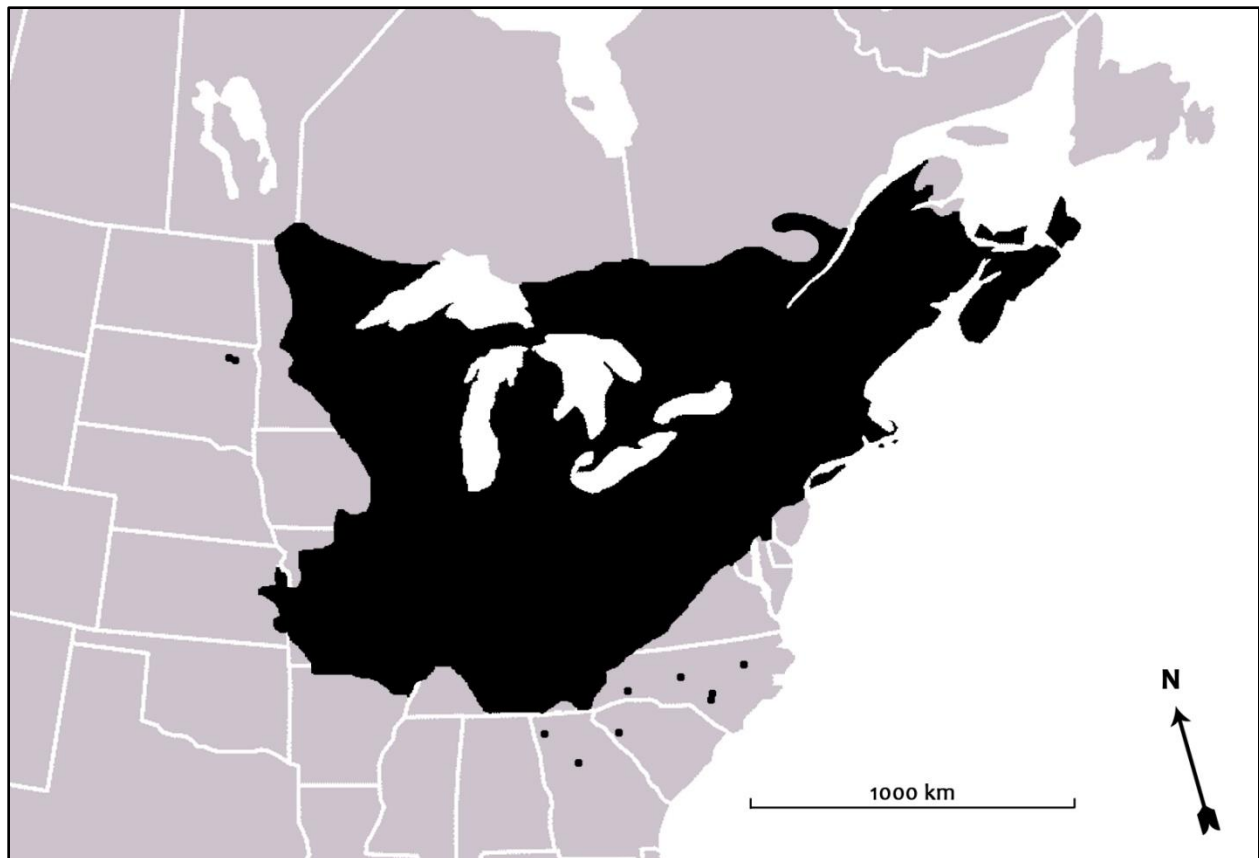


Figure 2.1. Sugar maple range map in eastern North America outlining the geographic range where the trees have been observed growing and reproducing (adapted from Farrar 1995).

2.1.3 Habitat, Life Expectancy and Size

Sugar maple prefers nutrient rich, moist soils that are well drained (Ritchie 1959). It is most commonly found in upland tolerant hardwood forests in the Maritimes mixed with yellow birch (*Betula alleghaniensis* Britt.), American beech (*Fagus grandifolia* Ehrh.), and sometimes red spruce (*Picea rubens* Sarg.) (Zelazny et al. 2003). Sugar maple is an extremely shade tolerant tree and it reaches full photosynthetic activity at approximately one quarter full sunlight. Due to its high shade tolerance, the species can survive for long periods in the forest understory before becoming a canopy tree. Sugar maple is a long lived northern hardwood species and can achieve life expectancies of 300 to 400 years. Its full size measures about 27 to 37 m in height and 76 to 91 cm diameter at breast height (Burns et al. 1990).

2.1.4 Foliar Phenology

Sugar maple, yellow birch, and American beech form many of the upland tolerant hardwood forests in the Maritimes (Zelazny et al. 2003) and it would be expected that strong competitive associations exist between these species. In fact, only days separate the spring time bud burst of sugar maple, yellow birch, and American beech (Richardson et al. 2006). The competitive advantage of being the first tree species to develop foliage in a deciduous forest is self-evident, however, the disadvantages could be more subversive. Late winter subzero temperature swings can not only damage new leaves, but early biological processes of dehardened tissues during winter thaws in yellow birch have been shown to put trees at risk for freezing damage of their roots (Cox and Zhu 2003). Typically, sugar maple requires 2500 hours of chilling temperatures before bud dormancy is broken in northern populations (Burns et al. 1990). Records gathered between 1989-2002 at Hubbard Brook (259m asl) in the White

Mountains of New Hampshire, positioned roughly at 44° N latitude and 72° W longitude, indicate the mean day for a sugar maple leaf development of 50% is May 14th and the mean day for 50% of leaf drop is October 18th; giving an average growing season of 157 days. For every additional 100 m increase in elevation, bud break occurs approximately 2.7 days later and leaf drop occurs approximately 2.5 days earlier (Richardson et al. 2006). The area where this data was collected roughly reflects the climatic conditions experienced in the Maritimes and is one degree of latitude farther south than the most southerly point of the study area in this thesis.

2.2 Dieback Phenomenon

2.2.1 Crown Dieback Defined

Crown dieback in trees is a type of branch-related mortality that first occurs at the terminal end of the branch and advances toward the bole. This phenomenon must appear in the upper crown of the tree to be considered dieback and have no obvious physical injury signs; in other words, inward to outward affliction (Auclair 2005). An obvious characteristic symptom of dieback is reduced radial growth due to the inability of the tree to fix enough carbon to form normal annual growth rings (Auclair 1993a).

Crown dieback was studied by many researchers throughout the 20th century. Early research centered on climatic causes then transitioned to atmospheric pollution theories of causation (Walker et al. 1990, Millers et al. 1989). More recently causation theories have moved forward to attribute thaw-freeze and drought as the major underlying problem (Bauce and Allen 1991, Auclair et al. 1993b, Auclair et al. 1996, Robitaille et al. 1995, Payette et al. 1996, Auclair 2005, Beier et al. 2008).

2.2.2 Dieback Research

In 2009 researchers from the west coast of North America released a report illustrating increasing mortality rates in forests from that area. They contributed evidence that this mortality occurring among young and old trees was connected to a changing climate in which water deficits are more frequent (van Mantgem et al. 2009). A year earlier in 2008, researchers in southeastern Alaska produced evidence supporting theories that warming winters were causing late winter severe thaw-freeze events manifesting in the decline and mortality of yellow cedar (*Chamaecyparis nootkatensis* (D. Don) Spach) (Beier et al. 2008). Most recently on the east coast, Auclair (2005) has shown a 22 year cycle of dieback affecting sugar maple, multiple ash species, multiple birch species, and red spruce. Another study from the same year assessed the spatial extent of past winter thaw-freeze events in relation to birch declines across eastern North America (Bourque et al. 2005). Previous to these more recent projects, Auclair completed extensive work in dieback associated with winter thaw-freeze in northern hardwoods of North America, western white pine (*Pinus monticola* D. Don) from the Pacific Northwest, and Norway spruce (*Picea abies* (L.) H. Karst) and silver fir (*Abies alba* Mill.) in Europe (Auclair et al. 1990, Auclair 1993, Auclair et al. 1996). This research along with many prior studies, consistently relate climatic events to externally expressed symptoms on various tree species covering many disjunct regions.

In a more directly related study to this work, Payette et al. (1996) completed an extensive dendrochronological investigation on the probable causes of sugar maple crown dieback during the 1980s in Quebec. The relevance to the present study is the geographic proximity of the sites sampled and the potential to consider the tree-ring chronologies produced from both sampling efforts as one network sharing similar climatic growth drivers. Although the methods used in the

Quebec study differed from the methods used here, the results offer a useful comparison. Among those results, Payette et al. (1996) concluded that winter thaw-freezes and summer droughts often coincided with periods of radial tree growth suppression. The conclusions of past field research was important evidence in the formulation of this study, and the results of experimental research were also essential.

2.2.3 Experimental Research

Over the past two decades, experimental work regarding thaw-freeze has been done with many researchers attempting to get at the root of the problem. Many studies on various tree species have illustrated that freezing and thawing of stem, branch, twig, and root portions of trees causes air bubbles to form in the xylem vessels of the wood (Sperry et al. 1988, Hacke and Sauter 1996, Zhu et al. 2002, Cox and Zhu 2003). These breaks in the fluid tension are more commonly referred to as xylem cavitations or xylem embolisms and can also be caused by water stress or drought conditions (Hacke and Sperry 2001). Different tree species have dissimilar xylem morphology, which triggers variance in response to climatic events amongst species (Hacke and Sperry 2001). The result of a high percentage of xylem cavitations is reduced water flow to the canopy and decreased canopy productivity, which can be extensive enough to cause the individual organism to suffer decreased vigor for several years or even cause death (Bergeron and Sedio 1999). Xylem cavitation is a regular part of seasonal change in many temperate tree species, but when severe winter temperature events happen, the root systems can be damaged in several potential poorly understood ways or depleted of the necessary energy to fully restore xylem conductivity (Robitaille et al. 1995, Hacke and Sauter 1996). These results can then be seen in crown dieback, potential mortality, and reduced radial growth or temporary growth suppression (Beier et al. 2008). Despite the research cited here, there is still a need to develop a

more specific understanding of winter ecological processes. The lack of winter study regarding sugar maple climate response will continue to affect the comprehension of potential effects of weather events during that time of year, ultimately resulting in continuing predictive uncertainty (Campbell et al. 2005).

2.2.4 Potential Connections to Ocean Conditions

Trees growing on most continents have shown strong connections to multidecadal oscillating ocean conditions (Gray et al. 2008, Cook and D'Arrigo 2002). Auclair et al. (1996) found a strong relationship among global climate phenomena and episodes of dieback in the northern temperate forests of eastern North America. More specifically, links were made between the Southern Oscillation Index (SOI) and Northern Hemisphere temperatures. While the influence of the SOI on northeastern areas of the North American continent is relatively weak (Auclair et al. 1996), Northern Hemisphere temperatures are also known to be modified by conditions in the North Atlantic Ocean (Sutton and Hodson 2005). This suggests North Atlantic Ocean conditions such as the North Atlantic Oscillation and the Atlantic Multidecadal Oscillation may play a role in the climatic drivers associated with tree growth and dieback episodes. In this regard, a winter-spring connection that may link these phenomena to thaw-refreeze events could also be underlying parts of the dieback processes. Direct assessments of these potential oceanic influences have yet to be addressed and they may provide important insights into tree responses in the Maritime Provinces.

Chapter 3

3.0 Study Area

3.1 Study Sites

Ten sampling sites were selected for this study and were mainly chosen near Adjusted Historic Canadian Climate Data (AHCCD) centres. Five locations near AHCCD centres were selected in New Brunswick, and two more were chosen in Nova Scotia (Fig. 3.1). Three more sites were selected in New Brunswick that did not have AHCCD centres nearby.

The study site area is bordered by Maine, U.S.A. at $67^{\circ} 47'$ W on the western side and by the Gaspé Peninsula, Quebec to the north at approximately 48° N. To the east the Gulf of St. Lawrence, and more specifically Chaleur Bay and Northumberland Strait, create a marine boundary at approximately $64^{\circ} 30'$ W, although the most westerly site is located in Nova Scotia closer to 62° W. Finally to the south, New Brunswick is bordered by another marine body in the Bay of Fundy and Nova Scotia is bordered by the Atlantic Ocean which both cross the 45° latitude on a 45° angle above which all sites are located (Fig. 3.1).

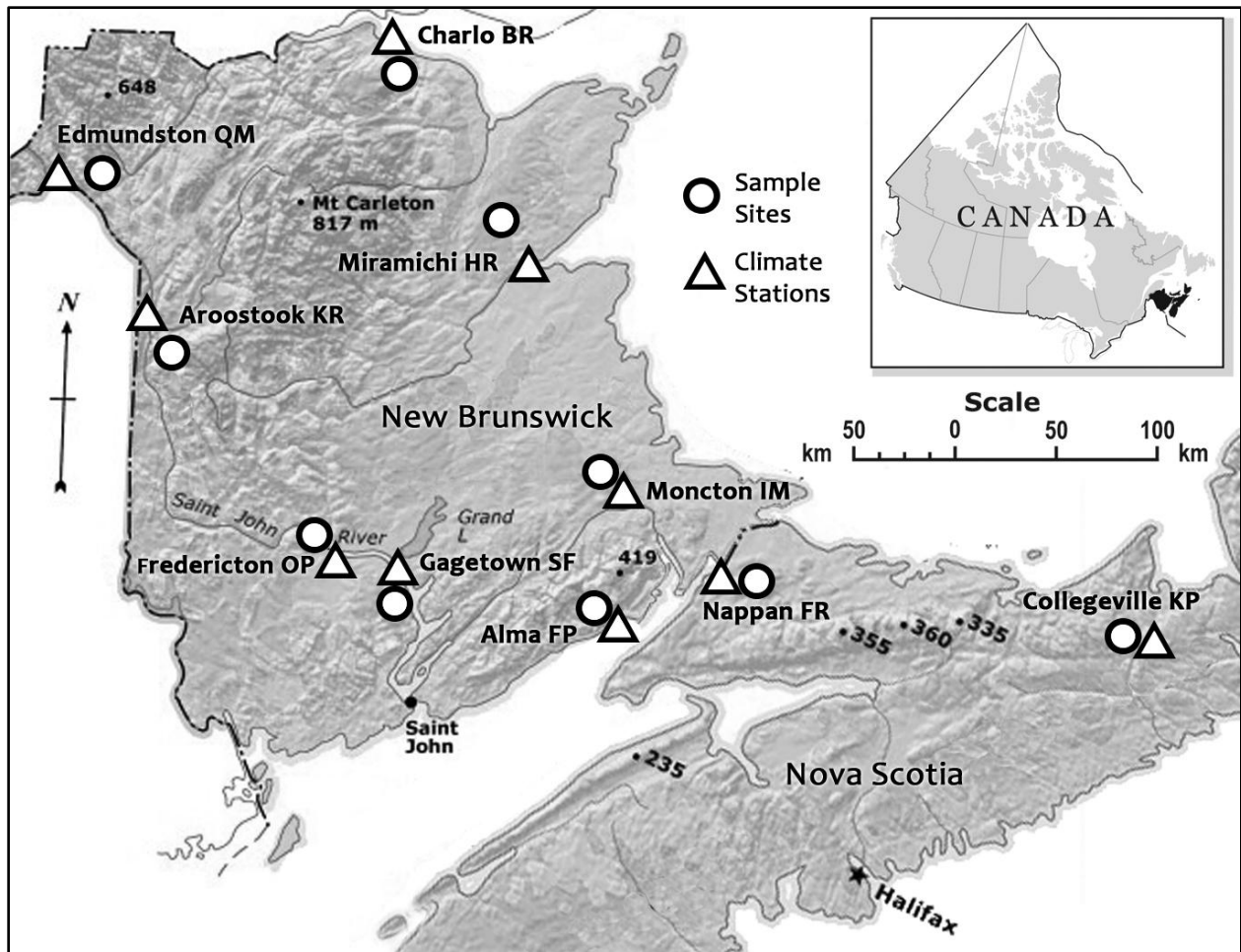


Figure 3.1. Study site map with the geographical positions of the ten sugar maple sample sites and ten climate stations from New Brunswick and Nova Scotia used in this study. Base map © 2001. Her Majesty the Queen in Right of Canada, Natural Resources Canada.

3.2 Climate

In the study site region, predominant winds flow from the west bringing with them a strong continental influence which subdues much of the marine effect produced by the various water bodies (Phillips, 1990). Coastal regions are still dominated by the marine influence and incursions of marine air masses into central areas do occur. The Gulf of St. Lawrence waters consistently freezes near land in winter and the surface warms substantially in summer months to a high of 18°C due to its shallow depths (Phillips, 1990). In the south, the Bay of Fundy

produces the highest tides in the world and its constantly-overturning deep waters produce surface temperatures ranging from a low of 0-4°C in winter to 8-12°C in summer, which results in foggy, cool air masses adjacent to the land (Phillips, 1990). Along New Brunswick's southern coast, fog normally occurs on a third of the days in July (Phillips, 1990). Finally the Atlantic Ocean carries the Gulf Stream off the southern coast of Nova Scotia, with mean 16°C waters mediating the temperature extremes in the southwest (Phillips, 1990).

Elevation in the region rises from sea level to a pinnacle of 820 m above sea level (asl), although most sample sites are found between 150m and 400m asl (Table 3.1). A quantitative description of each site can be found in Table 3.1. Due to a predominate westerly flow of air masses, combined with substantial continental effects to the north and west, and the many marine influences to the east and south, a complex set of localized climate conditions are created. July mean temperatures range through 16.5°C to 19.5°C and January mean temperatures range from -12.2°C to -6°C (Phillips, 1990, Clayden, 2000). Growing degree days above 5°C, range from slightly below 1300 to over 1800 across the region (Clayden, 2000). Precipitation normally ranges from 1000 mm to 1200 mm or higher in Nova Scotia depending upon the marine proximity and elevation (Phillips, 1990). Snowfall amounts typically accumulate from 300 to 400 cm in northwest New Brunswick accounting for 33% of annual precipitation (Phillips, 1990). In southern areas of New Brunswick, less than 20% of precipitation falls as snow totaling from 200 to 300 cm (Phillips, 1990). These mean temperatures and precipitation types can be substantially influenced in the winter months by the variation in air masses, from cold arctic, to warm maritime (Phillips, 1990).

Table 3.1. Tree-ring sample sites including the site elevation, position, distance from the nearest climate station, and the elevational difference between the site and climate station for each of the ten sample sites.

Site Name	Site Elevation (m)	Geographic Position (long/lat)	Distance From Climate Station (km)	Elevation Difference (m)
Benjamin River	267	47°54' N, 66°15' W	11	227
Quisibis Mountain	343	47°26' N, 68°01' W	25	188
Kintore Ridge	414	46°42' N, 67°38' W	12	305
Horseshoe Ridge	168	47°14' N, 65°43' W	31	135
Odell Park	70	45°57' N, 66°40' W	5	50
Slipp Farm	114	45°40' N, 66°08' W	14	80
Indian Mountain	157	46° 10' N, 64°55' W	19	85
Fundy Park	300	45°38' N, 65° 01' W	6	257
Fenwick Ridge	111	45°46' N, 64° 09' W	7	91
Keppoch Plateau	185	45°31' N, 62° 06' W	8	109

3.3 Biota

The Acadian Forest Region covers all of the Maritime Provinces except New Brunswick's central highlands. The Acadian Forest Region is distinguished as a mixed wood transition zone between the more northerly coniferous dominated forest and the more southerly deciduous dominated forests (Loo and Ives, 2003). Tree species such as yellow birch, sugar maple, American beech, eastern hemlock (*Tusga canadensis* (L.) Carriere), white pine (*Pinus strobus* L.), and balsam fir (*Abies balsamea* (L.) Mill.) are typical of the Acadian Forest Region. Red spruce is the most distinguishing feature of the Acadian Forest Region, occurring in most forest types (Mosseler et al., 2003). It should be noted that 300 to 400 years of land clearing and harvesting have substantially shifted forest composition and age distribution of the Acadian Forest Region to that of younger forests with less hardwood dominance (Loo and Ives, 2003, Mosseler et al., 2003). These anthropogenically manipulated forest characteristics affect this

study by changing the abundance and age classes of late-successional sugar maple, making it more difficult to find mature or old growth stands.

3.4 Individual Site Ecodistrict Descriptions

The following individual site descriptions detail the characteristics of the immediate area at each site and give a summary of the local ecodistrict based on the Ecological Land Classification for New Brunswick and the Ecological Land Classification for Nova Scotia. A general explanation of the major climatic features of the greater ecoregion is presented, followed by a more specific description of the climate and biota found within the smaller ecodistrict subsection.

Benjamin River (BR) – Tjigog Ecodistrict

This site is located on an inland plateau near the Bay of Chaleur at 267 m elevation (Fig. 3.1). The stand of sugar maple trees was unevenly aged and growing in a mixed stand with mature eastern white cedar (*Thuja occidentalis* L.), yellow birch, red spruce and balsam fir. There were minor components of red maple and white birch (*Betula papyrifera* Marsh.) in the area with a patchy, yet dense, American beech understory. The site is fairly flat and exhibited sporadic wet spots.

The Northern Uplands Ecoregion in which this ecodistrict is located is slightly cooler than other upland areas as most slopes face north (Zelazny et al. 2003). Although this region has a lower elevation than the adjacent highlands, winter temperatures are known to be extreme in areas far enough away from the Bay of Chaleur (Zelazny et al. 2003). The local climate of the ecodistrict is moderated by the Bay of Chaleur and it lies in the rain shadow of the highlands to the west and the Gaspé Peninsula to the north. These influences cause this site to receive a low

to medium amount of precipitation in the growing season relative to other sites and make fires more frequent here than most other parts of the study area (Zelazny et al. 2003). The moderation of temperatures by the Bay of Chaleur extend the growing season length within the ecodistrict, allowing species with more southern affinities to persist (Zelazny et al. 2003).

Quisibis Mountain (QM) – Madawaska Ecodistrict

This site is located in a hilly upland area at 343 m elevation near the base of the highest peak in the area, Quisibis Mountain. The site has the remnants of an old sugar shack and is dominated by uneven-aged sugar maple with minor components of mature yellow birch and American beech. The canopy was very tight and the slightly sloping site was well drained and facing southeast.

Unlike to the Northern Uplands Ecoregion, the Central Uplands Ecoregion, in which this site is located, slopes face predominantly south and west. The aspect of the slopes combined with the daytime cool air drainage into the numerous valley landforms results in warmer upland forests. This area is on the windward side of the highlands region where the effects of orthographic lifting bring higher precipitation and less frequent forest fires. The Madawaska Ecodistrict's high elevations produce a cool, damp climate which supports many hilltop tolerant hardwood stands (Zelazny et al. 2003).

Kintore Ridge (KR) – Brighton Ecodistrict

This is the highest site located at 414 m elevation on an unlogged portion of crown land. It is dominated by sugar maple mixed with mature beech, yellow birch, red spruce and balsam fir. Most of the site has vigorous beech undergrowth. The site is located on a well drained slope with a western aspect.

The Brighton Ecodistrict is another in the Central Uplands Ecoregion but with a much more southern geographic position. The elevation here results in higher precipitation amounts and cooler temperatures than other parts of the study area, however the location within the ecodistrict exposes the area to more moderate temperatures acquired from further down the slopes in the Saint John and Tobique river valleys. Tolerant hardwood stands are plentiful in this ecodistrict (Zelazny et al. 2003).

Horseshoe Ridge (HR) – Tabusintac Ecodistrict

This site is located at 168 m elevation and supports an even-age stand of sugar maple mixed with a minor portion of American beech and yellow birch. Vigorous American beech regeneration is common throughout the site. The landscape is generally flat yet the area appeared well drained.

Horseshoe Ridge is one of two sites sampled in the largest ecoregion of the Eastern Lowlands. The ecoregion lies in the rain shadow of the highland and upland regions and is therefore dry and prone to more frequent forest fires. The most noted example of this is the massive 1825 Miramichi fire which consumed the forests over much of the region (Zelazny et al. 2003). The Tabusintac Ecodistrict is cooled in summer by the waters of the Gulf of St. Lawrence. Tolerant hardwood stands where sugar maple is normally found occur infrequently in this ecoregion (Zelazny et al. 2003).

Odell Park (OP) – Aukpaque Ecodistrict

This site is found at 70 m elevation within the boundaries of a city park that is said to have never been logged. Much of the park is dominated by large old-growth eastern hemlock and white pine. The lower reaches are dominated by uneven-aged sugar maple with lesser

amounts of beech, white ash (*Fraxinus americana* L.), yellow birch and basswood (*Tilia americana* L.). The site features much exposed bedrock, is well drained and the aspect of the slope faces northeast. The park was established in 1954 and is criss-crossed by a number of hard packed trails.

Odell Park is on the edge of the warmest ecoregion of New Brunswick called the Grand Lake Lowlands. Due to the lag in heat transfer between the atmosphere and Grand Lake, the length of the growing season is extended and the frost free period is longer than any other area in New Brunswick (Zelazny et al. 2003). This results in warmer falls and an early finish of the winter season. The Aukpaque ecodistrict itself is located over the majority of the lower Saint John River Valley area. The sample site is located up river from Grand Lake but is still moderated by the large volume of water in the river (Zelazny et al. 2003). Although this ecodistrict supports many species with more southern affinities, the dominant stands are composed of red spruce, balsam fir, sugar maple, beech, white pine and hemlock. It should be noted that Odell Park borders on the Valley Lowlands Ecoregion and the Grand Lake Lowlands characteristics could be near their limits here (Zelazny et al. 2003).

Slipp Farm (SF) – Aukpaque Ecodistrict

This site is situated at 110 m elevation on private land. The tolerant hardwood stand of sugar maple, beech and yellow birch is uneven-aged and contains vigorous beech regeneration. Many of the trees found on this site contain cavities used by local wildlife. The terrain is flat and rocky on the top section of the plateau but the tolerant hardwood stand extends down an east facing slope, both of which are well drained. Limited logging has occurred on this site over long periods of history.

The Slipp Farm sugar maple sample site is located within the same ecoregion and ecodistrict as Odell Park, and its climatic exposure can be described through the ecological land classification in the same way. However, the Slipp Farm site is located roughly 18 km below the confluence of the Grand Lake drainage and the Saint John River in contrast to Odell Park which is situated approximately 45 km up river from the confluence. The Slipp Farm site is further away from the river edge and 40 m higher in elevation. These differences could cause some significant variation in local temperature between the two sites. The Slipp Farm lies on the boundary between the Aukpaque Ecodistrict of the Grand Lake Lowlands Ecoregion and the Yoho Ecodistrict of the Valley Lowlands Ecoregion. While both these ecodistricts are characterized as dry and partially rain-shadowed landscapes, it is unclear what, if any, differences exist in precipitation amounts (Zelazny et al. 2003).

Indian Mountain (IM) – Petitcodiac Ecodistrict

This site is on private land at 157 m elevation on the Indian Mountain plateau where the North River originates and later becomes the Petitcodiac River. Historically this stand of tolerant hardwoods, composed of uneven-aged sugar maple, yellow birch, beech, white ash and ironwood (*Ostrya virginiana* (Mill.) K. Koch), was used for maple syrup production. The site is relatively flat and incised with drainage channels making the slightly south facing slope well drained. A number of old wood roads traverse the stand although they are little used today. Minor amounts of logging have been carried out by the various land owners but more value was placed in the stand for maple sugar production thus allowing many of the trees to achieve old ages.

The large Eastern Lowlands Ecoregion covers this site and is influenced by the higher elevation areas to the northwest and southwest. These taller landforms cast a rain shadow over the lowlands as well as protecting it from onshore breezes off the Bay of Fundy. The result is a relatively dry climate with warm summers comparable to the Valley Lowlands Ecoregion and winter temperatures moderated by the Northumberland Strait. The particular ecodistrict which the Indian Mountain sugar maple stand is best characterized by is somewhat ambiguous. Indian Mountain, Steeves Mountain and Lutes Mountain form an area of higher elevation at the intersection of the low-elevation Castaway, Kouchibouguac and Petitcodiac ecodistricts. The Petitcodiac ecodistrict most likely lends the best climatic description as a transition zone between the warm, dry lowlands and the cool, wet Fundy Coastal Ecoregion (Zelazny et al. 2003). The elevation here would be expected to both increase precipitation amounts and result in cooler temperatures than the lowlands. Also the tolerant hardwood growing on the higher elevation areas here are somewhat of a departure from the typical lower elevation species comprised of intolerant hardwood and coniferous stands.

Fundy Park (FP) – Caledonia Ecodistrict

This site is situated at 300 m elevation in Fundy National Park. This tolerant hardwood stand is composed of uneven-aged sugar maple, yellow birch, beech and red spruce. Before the establishment of the park in 1948 the forests here were in high demand for spruce timber so it is unlikely this stand ever experienced significant harvesting pressure. The slope is relatively flat but maintained a slightly north facing aspect.

Geographically, this site is located within the Caledonia portion of the Central Uplands Ecoregion. This ecoregion's alternate ecodistricts are found in the northern part of New

Brunswick but share similar traits with this high elevation area. The climate within this ecodistrict is cool and moist keeping forest fire activity to a minimum. The elevation characteristics of the site allow the Caledonia Plateau an escape from the cool Bay of Fundy waters in the growing season. Although the site is within the Caledonia Ecodistrict it is important to note that the boundary of the Fundy Coastal Ecoregion is not far off. The steep temperature gradients emanating from the Bay of Fundy most likely affect this sample site. The cool waters of the Bay produce frequent fog days when in contact with warm humid summer air. This fog is hindered on its inland movement by the steep elevation of the Caledonia Uplands but it penetrates far enough inland to have some effect on this site. The slope of this site does face north, but it is located on the southern windward side of the uplands where orographic lifting is responsible for a high level of annual precipitation. There is a quick transition from the red spruce dominated coniferous forests in the Fundy Coastal Ecoregion to the tolerant hardwood stands common on the plateau area, describing the character of this site well (Zelazny et al. 2003).

Fenwick Ridge (FR) – Northumberland Lowlands Ecodistrict

This site is positioned at 111 m elevation on private land near the Trans Canada Highway. There is strong evidence here that it was once a maple sugar producing area. The forest is dominated by uneven-aged sugar maple with lesser amounts of yellow birch, white ash, ironwood, red spruce, beech and striped maple (*Acer pensylvanicum* L.). Regeneration on the site is shared between sugar maple in some areas and beech in others. The slope is gradual, the aspect faces east and the soil is medium, to well-drained. Many of the sugar maple trees on this site are hollow and very old.

The Northumberland Bras D'Or Lowlands Ecoregion description defines this area as a dry and warm environment during the growing season with some of the coolest temperatures found in Nova Scotia through the winter months. The Northumberland Strait influences the growing season temperatures with its warm waters but its winter freeze-over limits any warming impact during the coldest months. The Fenwick site is technically located in the Northumberland Lowlands Ecodistrict but it is also positioned very near the Cumberland Hills and Tantramar Marshes Ecodistricts. Presence in the rain shadow of the Cobequid Mountains limits the annual precipitation in the lowlands area to the smallest amount in Nova Scotia, leading to more frequent forest fires here than other areas of the province. However, the adjacent Cumberland Hills Ecodistrict receives slightly more precipitation which may be more likely along the Fenwick Ridge considering the relatively high elevation compared to the rest of the lowlands. Due to the proximity to other cooler ecodistricts, this area is most likely not as warm as the rest of the Northumberland Lowlands Ecodistrict. The tree species at this site are more characteristic of the Cumberland Hills ecodistrict as the lowlands are dominated by coniferous stands (Neily et al. 2003).

Keppoch Plateau (KP) – Pictou Anitgonish Highlands

This site occupies a low order stream valley at 185 m elevation. On the slopes, rising up from the stream, are dominant, uneven-aged sugar maple trees with components of yellow birch and beech. Although the forest is mature, it was not considered old-growth as there are few very old trees (150+). The small stream valley runs south to north and trees were sampled on both valley walls facing east and west. Trees away from the small stream are growing on well drained soils.

The Keppoch sampling site is situated within the Nova Scotia Uplands Ecoregion. This area characteristically has warm summers and relatively cold winters for Nova Scotia. Precipitation and snow fall amounts are comparably high in this ecoregion. Ice damage to trees can also be a problem for hardwoods here. The Keppoch area is more specifically located in the Pictou Antigonish Highlands Ecodistrict but the climatic difference has no further specification (Neily et al. 2003).

Chapter 4

4.0 Data Composition and Analysis Procedures

4.1 Instrumental Climate Data

Climate data used in this analysis was obtained through four sources. The most heavily relied upon data set was daily instrumental data from the Adjusted Historical Canadian Climate Data (AHCCD) set available through Environment Canada (Vincent and Gullet 1999, 2002). The second data source was daily snow depth reconstruction data accessed through the Canadian Daily Snow Depth Database Main Documentation (Brown and Braaten 1998). These two data sets were supplemented with the raw, unadjusted Canadian Daily Climate Data (CDCD), available through Environment Canada, and the U.S. Historical Climatology Network (USHCN) data (Williams et al. 2006). Several reasons arose for the need of supplemental data; the first, not all desired locations had AHCCD data available, and second, many days, weeks, and sometimes months worth of data were missing in the adjusted and reconstructed data. To fill these gaps, nearby climate data collection stations were used to provide the missing data at the station in question.

Nearby climate data sets were extracted from the CDCD data and sometimes used to extend the AHCCD data further back in time. By using data from other climate stations to infill missing data, a level of error was introduced into the chosen climate station series. Data from several stations, covering various periods of time, located at numerous elevations, and at assorted places within their communities had to be pieced together. Every effort was made to avoid using climate data of debatable quality, and instead to substitute missing values with data from the nearest, and most similar neighbour station. However, this was not always possible and the

original adjusted and homogenized data obtained from the AHCCD data set were altered in the end. The outcome of this compilation was that 10 complete data sets covering the time periods and areas outlined in Table 4.1. were constructed. From these data sets, both daily and monthly values were made available for the production of the climate variables needed in the analysis. It should also be noted that during the climate data set construction, lapse rates were applied to temperature and snow depth measurements in an attempt to account for the relatively large differences in elevation between climate stations and sample sites.

Table 4.1. Environment Canada climate station information for the main station used for each sample site. Climate station identification including, the station ID number, the common interval of data covered by all data types, the approximate geographic position (latitude and longitude in degrees and minutes), and the elevation above sea level is provided for each climate site.

Main Station Location	Station ID Number	Common Interval	Station Position	Station Elevation
Charlo, N.B.	8100885	1940-2005	47° 59' N, 66° 20' W	40 m
Edmundston, N.B.	810AL00	1936-2003	47° 21' N, 68° 11' W	155 m
Aroostook, N.B.	8100300	1932-2004	46° 48' N, 67° 43' W	91 m
Miramichi, N.B.	8101000	1876-2004	47° 01' N, 65° 28' W	33 m
Fredericton, N.B.	8101500	1878-2005	45° 52' N, 66° 32' W	20 m
Gagetown, N.B.	8101800	1928-2002	45° 47' N, 66° 09' W	34 m
Moncton, N.B.	8103200	1901-2005	46° 06' N, 64° 41' W	72 m
Alma, N.B.	8100200	1953-2002	45° 36' N, 64° 57' W	43 m
Nappan, N.S.	8203700	1917-2002	45° 46' N, 64° 15' W	20 m
Collegeville, N.S.	8201000	1919-2005	45° 29' N, 62° 01' W	76 m

4.2 Global Climate Model Data

Third Generation Coupled Global Climate Model (CGCM3), produced by the Canadian Centre for Climate Modeling and Analysis, was used to predict the future weather data applied in the tree growth forecasts. Monthly and daily data were calculated for the grid squares within the latitudes from 43°15' N to 48°50' N and longitudes from 61°52' W to 70°19' W (Fig. 4.1).

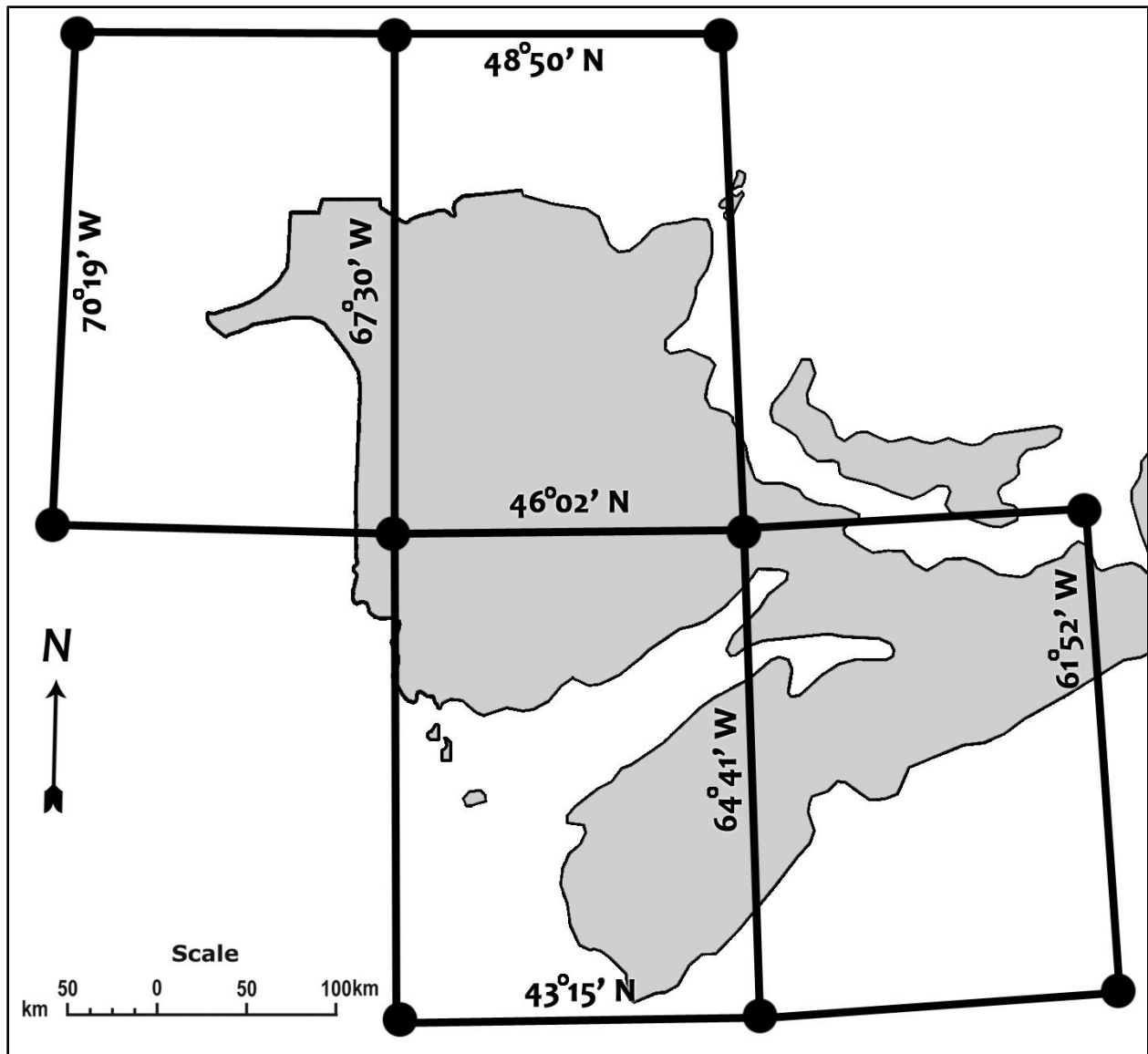


Figure 4.1. The CGCM3 produces a set of forecast data that is homogenous across a 2.81° X 2.81° grid square, and does so for a global grid. The CGCM3 output grid squares used in the study are illustrated over the Maritime provinces. Latitudinal and longitudinal boundaries for each grid square are also given. Base map © 2002. Her Majesty the Queen in Right of Canada, Natural Resources Canada.

4.3 Climate Change Scenarios

This study takes a conservative approach to future climate model data. Data used are based on two scenarios from the Special Report on Emissions Standard (SRES) published by the

IPCC (2007). The CGCM3 data used are based on the SRES B1 and SRES A1B scenarios. The B1 scenario is a low estimate and assumes a 550 parts per million (ppm) leveling of CO₂ emissions by the year 2100. The A1B scenario is an intermediate estimate and assumes a 720 ppm leveling of CO₂ emissions by the year 2100. These two scenarios were chosen from a range of scenarios which place atmospheric CO₂ concentrations between 550 ppm and 1000 ppm by the end of this century. As will be explained later, more extreme climate change scenarios were not deemed appropriate for this study.

4.4 Global Climate Model Calibration

The CGCM3 grid squares superimposed over the study area covered more than five degrees of latitude and over eight degrees of longitude, including several distinct water bodies. These grid squares overlap a zone much larger than the study area, and data represent an average homogenous result of temperature and precipitation over the entire heterogeneous region of each grid square. Because of this generalized upscaling, a “change factor” conversion was needed, at least on the basic monthly temporal scale. This was deemed possible, as a baseline climatological record from each climate station was available, and the calculations were relatively simple compared to a “statistical downscaling” approach (Diaz-Nieto and Wilby 2005).

For each month of every year, the CGCM3 data were subtracted from the point source data at each station for the longest period possible. The resulting calculations were then averaged for each month over the same period creating mean monthly divergence values. The divergence values were then added back onto the CGCM3 uniform data set to shift the magnitude of the values to that of the point source climate station values, and in doing so, they did not alter the variation of the data. The same operation was repeated for the daily data from

each climate station. The output divergence values were then applied to the future CGCM3 data adapting it to be representative for the future local climate at each site. A possible drawback to this process, is that the global climate model (GCM) data are not altered to reflect the local climate but only shifted to a similar magnitude as the local climate. Although not ideal, this was the most appropriate conversion possible given the relative large amount of data and the available time.

4.5 Climate Variables

The abiotic influence of climate on tree growth is complex. The combination of long- and short-term weather events that coalesce over time to form the climate can echo through the environment for days, years, decades and sometimes centuries after they occur. Although instrumentation to quantify this multidimensional continuous chain of weather events has evolved tremendously over the past century, we must still rely on the climatic description provided by those first meteorological instruments if we wish to peer relatively far back in time. Not only are we limited by the types of data collected by these early instruments, but we are also limited by the geographic extent within which measurements were taken.

In the Maritimes we are lucky to have a comparatively long climate record, reaching back over 130 years in some locations. The large majority of climate stations that extend back in time long enough to be of use to this study, are positioned within populated areas, often at low elevations. These older data records are subject to errors in documentation and collection as well as lack of uniform procedures and a lack of quality control (Vincent and Gullet 2002).

Many variables were constructed from the climate records made available through the sources listed above. The temporal periods of these variables are summarized in Table 4.2 and

Monthly Mean Temperature (MMT) Variable Set

Tmean – This variable set included mean monthly temperatures for each month over the three year period minus November and December of the current year. Also several months were aggregated into seasonal values to decrease the total number of variables in this set (Table 4.2).

Total Monthly Precipitation (TMP) Variable Set

Tprecip – This variable set included total monthly precipitation amounts from April to September in the current and first lagged years, and in the second lagged year, total seasonal precipitation amounts for spring and summer were provided (Table 4.2).

SD – This variable averaged monthly snow depth from December to March of each year and summed them in a snow depth index (Table 4.2). The purpose of this variable was to combine several variables to shrink the overall variable count, while providing a more representative perspective on the ecological effects of winter precipitation.

Daily Compiled Temperature (DCT) Variable Set

EvpStr – This variable averaged daily maximum temperatures in the months of July and August of all years. It is a representation of evapotranspirational stress (Table 4.2).

GDD – This variable summed the total number of growing degree days from May to October by summing mean daily temperatures above 5°C (Table 4.2).

TRF D – The ‘thaw/refreeze deep’ variable summed the freezing degree days (FDD) following a thaw, defined as a period accumulating 15 growing degree days in March, April or May (Table 4.2). Auclair et al. (1996), Payette et al. (1996), Bourque et al. (2005) and Brier et al. (2008) all defined a similar winter thaw-freeze variable.

TRFS – The ‘thaw/refreeze surficial’ variable represented the lowest negative temperature value ($<-4^{\circ}\text{C}$) following a period accumulating 15 growing degree days in March, April or May when no FDD (number of accumulated negative daily mean temperatures) were experienced but a nighttime freeze occurred (Table 4.2). Because many thaws represented the final thaw of the winter season, yet were not followed by an accumulation of FDD, it was felt a surficial freeze variable was necessary to describe significant, but short-term (one night freezing) events ($<-4^{\circ}\text{C}$) more commonly known as frost.

RtFr – This root freeze variable summed FDD for each winter month depending on the depth of snow present. The following accumulation of FDD was employed; FDD (base 0°C) were calculate when snow depth equaled zero to ten centimeters, FDD (base -5°C) were calculated when snow depth equaled 10 to 20 cm, FDD (base -10°C) were calculated when snow depth equaled 20 to 30 cm, FDD (base -15°C) were calculated when snow depth equaled 30 to 40 cm, no FDD were calculated when snow depth was greater than 40 cm. The FDD accumulation was determined for the months from December to March. FDD were calculated for each day in this time period using these constraints then summed for each month and the month in each year with the greatest absolute number of FDD represented that year (Table 4.2). Through experimental work, Robitaille et al. (1995) found freezes over bare ground caused reduced radial growth in sugar maple for several years following the event.

4.6 Climate Model Summary

The two northern CGCM3 grid square SRES A1b outputs used in this study were averaged, as were the two southern grid square SRES A1b outputs to produce two comparative data sets covering the years 2000 to 2100 (see Fig. 4.1). The comparative data sets were then

transposed using several of the DCT variable definitions and several seasonal temperature and precipitation parameters, creating two contiguous and contrasting climatic descriptions. This permitted the comparison of the future effects of climate change between the northern and southern regions of the study area. More specifically, a trend line was run through the mean of the forecast climatic descriptions. Values from the beginnings of these trend lines (the year 2000) and values from the ends (the year 2100) are used to quantify forecast climate change deviation between the latitudinally opposing regions.

4.7 Global Coupled Ocean-Atmosphere Interactions

Climate data representing global coupled ocean-atmosphere interactions (GCOAI) which vary at low frequencies relative to the annual scale of tree-rings were also used in the analysis of sugar maple response to climate. The Atlantic Multidecadal Oscillation (AMO), the North Atlantic Oscillation (NAO), the Southern Oscillation Index (SOI) and the Pacific Decadal Oscillation (PDO), were all assessed for relationships to sugar maple radial growth. The AMO is expressed by sea surface temperature (SST) anomalies between 0° - 70° N latitude in the Atlantic Ocean (Enfield et al. 2001). The NAO is identified through a principal component analysis of winter sea level pressure (SLP) anomalies measured between 20° N -70° N latitude and 90° W - 40° E longitude in the Atlantic Ocean (Hurrell et al. 2003). The Southern Oscillation Index (SOI) is the measured SST anomalies between 5° N - 5° S latitude and 170° W - 120° W longitude in the Pacific Ocean (Kaplan et al. 1998). The PDO is again identified through principal component analysis of SST above 20° N latitude in the Pacific Ocean (Mantua et al. 1997).

The AMO unsmoothed monthly index data (1856 -2008) were accessed through the Physical Sciences Division (PSD) of the Earth Systems Research Laboratory (ESRL) of the National Ocean and Atmospheric Administration (NOAA). Data for the winter (Dec-Mar) station based NAO index (1864 -2008) and the SOI signal monthly index data (1866 -2008) were both accessed through the Climate Analysis Section (CAS) of the Climate and Global Dynamics (CGD) division of the National Centre for Atmospheric Research (NCAR). The PDO standardized monthly index (1900 – 2008) was accessed through the Joint Institute for the Study of the Atmosphere and Ocean (JISAO).

4.8 Tree-Ring Data

At each sampling site at least 40 core samples were taken from 20 trees using a 5.1 mm increment boring tool. Sampling only occurred on sites where trees were over 150 years old to ensure the time period covered by the analysis was using only mature tree growth. Sites were also selected, based on their proximity to a nearby climate station. Due to the difficulties in finding suitable sampling sites over 150 years old near climate stations, other selection criteria such as slope, aspect, elevation, and substrate often had to be ignored. The resulting tree-ring data were therefore a consequence of an opportunistic sampling strategy. Although micro-site characteristics were largely disregarded, sugar maple is usually found in upland sites growing in tolerant hardwood stands in New Brunswick and Nova Scotia (Neily et al. 2003, Zelazny et al. 2003). All sites sampled, except one, were found in what would be considered pure tolerant hardwood stands (see section 3.4).

Increment cores were prepared using standard dendrochronological procedures (Stokes and Smiley 1968). Following preparation, all cores were visually cross-dated and then ring-

widths were measured to 0.001 mm using a VELMEX measuring system. Statistical cross-dating of the measured ring width patterns was carried out using the program COFECHA (Holmes 1992, Grissino-Mayer 2001). A small number of problematic cores with poor correlation values identified through this procedure were eliminated amounting to no more than four cores per sample site. The remaining cores for each site were standardized to remove non-climatic, low frequency growth signals, such as age-related trends and competition-induced growth suppression. Using the program ARSTAN (Cook 1985), ring-width series were double detrended, first using a negative exponential curve or linear regression, then using a spline of 50% frequency response, and indexed values for each chronology were produced creating master site chronologies. Following detrending procedures, the individual site chronologies were entered into correlation matrices to determine the strength of inter-site relationships.

4.9 Tree-ring Chronology Analysis

Each of the ten standardized tree-ring chronologies developed for this study were analyzed between trees to produce averaged individual site Pearson product-moment correlation coefficients (r -values based on overlapping 50-year segments) and an average mean sensitivity was calculated. Pearson's r -value describes the strength of linear dependence between each core's growth and an overall master chronology (all values over 0.3281 are significant at the 99% confidence interval), while the average mean sensitivity (AMS) calculation measures the high-frequency variation between annual rings by calculating average deviation (Fritts 1976, Grissino-Mayer 2001). Values of the AMS between 0.1 and 0.19 are considered low, values between 0.2 and 0.29 are considered moderate while any value over 0.3 is considered high and these values are recognized to be a good measure of a tree's sensitivity to climate (Grissino-Mayer 2001).

The relationship between the standardized chronologies of the ten sample sites were assessed using Pearson's r over the common interval of tree-ring data. Analysis across the range of sample sites is intended to reveal geographic patterns resulting from an uneven landscape and regional climatic variation. Relationships between the standardized chronologies of the ten sample sites are also assessed using Pearson's r over shorter time periods of 50 years overlapped by 25 years. Analysis across the range of sample sites using shorter time periods is intended to reveal temporal patterns resulting from climatic fluctuations or modifications of the sugar maple radial growth response to climate over time. Finally, the standardized chronologies for each site were assessed for relationships with the GCOAI data using Pearson's r to search for influence of these larger climatic fluctuations on the radial growth of sugar maple trees. Due to the low frequency multidecadal nature of the GCOAI phases, correlation analysis was performed on smoothed curves (10 year moving averages) of both the GCOAI and standardized tree ring curves. Correlations were calculated for the entire period of available instrumental data for each GCOAI.

4.10 Radial Growth-climate Analysis

A stepwise regression technique was used to establish and forecast the growth-climate relationship as it has in previous research using an "F to enter" of 0.20 and an "F to remove" of 0.25 (*c.f.*, Laroque and Smith 2003, Goldblum and Rigg 2005, Phillips and Laroque 2007, 2008, Girardin et al. 2008). In these forecasting studies, the tree-ring master chronologies were entered into the stepwise regression analysis as the dependent variable and mean monthly temperature along with total monthly precipitation values were entered as the independent variables. In addition to these independent variables, a one-year lag of radial tree growth was entered as an independent variable. This was done as autocorrelation, or the signature of radial growth

dependence on previous year's energy reserves, was not statistically removed from the tree-ring chronologies. A residual chronology is the accepted form of radial tree growth quantification with autocorrelation eliminated (Graumlich 1993, Tardiff et al. 2001, Goldblum and Rigg 2005, Girardin et al. 2008). Normally, when autocorrelation is not statistically removed, the prior year's radial growth is used as a variable in tree-ring modeling procedures to account for such high autocorrelation (Payette et al. 1996, Laroque and Smith 2003). However this can become problematic in radial growth forecasting as a heavy reliance on the prior growth variable will assure the model calibration and verification sections are continually corrected using the full information available through this model term. During forecasting excursions into future scenarios, the model must rely on the previous year's modeled radial growth for the prior growth variable values. Since the modeled radial growth only contains information from the included climate variables and does not contain the influence of the other normal non-climatic variables, the prior growth variable no longer maintains the ability to correct the model. This may result in divergence from the original performance of the model.

This study attempts to explain past climatic influence by omitting the prior growth variable and instead including past climate variables covering two lagged years. This can be problematic as large numbers of candidate variables regressed onto a relatively short time series may result in the selection of incorrect variables or an incomplete set of variables for model construction (Arbaugh and Peterson 1989). To minimize the inclusion of spurious variables and maximize the addition of important variables in the best subset, steps were taken to amalgamate biologically related variables (Table 4.2). It was thought that lagged variables would allow for easier identification of injurious winter events that have maximum effect the following year or the second year following occurrence.

Further to the previous growth variable replacement, adoption of a new method for model selection was employed. Previous forecast studies either set aside a portion of the radial tree growth/climate variable time series for cross-validation or used a 10% rule to select the variables for inclusion in the model to avoid “overfitting” (Laroque and Smith 2003, Phillips and Laroque 2006, 2007, Girardin et al. 2008). Cross-validation allows most of the data to be used in the stepwise regression for fitting the model and the rest of the data to be used to verify the model fit. Once all models are fit, the best verification is chosen or the 10% rule is applied to limit the selection of variables included in the model. With an increase in the number of variables entered into the stepwise regression analysis used in this study, it was necessary to maximize the length of the time series used in the regression to accommodate the relatively large number of variables, to the comparatively small number of observed years available.

The stepwise regression process outputs a range of models consisting of increasing quantities of explanatory variables until the “F to enter” and “F to remove” values constrain the process and all potential variables are included. To select the best subset model from the range of models created, Akaike’s Information Criteria corrected (AICc) for models with high variable to observation value ratios was used (Burnham 2002). This approach estimates Kullback-Leibler (K-L) information and the best model minimizes the K-L information or distance between reality and the model (Burnham 2002). The main drawback to this approach concerns models that are not in the set under consideration. Akaike’s Information Theory will select the best model from the available set, but if all the models in the set under consideration are poor, then the selected best model from this set will still remain poor. To assess the goodness-of-fit of the AICc-selected best model an adjusted coefficient of determination ($\text{adj } R^2$) was used. This gives a measure of how well the model, may predict future situations. The adjusted R^2 corrects the

coefficient of determination for increasing degrees of freedom in the model (Burnham and Anderson 1998). It only raises the adjusted R^2 value if an additional variable explains more variability than would be expected to occur by chance.

Chapter 5

5.0 Results and Model Outputs

5.1 Tree-ring Chronologies

The initial length of the tree-ring chronologies generated from the sampled trees in this study varied substantially, depending on the site. Although many trees were sampled with enough solid wood to measure over 200 years of radial growth, each site chronology was truncated at 1850 and all chronology analysis was performed on the shared 157 year common interval from 1850-2006. Intra-site r-values produced for each site through the mean series correlation statistic exemplify the common environmental response among trees at individual sites. Table 5.1 illustrates the mean site r-values ranging from 0.469 to 0.606 which signify that the majority of the trees in this study are all displaying a strong common signal. The relevance of these values can be put in a better context when compared with the lower sugar maple r-values produced by Tardiff et al. (2001) of 0.326 in Quebec and Goldblum and Rigg (2005) of 0.390 in Ontario. Average mean sensitivity values also calculated for each chronology range from 0.256 to 0.324 (Table 5.1). These sensitivity values produce a small general increasing trend from north to south and many sites approach or exceed 0.300 which indicates they are very sensitive to climate (Grissino-Mayer 2001). The r-values within the inter-site correlation matrix illustrate a large amount of variability in their relationships between site master chronologies (1850-2006), ranging from -0.084 to 0.537 (Table 5.2). These inter-site correlation values not only vary significantly between sites revealing inconsistent geographic patterns but those relationships change considerably through time. Table 5.3 illustrates the average r-values among all sites for five 50-year time periods, lagged 25 years, calculated over the 1850-2000 common interval. The

correlation values range from 0.182 to 0.336 representing periods of relative agreement and disagreement. Visual representations of radial growth curves for all sites are found in Figure 5.1.

Table 5.1. Statistics in this Table are calculated between individual tree ring indices produced for each sample site covering the common interval 1850-2006. Each site is represented by a minimum of 36 individual tree cores taken from a minimum of 17 trees. Intra-site correlations using Pearson's r-values illustrate the strength of relationships between sampled sugar maple trees at each site. Also presented are average mean sensitivity (AMS) values calculated using all trees at each site. Values for AMS are considered low from 0.1-0.19, intermediate from 0.2-0.29 and high from ≥ 0.3 (Grissino-Mayer 2001). * = ($p < 0.0001$).

Site	BR	QM	KR	HR	OP	SF	IM	FP	FR	KP
r	0.581*	0.578*	0.554*	0.606*	0.517*	0.572*	0.469*	0.537*	0.539*	0.497*
AMS	0.256	0.296	0.298	0.307	0.301	0.270	0.300	0.324	0.282	0.319

Table 5.2. The comparative relationships between all sugar maple chronologies are illustrated in this inter-site correlation matrix with Pearson's r-values for the common period 1850-2006. Pearson's r-values are calculated between standardized tree-ring curves for each site. Cells in this Table are shaded depending on the strength of the r-value indicated; darker shading represents higher r-values while lighter shading indicates lower r-values. * = ($p < 0.05$), ** = ($p < 0.01$).

Site	BR	QM	KR	HR	OP	SF	IM	FP	FR	KP
BR	1									
QM	0.273**	1								
KR	0.410**	0.532**	1							
HR	0.202*	0.392**	0.317**	1						
OP	0.034	0.361**	0.201*	0.537**	1					
SF	0.176*	0.112	0.091	-0.040	0.294**	1				
IM	0.043	0.126	0.133	0.087	0.240**	0.451**	1			
FP	0.144	0.254**	0.383**	0.369**	0.330**	0.277**	0.478**	1		
FR	-0.084	0.307**	0.064	0.264**	0.302**	0.074	0.232**	0.375**	1	
KP	0.108	0.287**	0.009	0.490**	0.496**	0.129	0.130	0.226**	0.433**	1

Table 5.3. Pearson's r-values averaged for all ten sugar maple chronologies over 50-year periods lagged by 25-years are presented. This Table was derived from individual inter-site correlation matrices calculated for each 50-year period. All five correlation values were composed of an average r-value computed between all sites in each individual matrix.

* = (p<0.05), ** = (p<0.01).

Time Period	1850-1899	1875-1924	1900-1949	1925-1975	1950-1999
Mean r-value	0.223	0.310*	0.336**	0.182	0.307*

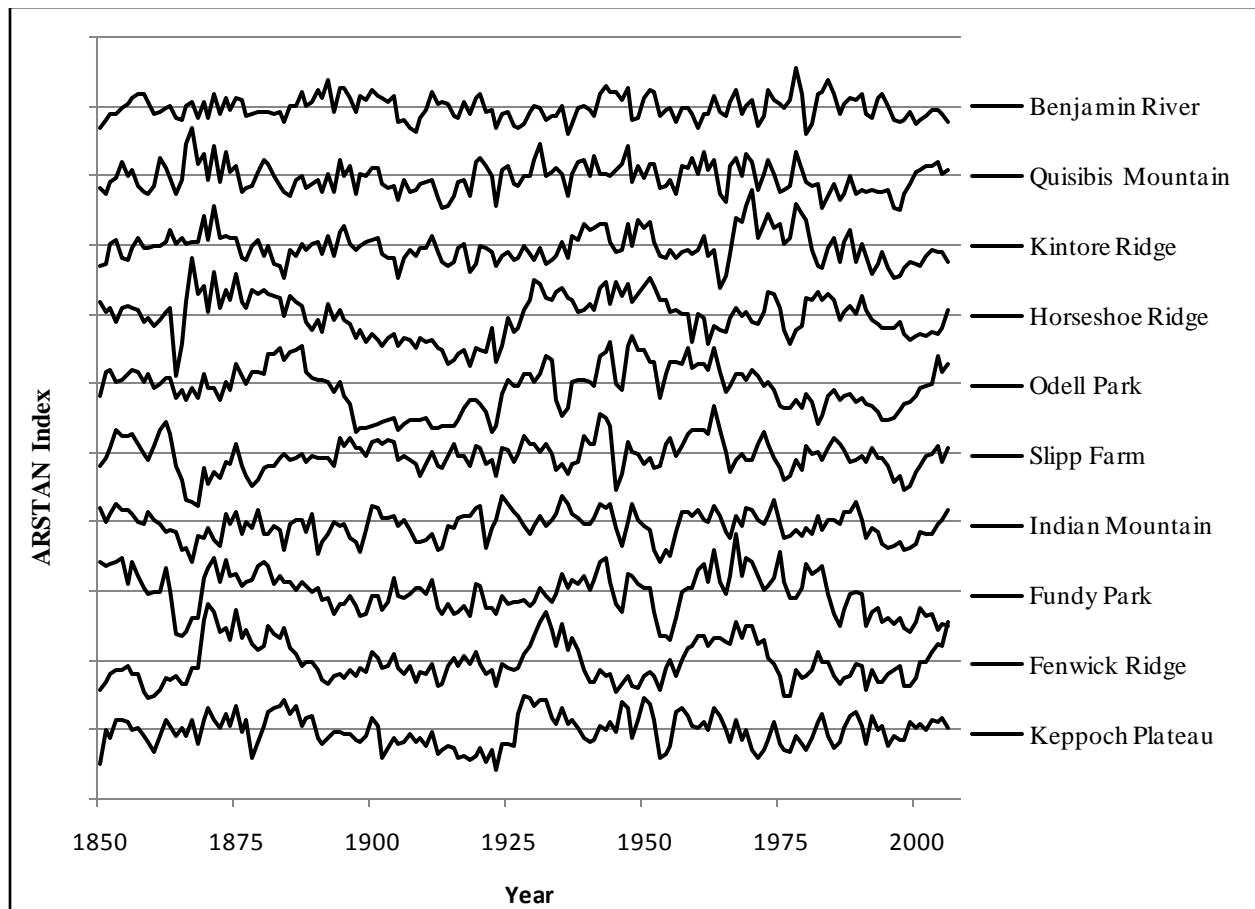


Figure 5.1. All ten sugar maple chronologies representing the ten sample sites are depicted over the truncated common interval from 1850-2006. All chronologies are standardized using the program ARSTAN and indexed curves are presented. Each curve fluctuates around an average of one represented by the horizontal strike-through lines. Sample depth at each site has a minimum of thirty cores extending back in time 100 years and at least 10 cores extending back 150 years. Site names are presented adjacent to each radial growth curve and order of sites is from north to south with occasional shuffling of sites to preserve nearest neighbour associations.

5.2 Relationship to Ocean-Atmosphere Interactions

Correlations between sugar maple chronologies and GCOAIs were completed using annual data and were also plotted using ten year moving averages (10-mavg). When the tree-ring chronologies were aggregated into one regional master chronology the AMO illustrated significant correlations with the strongest relationship occurring at a three year lag of the AMO (r-value = 0.368; $p < 0.01$, and r-value (10-mavg) = 0.582; $p < 0.01$). Although the master chronology produced a highly significant relationship with the AMO, six of the sites (Charlo (BJ), Aroostook (KR), Gagetown (SF), Moncton (IM), Alma (FP), Nappan (FR)) showed weak correlations while four of the sites (Edmundston (QM), Miramichi (HR), Fredericton (OP), Collegeville (KP)) showed very strong correlation values. Fredericton (OP) (r-value = 0.481; $p < 0.01$, and r-value (10-mavg) = 0.713; $p < 0.01$) and Collegeville (KP) (r-value = 0.371; $p < 0.01$, and r-value (10-mavg) = 0.738; $p < 0.01$) showed the highest values (Fig. 5.2).

The winter season measurements of the NAO index produced negative correlations with a large majority of sugar maple tree-ring chronologies in this study. Half of the sugar maple chronologies illustrate a significant negative correlation with the NAO index at a three year lag and nine of the sites illustrate a significant correlation to NAO at a three year lag under a ten year moving average. The regional standardized master chronology illustrated a significant negative correlation value with the strongest relationship occurring at a three year lag of NAO (r-value = -0.334; $p < 0.01$, and r-value (10-mavg) = -0.688; $p < 0.01$) (Fig. 5.3).

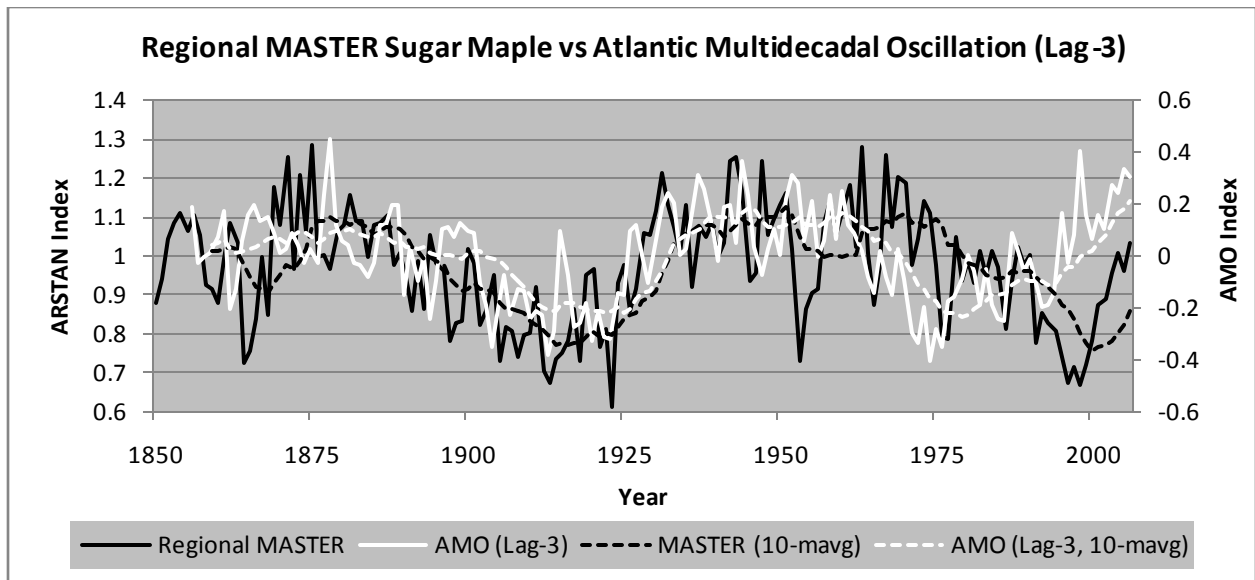


Figure 5.2. The standardized index of the regional master sugar maple tree-ring chronology plotted against the AMO at a three year lag. The curves of both the annual variability and smoothed decadal variability (10 year moving average) data are plotted for visual comparison.

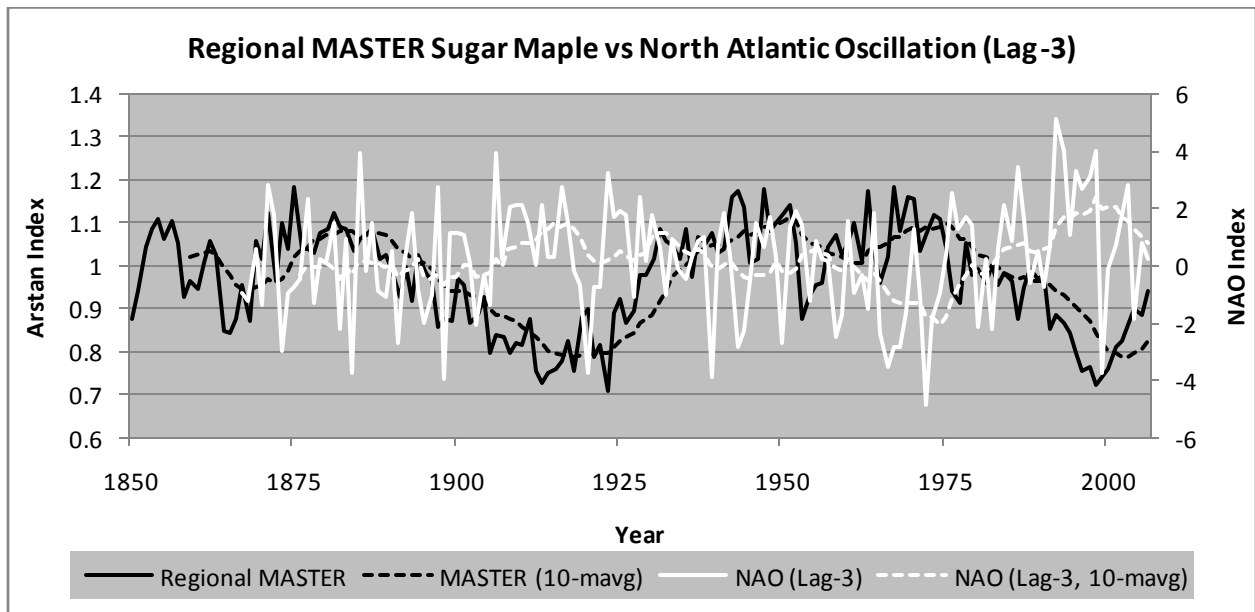


Figure 5.3. The standardized index of the regional master sugar maple tree-ring chronology plotted against the NAO at a three year lag. The curves of both the annual variability and smoothed decadal variability (10 year moving average) are plotted for visual comparison.

5.3 Thaw/Refreeze Variables

During the construction of the TRF Deep and Surficial variables, it was observed that forecasts of these variables were not consistent with historical occurrence and severity levels. The TRF Deep and Surficial variables are of limited use for forecasting as the CGCM3 daily April data illustrates a great range in the variability in temperatures (Fig. 5.4). These extreme day time to night time temperature swings result in future TRF Deep and Surficial variables of near annual occurrence with greater magnitude of negative daily minimum temperatures than what has actually been experienced in the past (Figure 5.4). This creates a large step in the data set in the year 2000 as the TRF Deep and Surficial variables transition from recorded data to modeled data (Figure 5.4).

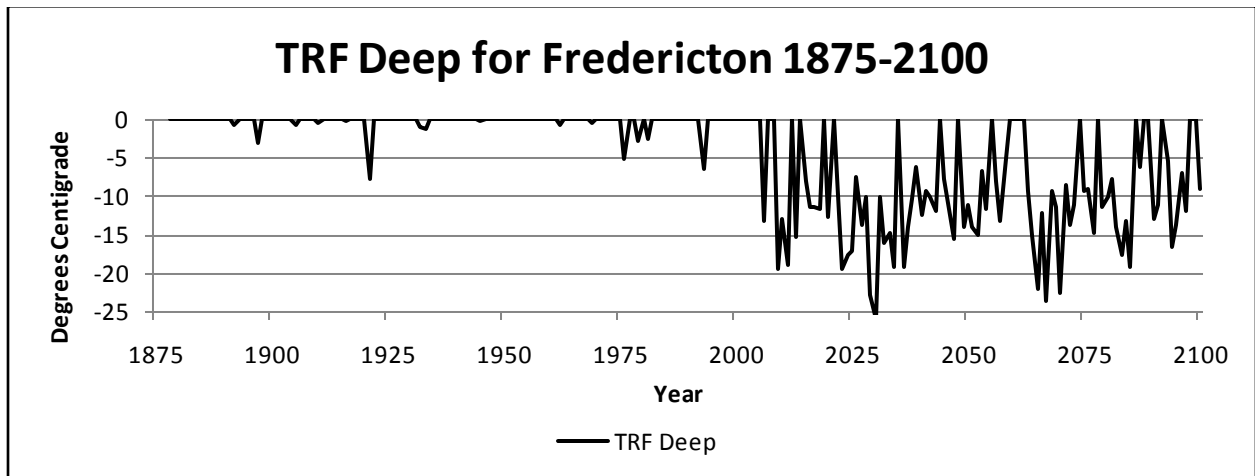


Figure 5.4. The Thaw/Refreeze Deep (TRF Deep) variable calculated using historical and forecast climate data for Fredericton is outlined. Noticeable is a large increase of occurrence in the data at the transition from historical to forecasted results around the year 2000.

5.4 Canadian Global Climate Model Third Generation Summaries

The following description highlights summarized information from the CGCM3 for the SRES A1b scenario based on a north versus south perspective of the study area (Table 5.4).

Table 5.4. Forecast climatic changes expected by the end of the 21st century for the SRES A1b scenario produced by the CGCM3. T DJFM = winter temperature, RtFr = root freeze, GDD = growing degree days, EvpStr = evapotranspiration stress, T Apr = April temperature, P MAJ = spring precipitation and P JAS = summer precipitation.

Variable	Northern CGCM3 Grid Square		Southern CGCM3 Grid Square	
	2000	2100	2000	2100
T DJFM	-14°C	-8°C	-7.5°C	-1.5°C
Snow Depth	280 cm	255 cm	125 cm	40 cm
RtFr	-120 FDD	-70 FDD	-145 FDD	-75 FDD
GDD	1075 GDD	1550 GDD	1550 GDD	2350 GDD
EvpStr	20°C	22°C	23°C	27°C
T Apr	-2°C	2.5°C	1.5°C	7°C
P MAJ	95 mm	120 mm	105 mm	115 mm
P JAS	112 mm	110 mm	95 mm	85 mm

Notable changes in forecasted climate means include a near 70% reduction in winter snow depth in southern areas of the Maritimes by the end of the 21st century. The root freeze index shows a 42% drop in northern regions and a 48% drop in southern regions even though the protective snow cover is forecast to be substantially reduced in the south. This is mainly due to a projected 6°C rise in winter temperatures by the end of the current century. The number of growing degree days is predicted to make large increases, intensifying to a 44% surge in the north while the south should experience 52% amplification. Average July and August temperature daily maximums are projected to increase by 2°C in the north and 4°C the south. Average April temperatures are forecast to rise by 4.5°C in the north and by 5.5°C in the south. Spring precipitation is expected to increase by 26% in the north and only 9% in the south while little change in summer precipitation is forecast for the north but an 11% decrease should be realized in the south.

5.5 Radial Growth Future Forecasts

This section illustrates the results of the stepwise regression models based on the MMT/TMP variable sets. All individual tree-ring master chronologies, model calibration, and future model forecasts are illustrated in Figures 5.5 to 5.24. Where possible, models were calibrated over a 76-year period from 1930 to 2005 however, in some cases, a common interval of climate data reaching back to 1930 was not available so several models are calibrated on a shorter time period (see Table 5.5).

Since Fredericton had the least distance between climate station and sugar maple sample site, two auxiliary models were produced, one using the TRF Deep variable in place of the April temperature variable and the other using both the TRF Deep variable in place of the April temperature variable and the AMO index (Figs. 5.25 and 5.26). These clarification models are named Fredericton (OP2) and Fredericton (OP3) respectively, and the information regarding these models is found in Tables 5.5 and 5.6.

Table 5.5. The regression model summary information for the AICc optimum variable subset. Model information including the variable type, period and length of model calibration, the number of included variables in each model and the amount of explained variance is presented. Explained variance is represented by an adjusted R² value for each model which is assessed for significance by an ANOVA. * = (p≤0.001)

Site	Variable Type	Model Calibration Period	Calibration Period Length	Included Model Variables	Model Adjusted R ²
Charlo (BR)	Monthly	1940-2005	66 yrs	6	0.346*
Edmundston (QM)	Monthly	1936-2003	68 yrs	10	0.542*
Aroostook (KR)	Monthly	1932-2004	73 yrs	7	0.237*
Miramichi (HR)	Monthly	1930-2004	75 yrs	12	0.438*
Fredericton (OP1)	Monthly	1930-2005	76 yrs	11	0.321*
Gagetown (SF)	Monthly	1928-2002	75 yrs	11	0.406*
Moncton (IM)	Monthly	1930-2005	76 yrs	8	0.373*
Alma (FP)	Monthly	1953-2002	50 yrs	11	0.520*
Nappan (FR)	Monthly	1930-2002	73 yrs	10	0.347*
Collegeville (KP)	Monthly	1930-2005	76 yrs	12	0.319*
Fredericton (OP2)	Monthly w/TRF	1918-2005	88 yrs	12	0.446*
Fredericton (OP3)	Monthly w/TRF &	1878-2005	128 yrs	11	0.543*

Table 5.6. The regression model variables included in the AICc optimum variable subset for each site. The prefix denotes whether a variable is positive (+) or negative (-), as well as temperature (T) or precipitation (P). The root denotes the month or combination of months contributing to the variable, or a non-monthly associated variable such as snow depth, Thaw/Refreeze Deep (TRF), or Atlantic Multidecadal Oscillation (AMO). The suffix denotes the year of occurrence of the specific variable where “a” = current year, “b” = 1st lagged year, and “c” = 2nd lagged year.

Charlo (BR)	Edmundston (QM)	Aroostook (KR)	Miramichi (HR)	Gagetown (SF)	Moncton (IM)
-T Jul b	+T Jul a	+P Jun b	-Snow Depth b	-T Aug b	-T OND c
+P Jun b	+T Sep b	+P Jun a	-T OND c	-T Mar a	-T Mar a
-T OND c	-Snow Depth b	+T Jul a	-T Jun c	-T Aug a	-P May b
-P Sep a	-T Apr a	-T Sep a	-Snow Depth a	+T Oct a	+Snow Depth c
-T Jan c	-P May a	+P Sep a	-Snow Depth c	+P Aug b	+T May a
+ T Jul a	+P Sep a	-T Apr b	-T May a	-T Jul b	-T Apr b
	+P Apr a	+Snow Depth c	+P Apr a	-T Jan b	+P Aug b
	-T Jul b		+P Jun a	+P Apr a	-T Feb a
	-Snow Depth c		-T Jun b	-P May a	
	-P Jul b		+T Jul a	-T Jun c	
			+T Jul b	-T Jun b	
			-T Aug b		
Alma (FP)	Nappan (FR)	Collegeville (KP)	Fredericton (OP1)	Fredericton (OP2)	Fredericton (OP3)
-T JAS c	-T Aug b	-P May b	+T Oct a	-TRF b	+ AMO
-T Apr a	-T Apr a	-T Aug b	-T Jun a	-TRF c	+P Aug a
-T Jul b	-P AMJ c	-P Jul a	-T Jun b	-TRF a	+P Jul b
+P Jul a	+P Jun b	+P Apr a	-P Jun b	+T Oct a	+P Aug b
+T Sep a	-T JASc	-P May a	+T OND c	+P Jun a	+Snow Depth c
-P Sep a	+T Jun b	+T Sep a	-T Apr b	+T OND b	+T Aug a
-T Apr c	-P May b	-T Jun b	-T Jun c	-T Jun b	-T May c
+P Jun b	-P Sep b	-P Aug b	-T Mar a	-Snow Depth b	+Snow Depth a
+T Oct a	+T Oct a	+P Apr b	-T Apr c	-T Jun a	+T Aug b
+T Mar b	-P May a	-T Feb c	-P May a	-T Feb b	-TRF b
-T Apr b		+T Jan a	+P Apr a	-T Jun c	-TRF c
		+T Sep b		-P May a	

Charlo (BR)

The regression model for this site used the Charlo climate data regressed against the Benjamin River sugar maple chronology. This six variable optimal-subset model explained 35% of variance using a climate record covering the period 1940-2005 (Table 5.5). Tables 5.6 and 5.7 both detail the variables included in the AICc selected best model. Model outputs for the two SRES scenarios are visually illustrated in Fig. 5.5 and Fig. 5.6. The forecast for the SRES B1 scenario depicts an approximate 30% radial growth reduction by the end of the 21st century (Fig. 5.5). Alternatively the forecast for the SRES A1b scenario plots an estimated 50% reduction in radial growth by the year 2100 (Fig 5.6).

Table 5.7. The regression model variables from the best subset model representing the Charlo climate data regressed against the Benjamin River sugar maple chronology are illustrated. The monthly variables used in this regression model are represented in the Table by: white = positive variable association, black = negative variable association, gray = variable not included in this model.

BR	2 nd Year Lag												1 st Year Lag												Current Year											
Month	J	F	M	A	M	J	J	A	S	O	N	D	J	F	M	A	M	J	J	A	S	O	N	D	J	F	M	A	M	J	J	A	S	O	N	D
Temp	█									█	█	█																								
Precip																																				

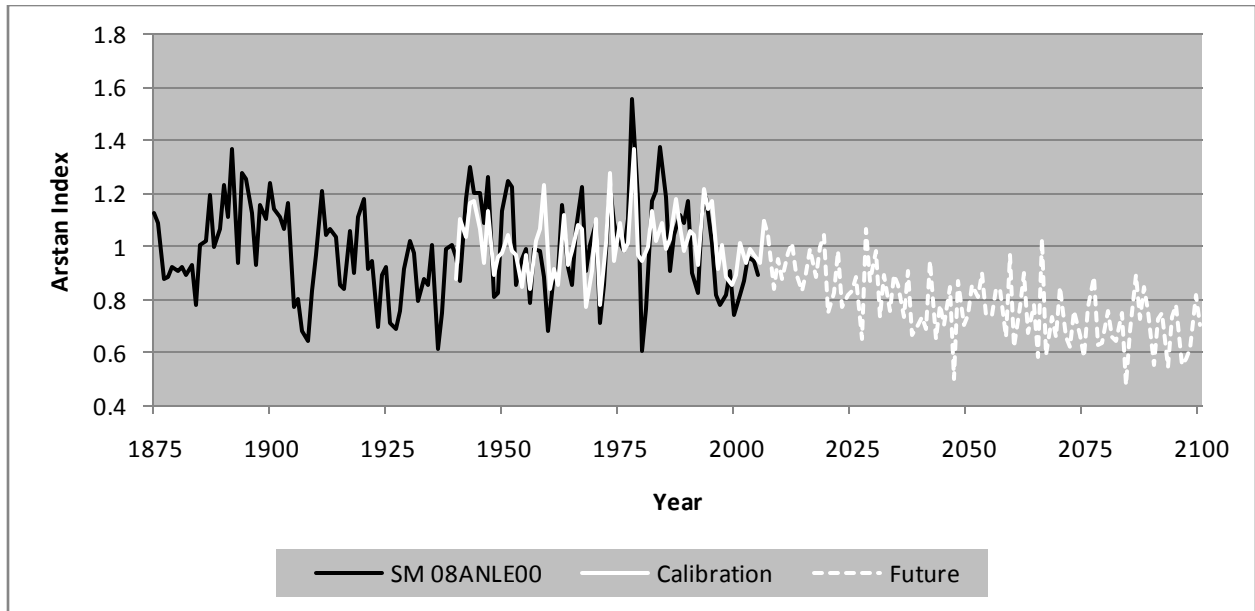


Figure 5.5. The regression model defined in this Figure used climate data from Charlo and the sugar maple chronology from Benjamin River (BR). The black line illustrates the historic sugar maple radial growth curve for BR (Chronology MAD Lab code = 08ANLE00). The unbroken white line details the model calibration period. The broken white line estimates the future growth response of sugar maple using the SRES B1 scenario.

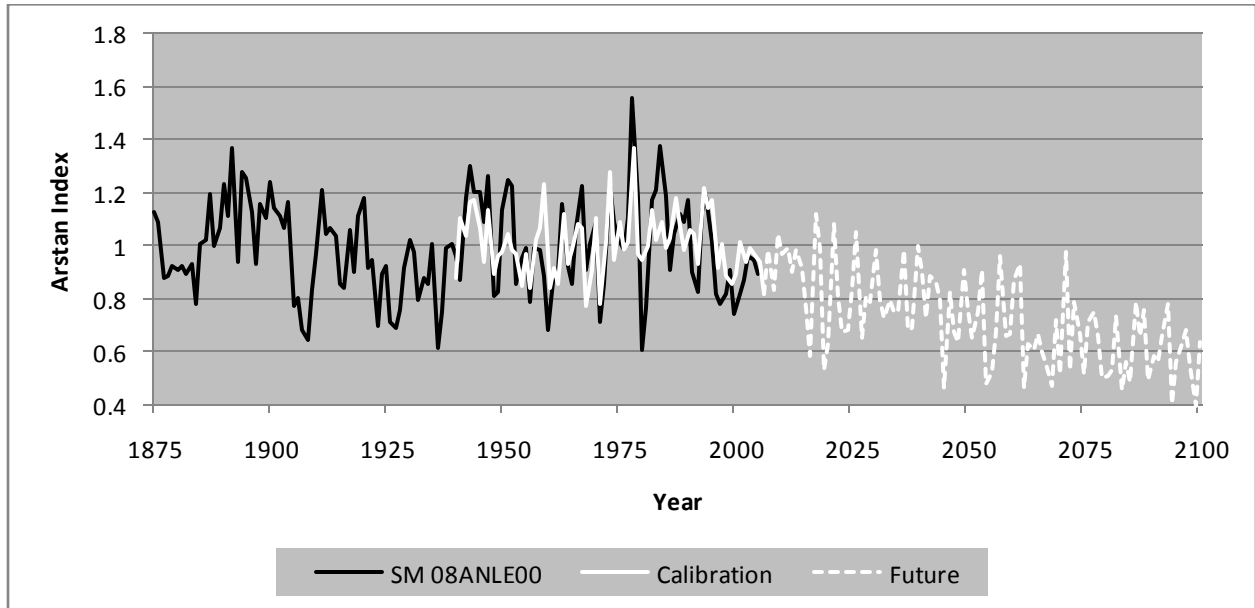


Figure 5.6. The regression model defined in this Figure used climate data from Charlo and the sugar maple chronology from Benjamin River (BR). The black line illustrates the historic sugar maple radial growth curve for BR (Chronology MAD Lab code = 08ANLE00). The unbroken white line details the model calibration period. The broken white line estimates the future growth response of sugar maple using the SRES A1b scenario.

Edmundston (QM)

The regression model for this site used the Edmundston climate data regressed against the Quisibis Mountain sugar maple chronology. This 10 variable optimal subset model explained 54% of variance using a climate record covering the period 1936-2003 (Table 5.5). Tables 5.6 and 5.8 both detail the variables included in the AICc selected best model. Model outputs for the two SRES scenarios are visually illustrated below in Fig. 5.7 and Fig. 5.8. The forecast for the SRES B1 scenario depicts no change radial growth rates by the end of the 21st century (Fig. 5.7). Alternatively the forecast for the SRES A1b scenario plots an estimated 10% increase in radial growth by the year 2100 (Fig 5.8).

Table 5.8. The regression model variables from the best subset model representing the Edmundston climate data regressed against the Quisibis Mountain sugar maple chronology are illustrated. The monthly variables used in this regression model are represented in the Table by: white = positive variable association, black = negative variable association, gray = variable not included in this model.

QM	2 nd Year Lag										1 st Year Lag										Current Year															
Month	J	F	M	A	M	J	J	A	S	O	N	D	J	F	M	A	M	J	J	A	S	O	N	D	J	F	M	A	M	J	J	A	S	O	N	D
Temp																																				
Precip																																				

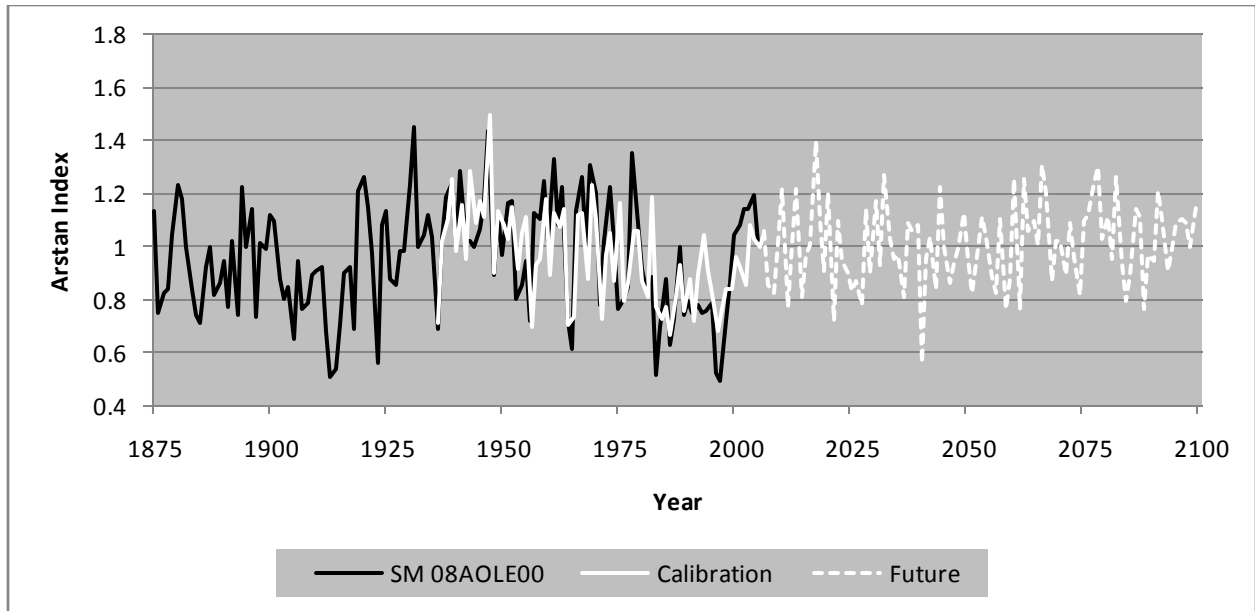


Figure 5.7. The regression model defined in this Figure used climate data from Edmunston and the sugar maple chronology from Quisibis Mountain. The black line illustrates the historic sugar maple radial growth curve for QM (Chronology MAD Lab code = 08AOLE00). The unbroken white line details the model calibration period. The broken white line estimates the future growth response of sugar maple using the SRES B1 scenario.

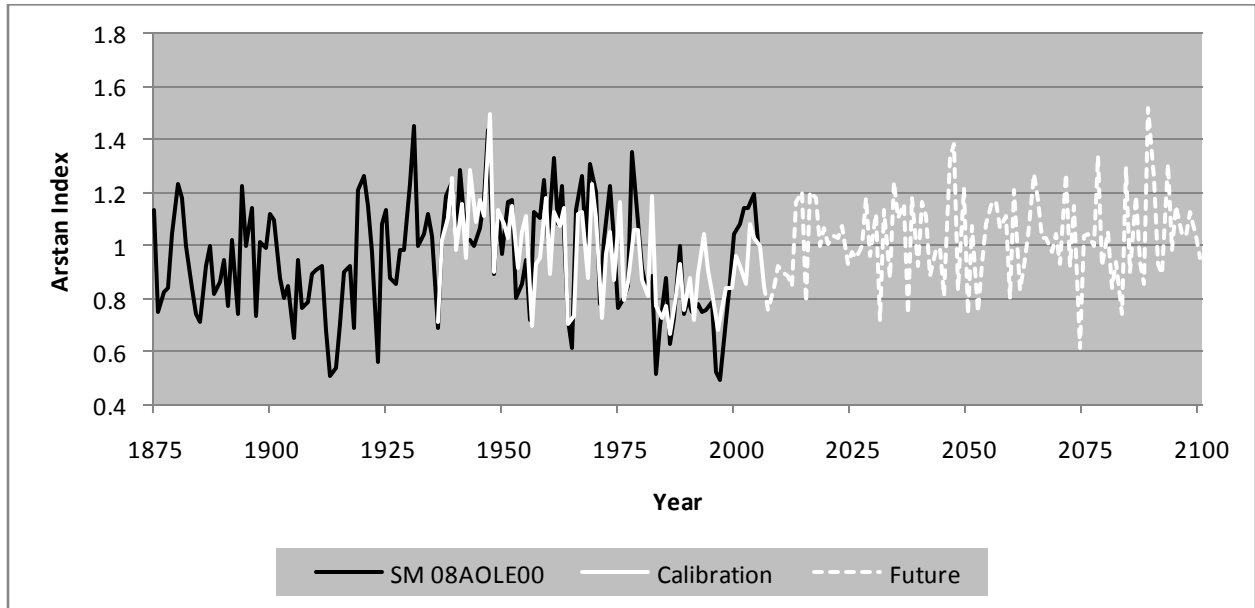


Figure 5.8. The regression model defined in this Figure used climate data from Edmunston and the sugar maple chronology from Quisibis Mountain. The black line illustrates the historic sugar maple radial growth curve for QM (Chronology MAD Lab code = 08AOLE00). The unbroken white line details the model calibration period. The broken white line estimates the future growth response of sugar maple using the SRES A1b scenario.

Aroostook (KR)

The regression model for this site used the Aroostook climate data regressed against the Kintore Ridge sugar maple chronology. This seven-variable optimal subset model explained 24% of variance using a climate record covering the period 1932-2004 (Table 5.5). Tables 5.6 and 5.9 both detail the variables included in the AICc selected best model. Model outputs for the two SRES scenarios are visually illustrated below in Fig. 5.9 and in Fig. 5.10. The forecast for the SRES B1 scenario depicts an approximate 20% radial growth reduction by the end of the 21st century (Fig. 5.9). Also, the forecast for the SRES A1b scenario plots an estimated 20% reduction in radial growth by the year 2100 (Fig 5.10).

Table 5.9. The regression model variables from the best subset model representing the Aroostook climate data regressed against the Kintore Ridge sugar maple chronology are illustrated. The monthly variables used in this regression model are represented in the Table by: white = positive variable association, black = negative variable association, gray = variable not included in this model.

KR	2 nd Year Lag										1 st Year Lag										Current Year															
Month	J	F	M	A	M	J	J	A	S	O	N	D	J	F	M	A	M	J	J	A	S	O	N	D	J	F	M	A	M	J	J	A	S	O	N	D
Temp																																				
Precip																																				

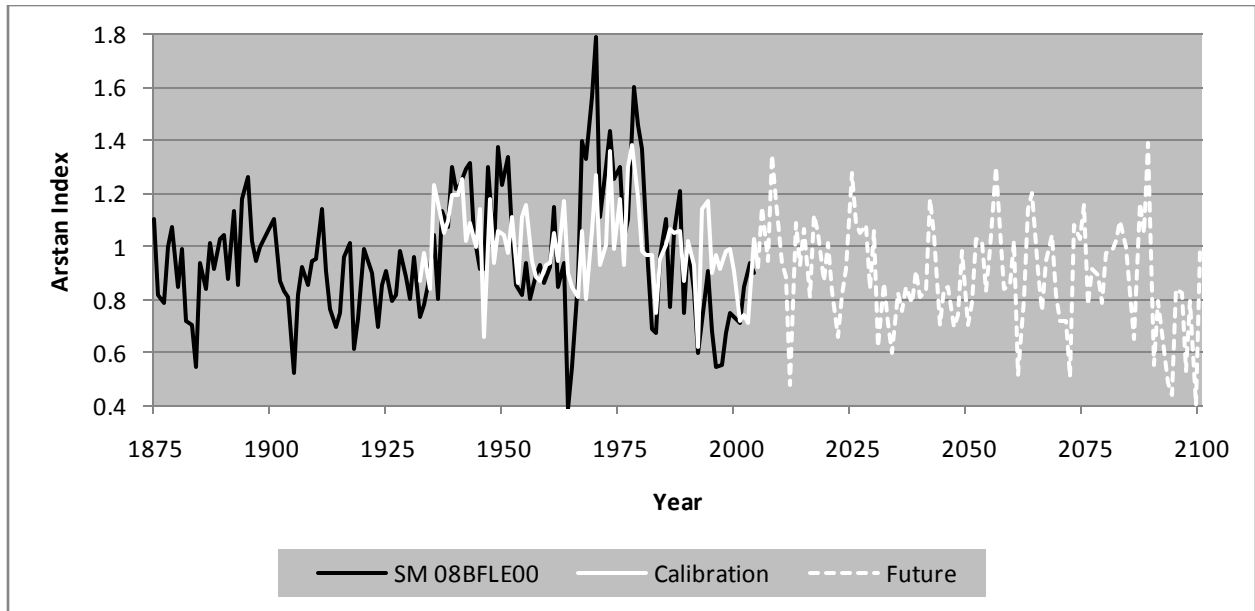


Figure 5.9. The regression model defined in this Figure used climate data from Aroostook and the sugar maple chronology from Kintore Ridge. The black line illustrates the historic sugar maple radial growth curve for KR (Chronology MAD Lab code = 08BFLE00). The unbroken white line details the model calibration period. The broken white line estimates the future growth response of sugar maple using the SRES B1 scenario.

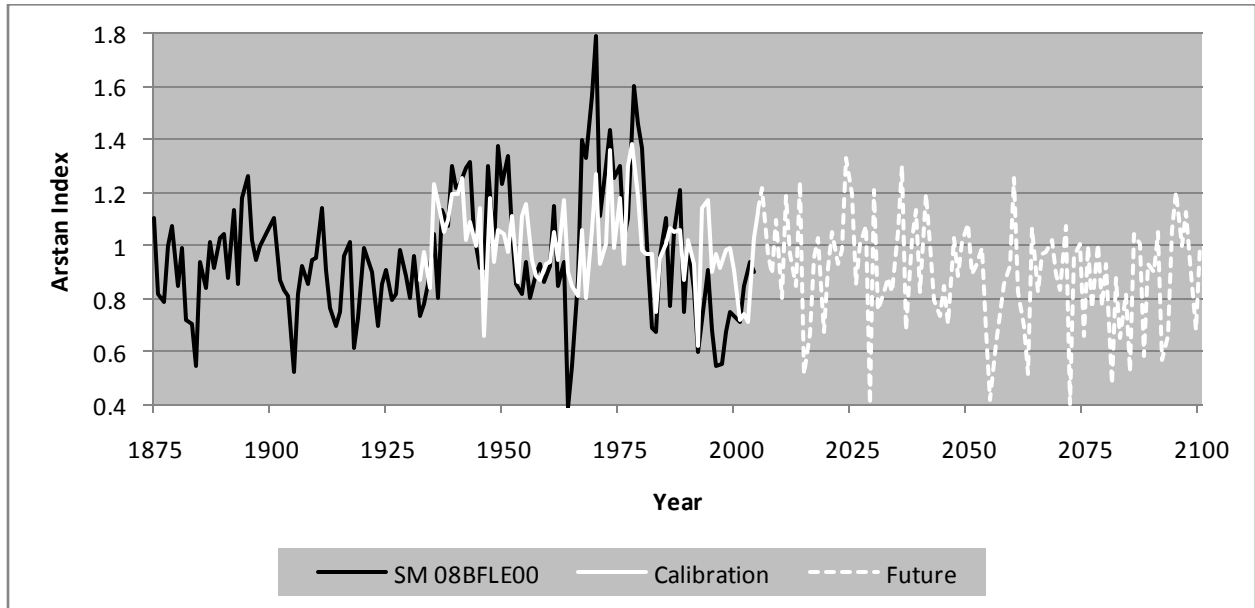


Figure 5.10. The regression model defined in this Figure used climate data from Aroostook and the sugar maple chronology from Kintore Ridge. The black line illustrates the historic sugar maple radial growth curve for KR (Chronology MAD Lab code = 08BFLE00). The unbroken white line details the model calibration period. The broken white line estimates the future growth response of sugar maple using the SRES A1b scenario.

Miramichi HR

The regression model for this site used the Miramichi climate data regressed against the Horseshoe Ridge sugar maple chronology. This 12-variable optimal subset model explained 44% of variance using a climate record covering the period 1930-2005 (Table 5.5). Tables 5.6 and 5.10 both detail the variables included in the AICc selected best model. Model outputs for the two SRES scenarios are visually illustrated below in Fig. 5.11 and Fig. 5.12. The forecast for the SRES B1 scenario depicts an approximate 50% radial growth reduction by the end of the 21st century (Fig. 5.11). Alternatively the forecast for the SRES A1b scenario plots an estimated 60% reduction in radial growth by the year 2100 (Fig 5.12).

Table 5.10. The regression model variables from the best subset model representing the Miramichi climate data regressed against the Horseshoe Ridge sugar maple chronology are illustrated. The monthly variables used in this regression model are represented in the Table by: white = positive variable association, black = negative variable association, gray = variable not included in this model.

HR	2 nd Year Lag												1 st Year Lag												Current Year											
Month	J	F	M	A	M	J	J	A	S	O	N	D	J	F	M	A	M	J	J	A	S	O	N	D	J	F	M	A	M	J	J	A	S	O	N	D
Temp																																				
Precip																																				

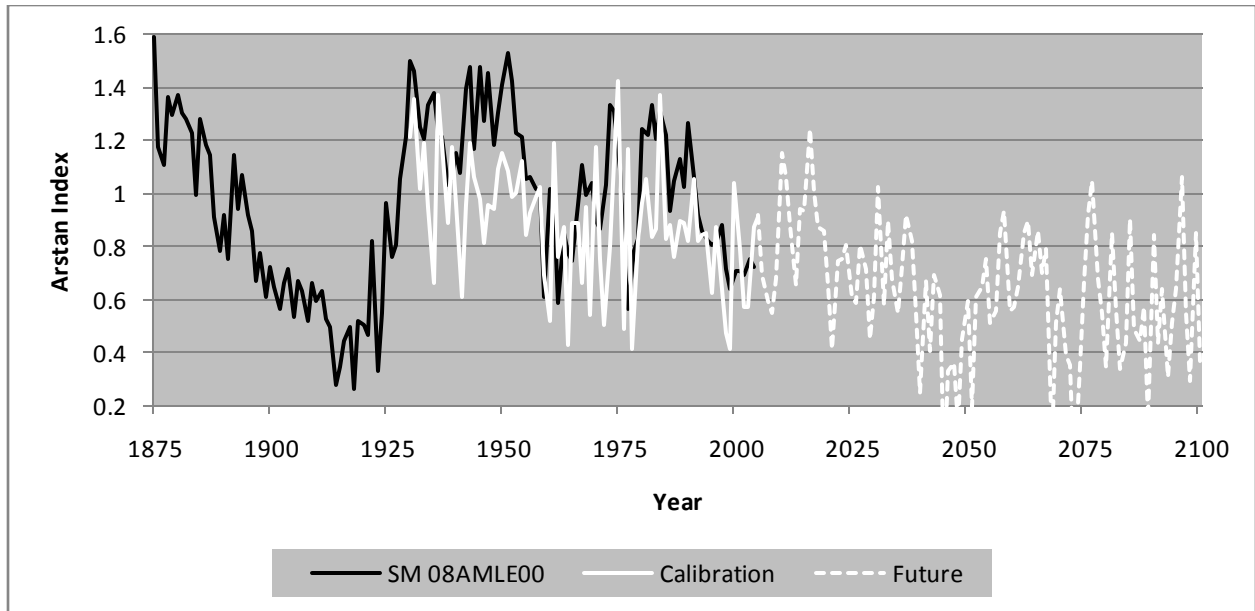


Figure 5.11. The regression model defined in this Figure used climate data from Miramichi and the sugar maple chronology from Horseshoe Ridge. The black line illustrates the historic sugar maple radial growth curve for HR (Chronology MAD Lab code = 08AMLE00). The unbroken white line details the model calibration period. The broken white line estimates the future growth response of sugar maple using the SRES B1 scenario.

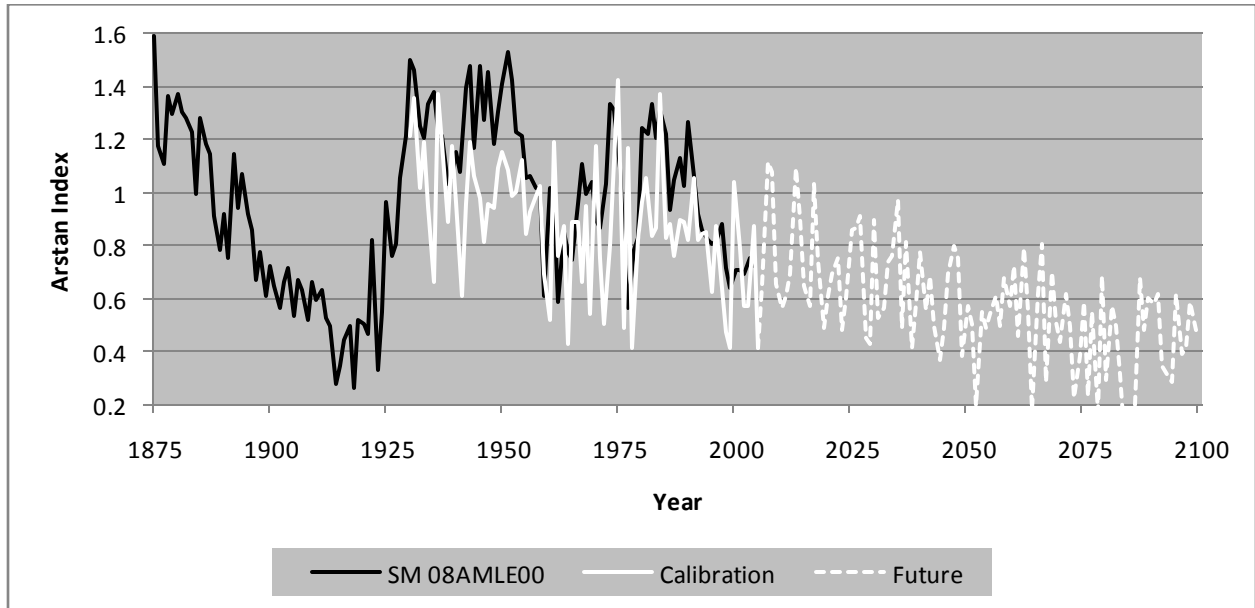


Figure 5.12. The regression model defined in this Figure used climate data from Miramichi and the sugar maple chronology from Horseshoe Ridge. The black line illustrates the historic sugar maple radial growth curve for HR (Chronology MAD Lab code = 08AMLE00). The unbroken white line details the model calibration period. The broken white line estimates the future growth response of sugar maple using the SRES A1b scenario.

Fredericton (OP1)

The regression model for this site used the Fredericton climate data regressed against the Odell Park sugar maple chronology. This 11-variable optimal subset model explained 32% of variance using a climate record covering the period 1930-2005 (Table 5.5). Tables 5.6 and 5.11 both detail the variables included in the AICc selected best model. Model outputs for the two SRES scenarios are visually illustrated below in Fig. 5.13 and Fig. 5.14. The forecast for the SRES B1 scenario depicts an approximate 90% radial growth reduction by the end of the 21st century (Fig. 5.13). Alternatively the forecast for the SRES A1b scenario plots an estimated 100% reduction in radial growth by the year 2100 (Fig 5.14).

Table 5.11. The regression model variables from the best subset model representing the Fredericton climate data regressed against the Odell Park sugar maple chronology are illustrated. The monthly variables used in this regression model are represented in the Table by: white = positive variable association, black = negative variable association, gray = variable not included in this model.

OP1	2 nd Year Lag										1 st Year Lag										Current Year															
Month	J	F	M	A	M	J	J	A	S	O	N	D	J	F	M	A	M	J	J	A	S	O	N	D	J	F	M	A	M	J	J	A	S	O	N	D
Temp																																				
Precip																																				

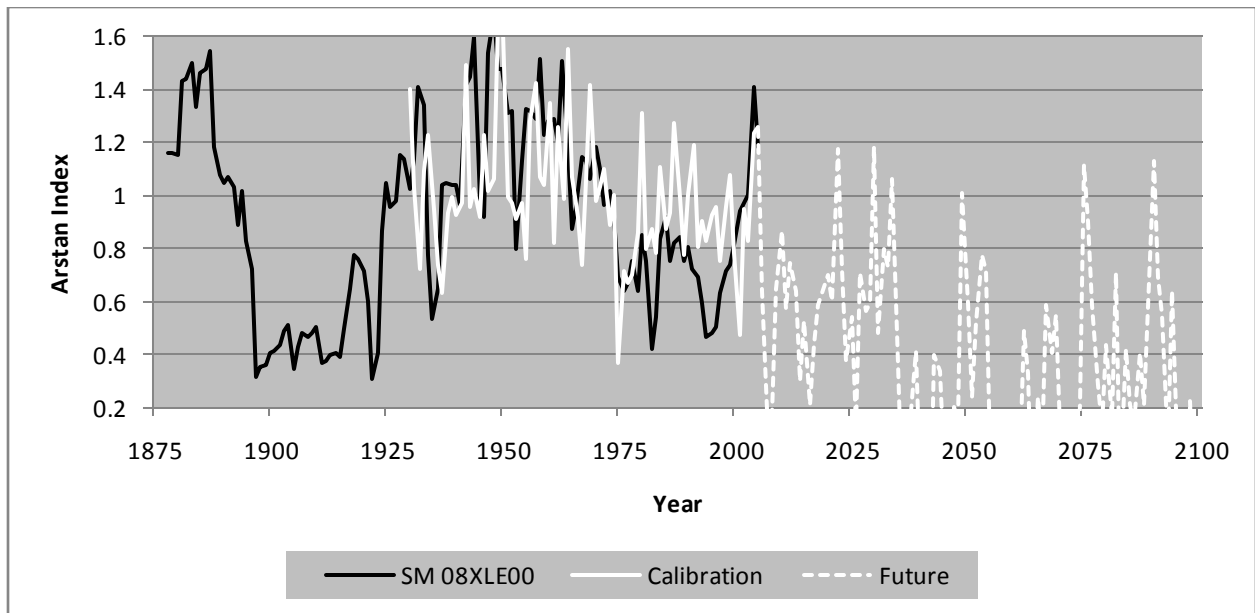


Figure 5.13. The regression model defined in this Figure used climate data from Fredericton and the sugar maple chronology from Odell Park. The black line illustrates the historic sugar maple radial growth curve for OP (Chronology MAD Lab code = 08XLE00). The unbroken white line details the model calibration period. The broken white line estimates the future growth response of sugar maple using the SRES B1 scenario.

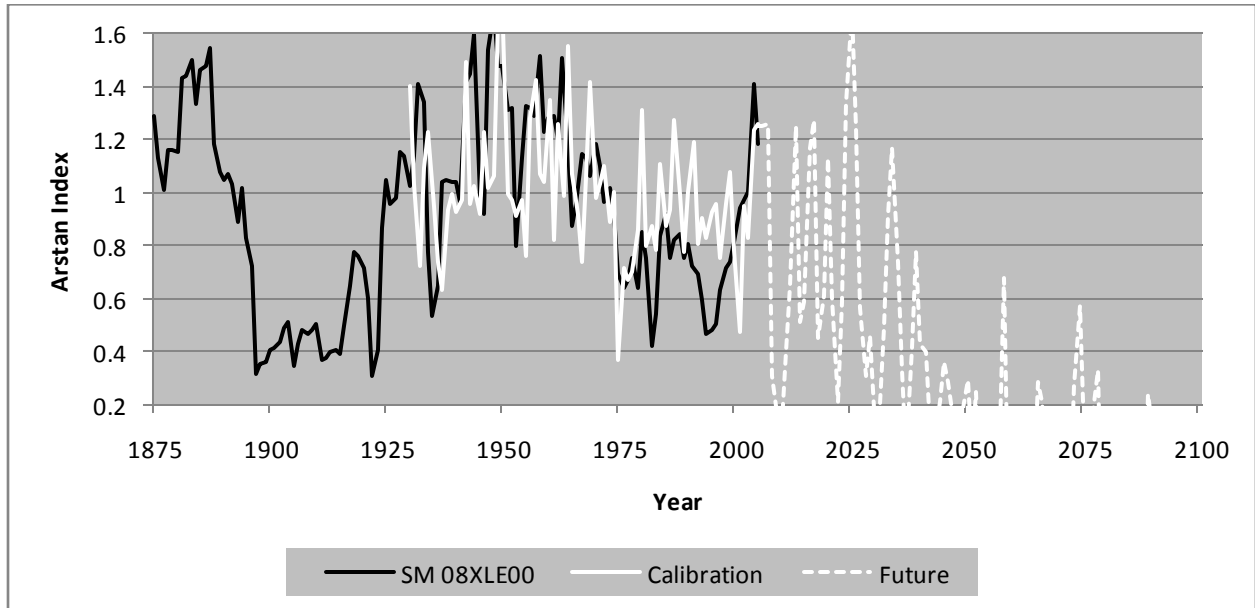


Figure 5.14. The regression model defined in this Figure used climate data from Fredericton and the sugar maple chronology from Odell Park. The black line illustrates the historic sugar maple radial growth curve for OP (Chronology MAD Lab code = 08XLE00). The unbroken white line details the model calibration period. The broken white line estimates the future growth response of sugar maple using the SRES A1b scenario.

Gagetown (SF)

The regression model for this site used the Gagetown climate data regressed against the Slipp Farm sugar maple chronology. This ten-variable optimal subset model explained 41% of variance using a climate record covering the period 1928-2002 (Table 5.5). Tables 5.6 and 5.12 both detail the variables included in the AICc selected best model. Model outputs for the two SRES scenarios are visually illustrated below in Fig. 5.15 and Fig. 5.16. The forecast for the SRES B1 scenario depicts an approximate 80% radial growth reduction by the end of the 21st century (Fig. 5.15). Alternatively the forecast for the SRES A1b scenario plots an estimated 100% reduction in radial growth by the year 2100 (Fig 5.16).

Table 5.12. The regression model variables from the best subset model representing the Gagetown climate data regressed against the Slipp Farm sugar maple chronology are illustrated. The monthly variables used in this regression model are represented in the Table by: white = positive variable association, black = negative variable association, gray = variable not included in this model.

SF	2 nd Year Lag										1 st Year Lag										Current Year														
	J	F	M	A	M	J	J	A	S	O	N	D	J	F	M	A	M	J	J	A	S	O	N	D	J	F	M	A	M	J	J	A	S	O	N
Temp																																			
Precip																																			

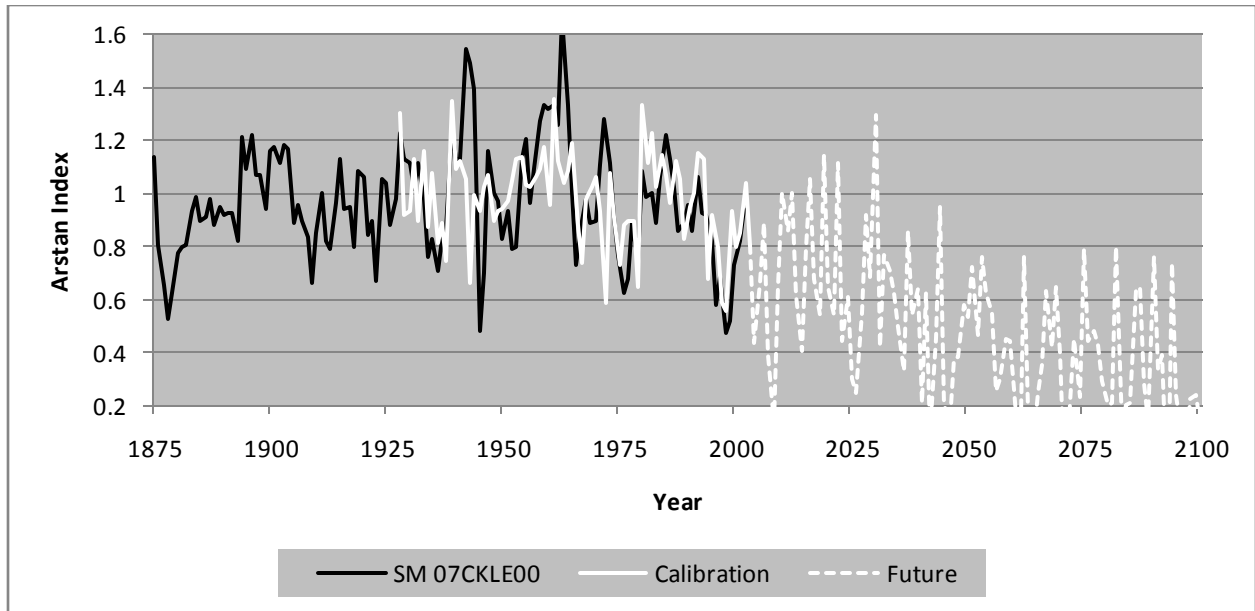


Figure 5.15. The regression model defined in this Figure used climate data from Gagetown and the sugar maple chronology from Slipp Farm. The black line illustrates the historic sugar maple radial growth curve for SF (Chronology MAD Lab code = 07CKLE00). The unbroken white line details the model calibration period. The broken white line estimates the future growth response of sugar maple using the SRES B1 scenario.

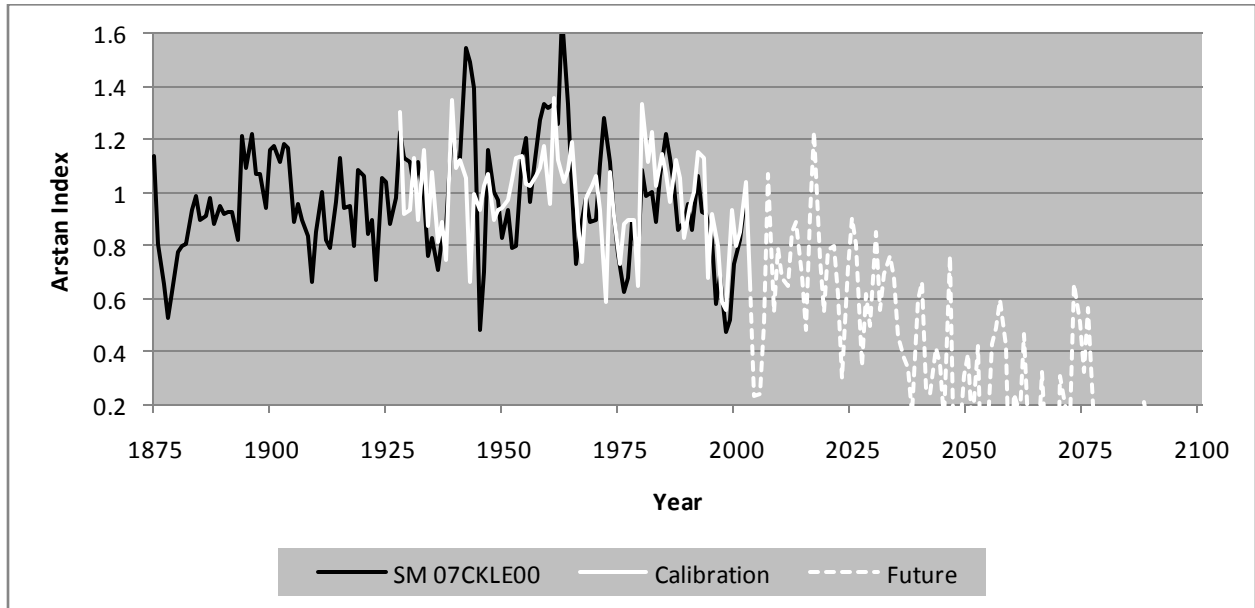


Figure 5.16. The regression model defined in this Figure used climate data from Gagetown and the sugar maple chronology from Slipp Farm. The black line illustrates the historic sugar maple radial growth curve for SF (Chronology MAD Lab code = 07CKLE00). The unbroken white line details the model calibration period. The broken white line estimates the future growth response of sugar maple using the SRES A1b scenario.

Moncton (IM)

The regression model for this site used the Moncton climate data regressed against the Indian Mountain sugar maple chronology. This eight-variable optimal subset model explained 37% of variance using a climate record covering the period 1930-2005 (Table 5.5). Tables 5.6 and 5.13 both detail the variables included in the AICc selected best model. Model outputs for the two SRES scenarios are visually illustrated below in Fig. 5.17 and Fig. 5.18. The forecast for the SRES B1 scenario depicts an approximate 50% radial growth reduction by the end of the 21st century (Fig. 5.17). Alternatively the forecast for the SRES A1b scenario plots an estimated 70% reduction in radial growth by the year 2100 (Fig 5.18).

Table 5.13. The regression model variables from the best subset model representing the Moncton climate data regressed against the Indian Mountain sugar maple chronology are illustrated. The monthly variables used in this regression model are represented in the Table by: white = positive variable association, black = negative variable association, gray = variable not included in this model.

IM	2 nd Year Lag												1 st Year Lag												Current Year											
Month	J	F	M	A	M	J	J	A	S	O	N	D	J	F	M	A	M	J	J	A	S	O	N	D	J	F	M	A	M	J	J	A	S	O	N	D
Temp																																				
Precip																																				

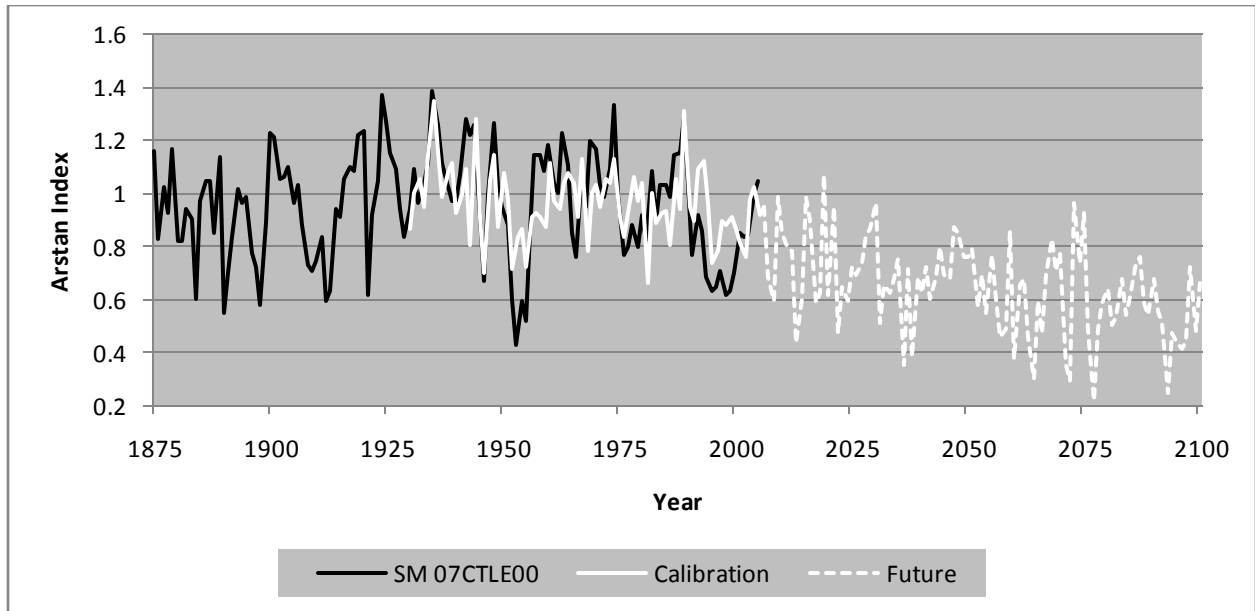


Figure 5.17. The regression model defined in this Figure used climate data from Moncton and the sugar maple chronology from Indian Mountain. The black line illustrates the historic sugar maple radial growth curve for IM (Chronology MAD Lab code = 07CTLE00). The unbroken white line details the model calibration period. The broken white line estimates the future growth response of sugar maple using the SRES B1 scenario.

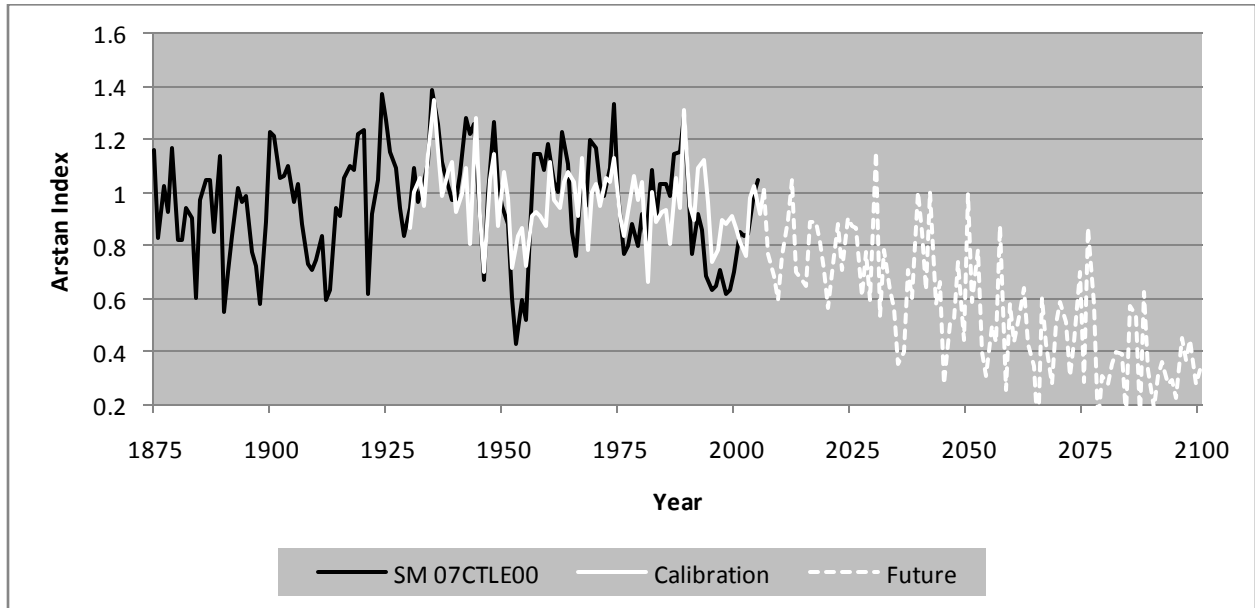


Figure 5.18. The regression model defined in this Figure used climate data from Moncton and the sugar maple chronology from Indian Mountain. The black line illustrates the historic sugar maple radial growth curve for IM (Chronology MAD Lab code = 07CTLE00). The unbroken white line details the model calibration period. The broken white line estimates the future growth response of sugar maple using the SRES A1b scenario.

Alma (FP)

The regression model for this site used the Fundy climate data regressed against the Fundy Park sugar maple chronology. This 11-variable optimal subset model explained 52% of variance using a climate record covering the period 1953-2005 (Table 5.5). Tables 5.6 and 5.14 both detail the variables included in the AICc selected best model. Model outputs for the two SRES scenarios are visually illustrated below in Fig. 5.19 and Fig. 5.20. The forecast for the SRES B1 scenario depicts an approximate 100% radial growth reduction by the end of the 21st century (Fig. 5.19). Also the forecast for the SRES A1b scenario plots an estimated 100% reduction in radial growth by the year 2100 (Fig 5.20).

Table 5.14. The regression model variables from the best subset model representing the Alma climate data regressed against the Fundy Park sugar maple chronology are illustrated. The monthly variables used in this regression model are represented in the Table by: white = positive variable association, black = negative variable association, gray = variable not included in this model.

FP	2 nd Year Lag												1 st Year Lag												Current Year											
Month	J	F	M	A	M	J	J	A	S	O	N	D	J	F	M	A	M	J	J	A	S	O	N	D	J	F	M	A	M	J	J	A	S	O	N	D
Temp				█			█	█	█								█		█								█									
Precip																																				

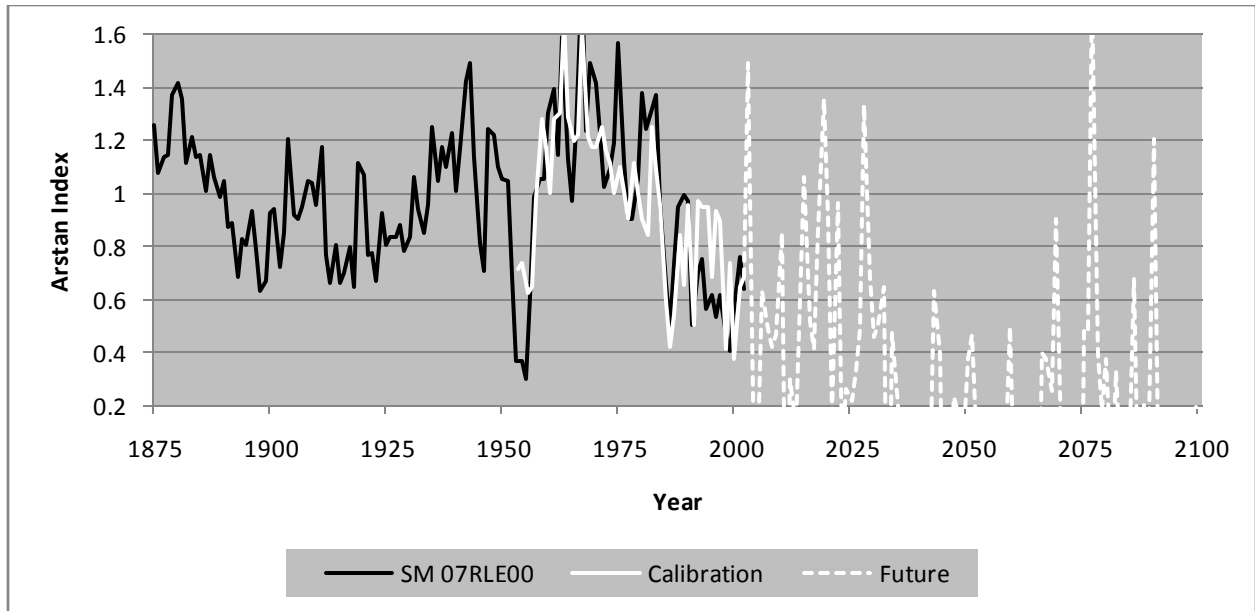


Figure 5.19. The regression model defined in this Figure used climate data from Alma and the sugar maple chronology from Fundy Park. The black line illustrates the historic sugar maple radial growth curve for FP (Chronology MAD Lab code = 07RLE00). The unbroken white line details the model calibration period. The broken white line estimates the future growth response of sugar maple using the SRES B1 scenario.

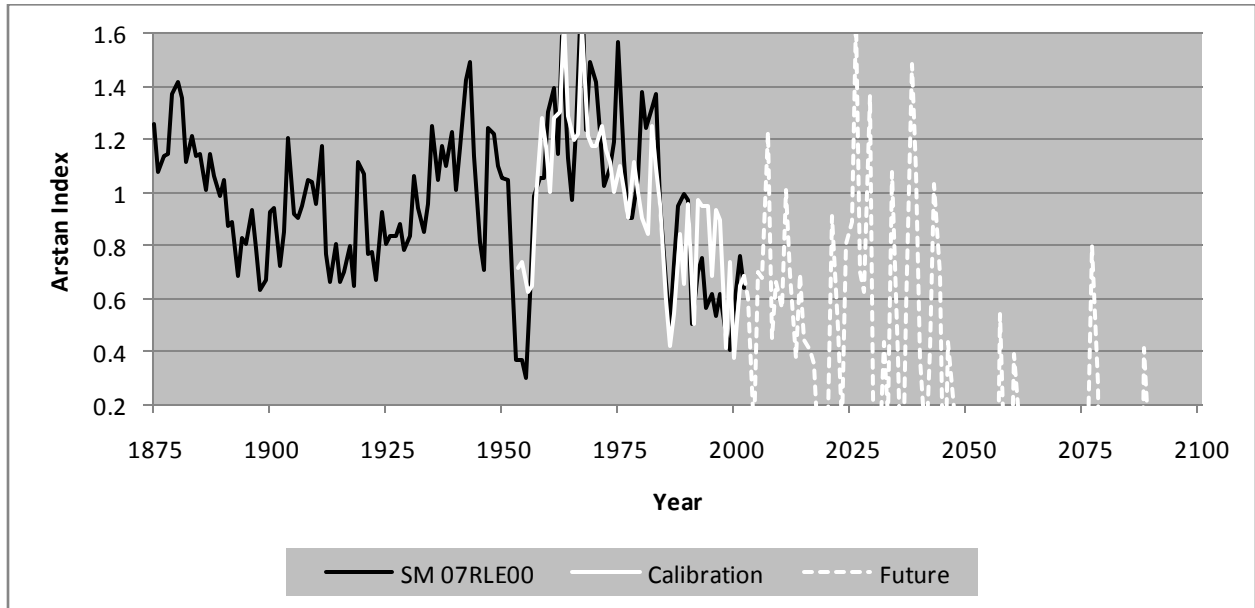


Figure 5.20. The regression model defined in this Figure used climate data from Alma and the sugar maple chronology from Fundy Park. The black line illustrates the historic sugar maple radial growth curve for FP (Chronology MAD Lab code = 07RLE00). The unbroken white line details the model calibration period. The broken white line estimates the future growth response of sugar maple using the SRES A1b scenario.

Nappan (FR)

The regression model for this site used the Nappan climate data regressed against the Fenwick Ridge sugar maple chronology. This 10-variable optimal subset model explained 35% of variance using a climate record covering the period 1930-2002 (Table 5.5). Tables 5.6 and 5.15 both detail the variables included in the AICc selected best model. Model outputs for the two SRES scenarios are visually illustrated below in Fig. 5.21 and Fig. 5.22. The forecast for the SRES B1 scenario depicts an approximate 50% radial growth reduction by the end of the 21st century (Fig. 5.21). Also the forecast for the SRES A1b scenario plots an estimated 90% reduction in radial growth by the year 2100 (Fig 5.22).

Table 5.15. The regression model variables from the best subset model representing the Nappan climate data regressed against the Fenwick Ridge sugar maple chronology are illustrated. The monthly variables used in this regression model are represented in the Table by: white = positive variable association, black = negative variable association, gray = variable not included in this model.

FR	2 nd Year Lag												1 st Year Lag												Current Year											
Month	J	F	M	A	M	J	J	A	S	O	N	D	J	F	M	A	M	J	J	A	S	O	N	D	J	F	M	A	M	J	J	A	S	O	N	D
Temp																																				
Precip																																				

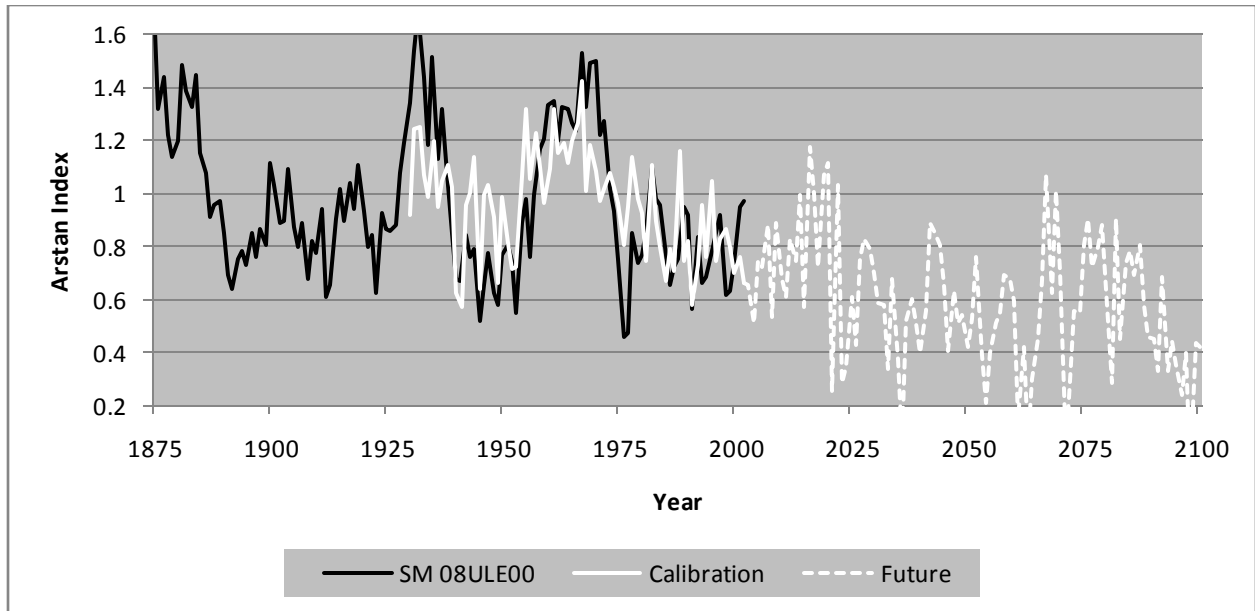


Figure 5.21. The regression model defined in this Figure used climate data from Nappan and the sugar maple chronology from Fenwick Ridge. The black line illustrates the historic sugar maple radial growth curve for FR (Chronology MAD Lab code = 08ULE00). The unbroken white line details the model calibration period. The broken white line estimates the future growth response of sugar maple using the SRES B1 scenario.

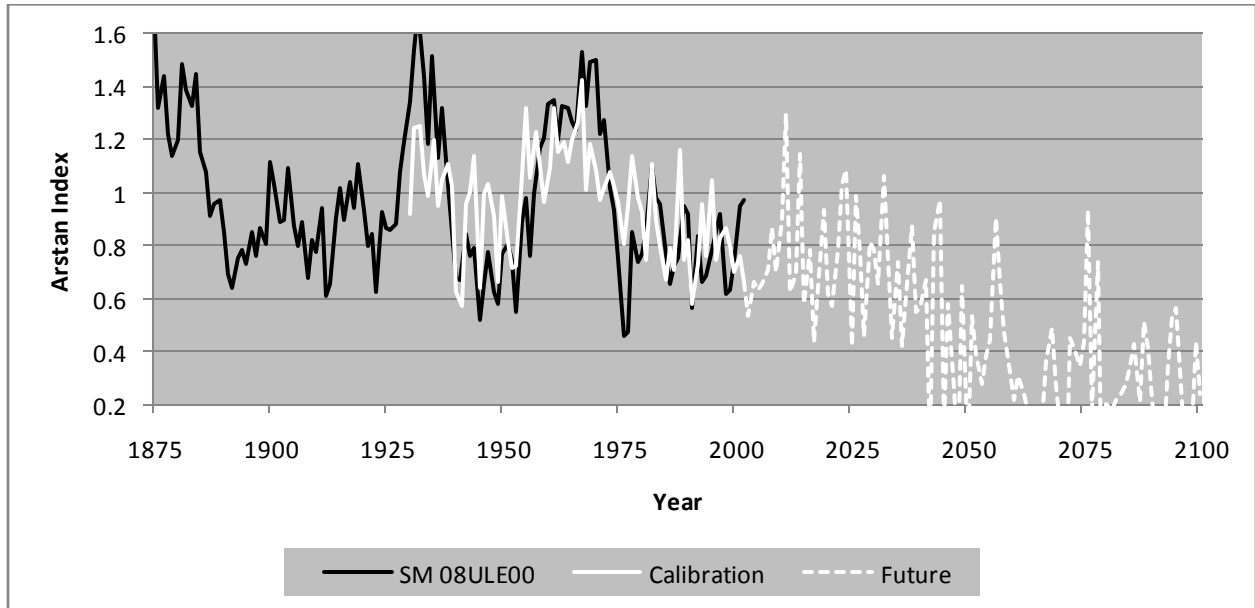


Figure 5.22. The regression model defined in this Figure used climate data from Nappan and the sugar maple chronology from Fenwick Ridge. The black line illustrates the historic sugar maple radial growth curve for FR (Chronology MAD Lab code = 08ULE00). The unbroken white line details the model calibration period. The broken white line estimates the future growth response of sugar maple using the SRES A1b scenario.

Collegeville (KP)

The regression model for this site used the Collegeville climate data regressed against the Keppoch Plateau sugar maple chronology. This 12-variable optimal subset model explained 32% of variance using a climate record covering the period 1930-2005 (Table 5.5). Tables 5.6 and 5.16 both detail the variables included in the AICc selected best model. Model outputs for the two SRES scenarios are visually illustrated below in Fig. 5.23 and Fig. 5.24. The forecast for the SRES B1 scenario depicts no change in radial growth by the end of the 21st century (Fig. 5.23). Alternatively the forecast for the SRES A1b scenario plots an estimated 20% reduction in radial growth by the year 2100 (Fig 5.24).

Table 5.16. The regression model variables from the best subset model representing the Collegeville climate data regressed against the Keppoch Plateau sugar maple chronology are illustrated. The monthly variables used in this regression model are represented in the Table by: white = positive variable association, black = negative variable association, gray = variable not included in this model.

KP	2 nd Year Lag												1 st Year Lag												Current Year											
	J	F	M	A	M	J	J	A	S	O	N	D	J	F	M	A	M	J	J	A	S	O	N	D	J	F	M	A	M	J	J	A	S	O	N	D
Temp		█															█	█		█																
Precip																		█																		

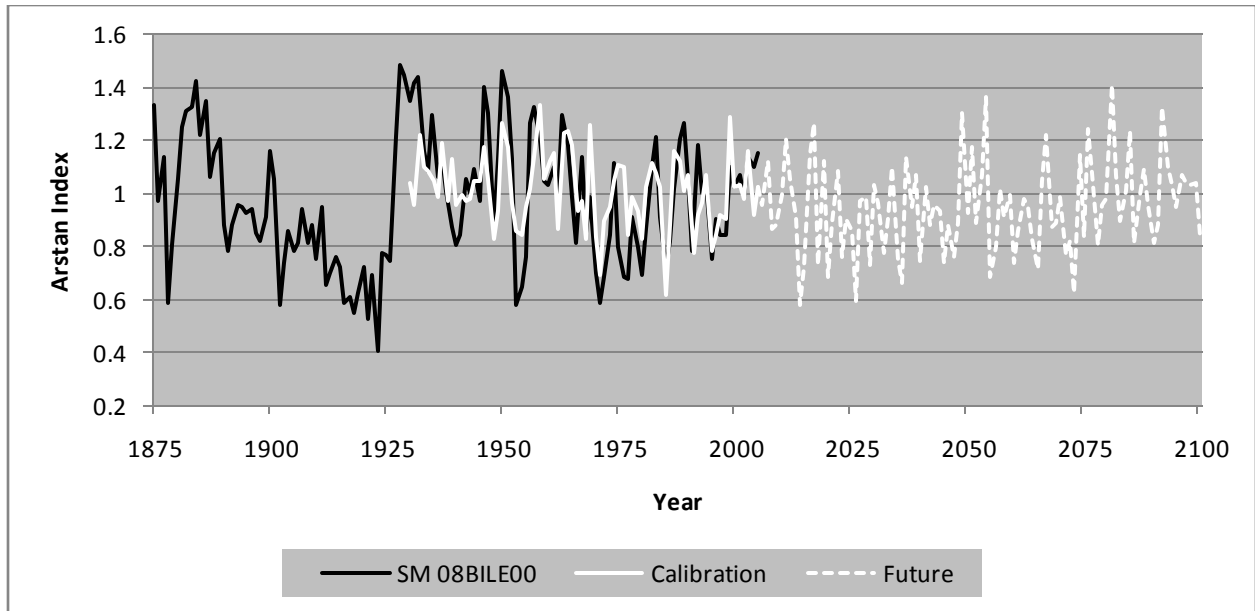


Figure 5.23. The regression model defined in this Figure used climate data from Collegeville and the sugar maple chronology from Keppoch Plateau. The black line illustrates the historic sugar maple radial growth curve for KP (Chronology MAD Lab code = 08BILE00). The unbroken white line details the model calibration period. The broken white line estimates the future growth response of sugar maple using the SRES B1 scenario.

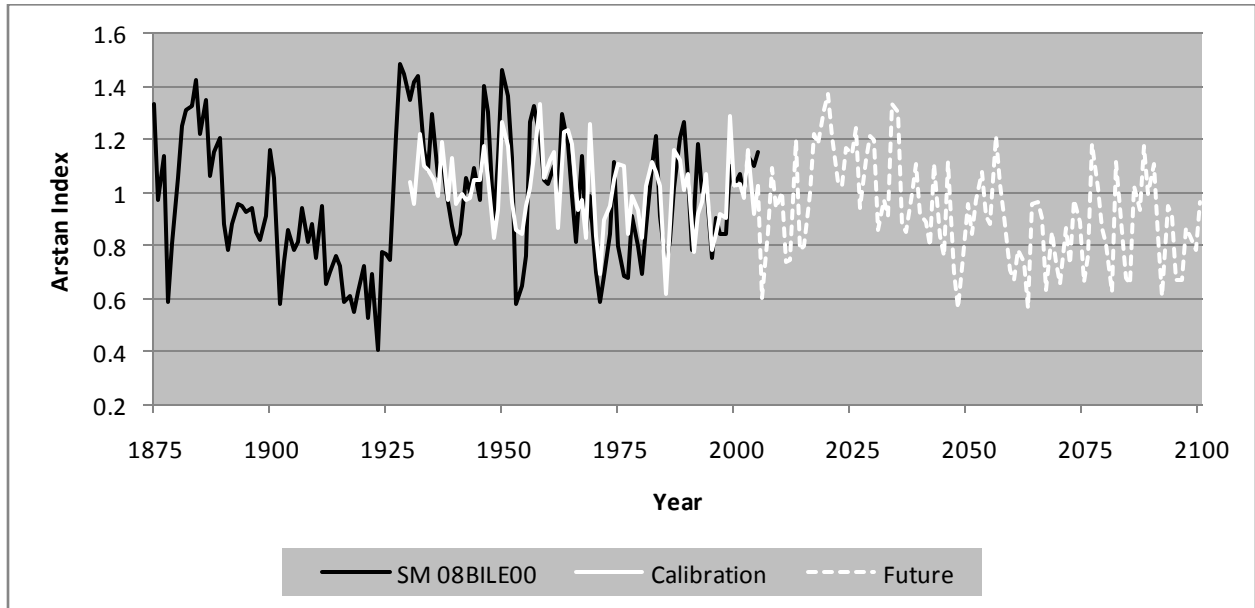


Figure 5.24. The regression model defined in this Figure used climate data from Collegeville and the sugar maple chronology from Keppoch Plateau. The black line illustrates the historic sugar maple radial growth curve for KP (Chronology MAD Lab code = 08BILE00). The unbroken white line details the model calibration period. The broken white line estimates the future growth response of sugar maple using the SRES A1b scenario.

Fredericton (OP2)

The Fredericton OP2 regression model used the Fredericton climate data regressed against the Odell Park sugar maple chronology. This is a supplementary model meant to test the TRF Deep variable. The April temperature variable was removed in the current year, as well as both of the lagged years from the MMT variable set. They were then replaced with the TRF Deep variables from the DCT variable set. The AICc selected 12-variable model, explains 45% of variance using climate data covering the period 1918-2005 (Table 5.5). Although a longer time period is calibrated in this model, it results in a 13% increase in explained variance as the selected best subset model included the TRF Deep variable from current year, 1st year lag, and 2nd year lag as the top three variables (Tables 5.6 and 5.17). The TRF Deep variables aid the model in achieving an increased descriptive capacity regarding the radial growth suppression periods which was not evident in the original Fredericton OP1 model. However, it is not possible with the Fredericton OP2 regression model to forecast future growth as there is currently no reliable future forecast of the TRF Deep variable. Therefore, only the past radial growth and model calibration period is presented (Fig. 5.25). Of note in Figure 5.25 are the thaw/refreeze events defined by the TRF Deep variable. The thaw/refreeze events are normally followed by large growth reduction periods lasting several years before normal sugar maple radial growth resumes (Fig. 5.25). Several thaw/refreeze events do not correspond to radial growth reductions, a situation also observed by Auclair et al. (1996) in relation to decreasing sugar maple dieback during a portion of the identified freeze and drought events in other areas of the sugar maple range.

Table 5.17. The regression model variables from the best subset model representing the Fredericton climate data regressed against the Odell Park sugar maple chronology are illustrated. The monthly variables used in this regression model are represented in the Table by: white = positive variable association, black = negative variable association, gray = variable not included in this model. The April temperature variable has been replaced in current year, 1st lagged year, and 2nd lagged year, with the TRF Deep variable symbolized as: * = TRF Deep.

OP2	2 nd Year Lag												1 st Year Lag												Current Year											
Month	J	F	M*	M	J	J	A	S	O	N	D	J	F	M*	M	J	J	A	S	O	N	D	J	F	M*	M	J	J	A	S	O	N	D			
Temp																																				
Precip																																				

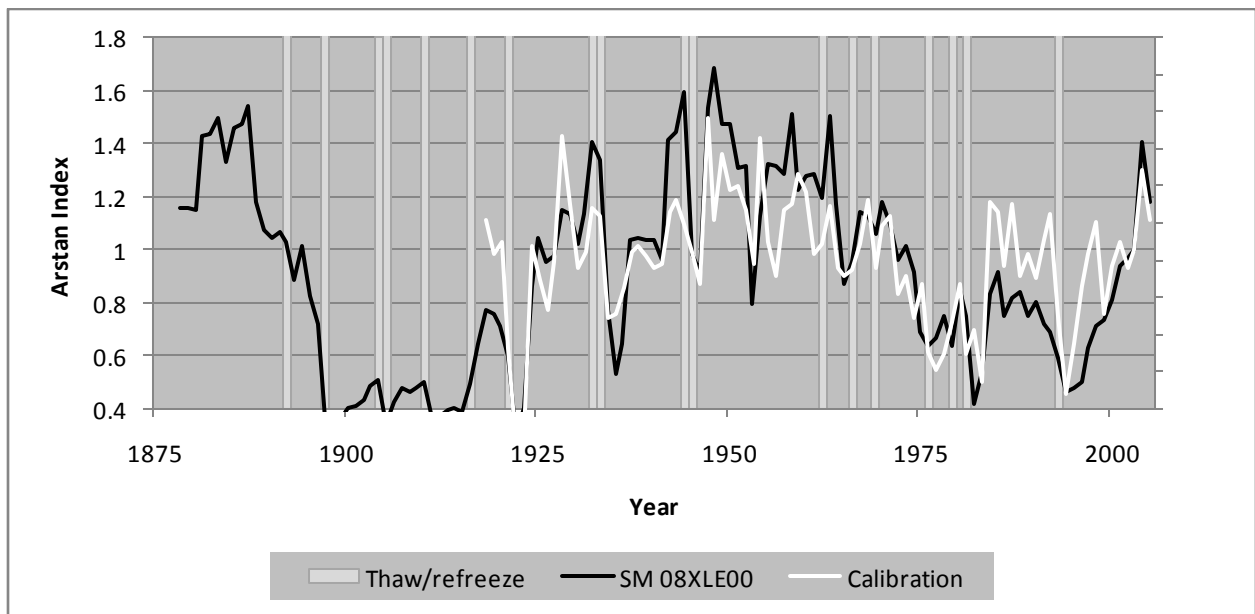


Figure 5.25. The regression model defined in this Figure used climate data from Fredericton station and the sugar maple chronology from Odell Park. The black line illustrates the historic sugar maple radial growth curve for OP (Chronology MAD Lab code = 08XLE00). The unbroken white line details the model calibration period. The light grey bars indicated thaw/refreeze events defined by the TRF Deep variable. The thaw/refreeze component is only meant to position the events in time and does not detail severity of the event.

Fredericton OP3

The Fredericton OP3 regression model used the Fredericton climate data regressed against the Odell Park sugar maple chronology. This supplementary model was constructed to test the TRF Deep variable, as well as to better understand how the AMO index has influenced sugar maple trees in the region. The April temperature variable was removed from the regression input list in the current year and both lagged years from the MMT variable set. The variables were then replaced with the TRF Deep variables from the DCT variable set. Also the AMO index at a three year lag was entered as another independent variable in the stepwise regression analysis.

The results of the analysis produced an 11 variable model, explaining 54% of the variance using climate terms covering the period 1878-2005 (Table 5.5). A 13% increase in explained variance was realized with this model despite a much longer period of calibration (1878-2005). The selected best subset model included the AMO index (lagged three years) as the top variable, as well as the TRF Deep variable from 1st year lag, and 2nd year lag (Tables 5.6 and 5.18). It is not possible with the Fredericton OP3 regression model to forecast future growth, as there is currently no reliable future forecast of the TRF Deep variable or the AMO index. Therefore, only the past radial growth and model calibration period is presented (Fig. 5.26). Figure 5.26 details the thaw/refreeze events defined by the TRF Deep variable.

Table 5.18. The regression model variables from the best subset model representing the Fredericton climate data regressed against the Odell Park sugar maple chronology are illustrated. The monthly variables used in this regression model are represented in the Table by: white = positive variable association, black = negative variable association, gray = variable not included in this model. This regression model is a supplementary model testing the TRF Deep variable and AMO index. The April temperature variable has been replaced in 1st lagged year, and 2nd lagged year with the TRF Deep variable symbolized as: * =TRF Deep. The AMO index (lagged three years) has also been added as another independent variable symbolized as: ω = AMO

OP3	2 nd Year Lag												1 st Year Lag												Current Year											
	Month	J	F	M*	M*	J	J	A	S	O	N	D	J	F	M*	M*	J	J	A	S	O	N	D	J	F	M*	M*	J	J	A	S	O	ω			
Temp																																				
Precip																																				

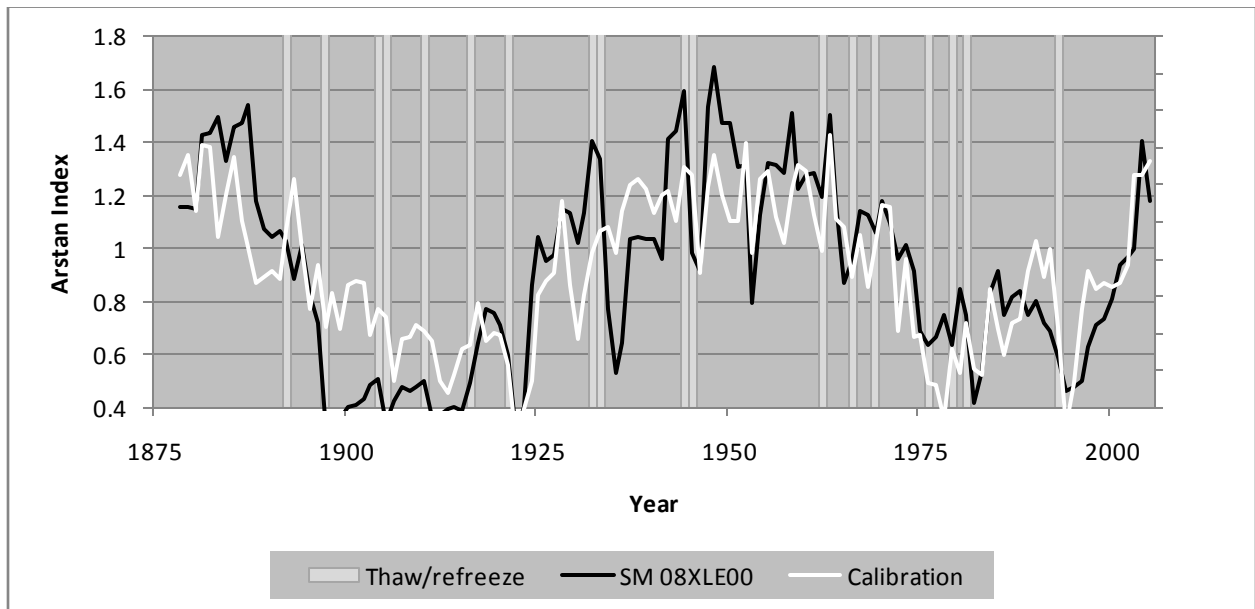


Figure 5.26. The regression model defined in this Figure used climate data from Fredericton and the sugar maple chronology from Odell Park. This regression model is a supplementary model testing the TRF Deep variable and AMO index (lagged three years). The black line illustrates the historic sugar maple radial growth curve for OP (Chronology MAD Lab code = 08XLE00). The unbroken white line details the model calibration period. The light grey bars indicated thaw/refreeze events defined by the TRF Deep variable. The thaw/refreeze component is only meant to position the events in time and does not detail the severity of the events.

5.6 Common Variable Aggregation and Verification

The following description highlights shared variables and geographic patterns among the regression outputs based on the MMT/TMP variable set (Table 5.19). Variables that occur infrequently are largely ignored as there is a high probability they may be spurious in nature. The summary follows a seasonal narrative beginning in winter.

Table 5.19. Aggregated variables from radial growth forecast models for verification of the most influential climate terms. Variables from the AICc selected model for each sample site are included in the Table. All variables including those from lagged years are displayed under the month of occurrence with indifference as to the number of years before radial growth.

Temperature variables are arranged in the top half of the Table and precipitation variables are arranged in the bottom half of the Table. Black cells are negative associations to numerically high values of the variable and white cells are positive associations to numerically high values of the variable. Numbers in each cell represent the number of occurrences of a variable in a particular model (three is the maximum per model as no month can occur in more than the current year, 1st lagged year, and 2nd lagged year). DJFM/Snow Depth is the winter snow depth index, ⁻ = T ONDC, - = T JASc, ₋ = P AMJc where the seasonal variable actually represents three months but the value is assigned to the first month in the season.

MMT	Jan	Feb	Mar	Apr	May	Jun	Jul	Aug	Sep	Oct	Nov	Dec
BR	1						1 1			1 ⁻	-	-
QM				1			1 1		1			
KR				1			1		1			
HR					1	2	2	1		1 ⁻	-	-
OP			1	2		3				2 ⁻	-	-
SF	1		1			2	1	2		1		
IM		1	1	1	1					1 ⁻	-	-
FP				3			2-	-	-	1		
FR				1		1	1-	1-	-	1		
KP		1 1				1		1	2			
Total	2	1 2	0 3	0 9	1 1	8 1	6 5	5 0	1 4	3 4	0 0	0 0
TMP	DJFM/Snow Depth			Apr	May	Jun	Jul	Aug	Sep	Oct	Nov	
BR						1			1			
QM	2				1 1		1		1			
KR				1		2			1			
HR	3				1	1						
OP				1	1	1						
SF				1	1			1				
IM	1				1			1				
FP							1		1			
FR					3	1			1			
KP				-	2 2		1	1				
Total	5			2	0 6	9	1 5	2 1	1 2	1 4	0 0	

Two of the most northerly sites had five links to lower snow depths. Cold Marches were a commonly shared variable for southern New Brunswick sites on the north side of the Caledonia Uplands. An affinity for cold Aprils was the most commonly selected variable with nine links

by six different sites with a near random distribution. Five sites away from the Bay of Fundy had six positive associations with wet Aprils. Six sites showed nine links to dry Mays. Eight links to cool Junes were made by four sites away from the Bay of Fundy but with a southern geographic position. Conversely, six connections to wet Junes were selected by five sites distributed in northern areas and near the Bay of Fundy.

Summer temperature and precipitation associations are the most polarized variables. Sites in the south prefer cool Julys and Augusts, while central areas have no selected preferences, and northern areas link to a combination of warmer and cooler Julys and Augusts. Six links to summer precipitation variables from five sites were selected but they showed no discernable geographic pattern. Three sites made four connections to warmer Septembers, while one site indicated a cooler September, and no overall spatial pattern was evident to these variables. Sites near the Bay of Fundy preferred dry Septembers while northern sites more often selected wet Septembers. Sites near the Bay of Fundy and Grand Lake linked to warmer Octobers, while sites located along the eastern marine boundary of the study area preferred cool falls.

Chapter 6

6.0 Discussion and Synthesis

6.1 Radial Growth Forecasts and Regional Climate Change

6.1.1 *Dendrochronological Insights*

Tree-ring analysis of the sampled sugar maple trees across all sites provides crucial insight into relationships among the tree species and climate. The dendrochronological analysis among the individual sugar maple trees at each site indicated a strong common signal (Table 5.1). Analysis of the similarity between the average tree-ring indices developed from each sampling site illustrates a complex pattern across the landscape (Table 5.2). Further to this complex geographical pattern, is an even more elaborate temporal relationship among the sites (Table 5.3). These temporal and geographic patterns signify a heterogeneous influence upon sugar maple radial growth over the landscape. Measures of sensitivity (Table 5.1) provide evidence that the large majority of the sugar maple tree-ring chronologies are highly sensitive to their environments. Climate, a wide ranging, similar growth input common to trees at all sites, is most likely responsible for much of the variation in the radial growth of sugar maple trees studied in this project, and has been illustrated in other sugar maple studies (Payette et al. 1996, Tardif et al. 2001). Therefore, climate has been substantially influencing sugar maple radial growth across each study area, but climatic event effects have altered the radial growth characteristics substantially from place to place.

6.1.2 Stability of Radial Growth

Central to the success of robust model building is the consistency of the radial growth response to climate over time (Fritts 1976). If a tree alters its mode of growth because of a changing climate, or if a tree reacts differently to the climate as it ages, attempts to model that relationship would be difficult due to the complexity of the ever-adjusting relationship. As evidenced in Table 5.3, the temporal consistency of the radial growth response to climate among sugar maple is highly variable. This illustrates that the sample sites have been altering their radial growth responses relative to each other over time. Visually, this modification in radial growth response can be assessed in Figure 5.1. Over annual to biennial periods, little conformity is visible, while multidecadal time periods exhibit greater similarity. More specifically, the periods from 1900-1925 and 1980-2000 exhibit below average radial growth rates across most sites, while the period covering 1930-1980 generally displays above average radial growth rates across most sites (Fig. 5.1). Low frequency multidecadal radial growth influences can be more easily observed in the regional master sugar maple chronology used in Fig. 5.2. During low frequency radial growth suppression periods linked with GCOAIs, it is suspected a new set of climatic radial growth drivers and limitations come into play. This seems to agree with a study by Tardif et al. (2001) in Quebec, which also found unstable radial growth to climate relationships with sugar maples.

6.1.3 Explained Variance

In this study's results, between 24 and 54% of annual radial growth variance was explained. These values were derived through an adjusted coefficient of determination and without using a prior growth variable. Some context can be given regarding the strength of these

results by comparing them with the unadjusted coefficients of determination results from models produced in other studies.

Lane et al. (1993) produced five sugar maple models and their results explained 24 to 79% of the variance. In 27 sugar maple models, Payette et al. (1996) produced explained variance values from 19.5 to 65.7%. Using radial growth chronologies from three species including sugar maple, eastern hemlock and American beech, Tardif et al. (2001) developed models explaining 53 to 54% of variance. In 2003, Laroque and Smith produced five models from Douglas-fir (*Pseudotsuga menziesii* Carrière), western red-cedar (*Thuja plicata* Donn ex D. Don), western hemlock (*Tsuga heterophylla* (Raf.) Sarg.), mountain hemlock (*Tsuga mertensiana* (Bong.) Carr.), and yellow cedar (*Chamaecyparis nootkatensis* (D. Don) Spach) that explained between 55 and 68% of the variance. Goldblum and Rigg (2005) created three models using sugar maple, white spruce and balsam fir which explained 39 to 61% of the variance. Most recently, Girardin et al. (2008) produced three radial growth models using jack pine (*Pinus banksiana* Lamb.), black spruce and trembling aspen (*Populus tremuloides* Michx.) with explained variances between 48 and 56%. Characteristics of these models such as model selection technique, the species being modeled and the lack of adjustment regarding the coefficients of determination, make the comparison with this study difficult. Girardin et al. (2008) also produced adjusted coefficients of determination which resulted in a smaller explained variance of 42 to 49% and are more directly comparable with the values associated with this study.

6.1.4 Verifying Climate Terms Across Models

Due to low frequency climate fluctuation, and frequent suppression periods throughout the radial growth chronologies of sugar maple trees used in this study, model building applying stepwise regression was somewhat impaired. A lack of sufficient stability and consistency in the radial growth to climate relationship necessitated a reduction in the length of time applicable for analysis. For example, when a long period (i.e., 1900-2006) was selected for model calibration, the stepwise regression analysis was forced to explain radial growth variance using driving variables from time periods that represented both suppression and intensified radial growth intervals. This resulted in an overly complicated calibration period for such intervals, which subsequently led to the selection of an insufficient number of variables to provide a good explanation of the radial growth variance. Therefore, a strategy was developed to eliminate the most problematic time period (1900-1930) from the analysis, where it appeared that a conflicting radial growth response was at play (Table 5.3). During this time period climatic influences of GCOAIs may have altered the radial growth/climate response. When the shorter time period from 1930-2006 was modeled, a significant explanation of the variance was quickly achieved. The large variable set, combined with a shortened time period over which the regression analysis could be run, potentially introduced spurious variables into the models (Burnham 2002). This may have over-estimated the importance of some of the significant variables, and therefore limited the strength of the resulting model forecasts. Despite the lack of robust regression models made from the longest possible climate data set, when the outputs are viewed in aggregate and cross referenced between sites, the verification of the most important variables is produced allowing inference to be based on multiple models (Burnham 2002).

6.1.5 Common Model Variables

Although the wide range of influences on radial growth produce a less than ideal situation for model construction, the opportunity for cross referencing the ten models is unprecedented. This natural variability in the response of all of the sugar maple radial growth to climate models makes the option of verifying the terms across all models an essential quality check process. Through cross referencing, it then becomes possible to filter out potential spurious results, and identify common variables of wider influence. By examining these most commonly selected variables from the 10 regression model outputs, a general illustration of how sugar maple trees have responded to Maritime climates over the past 75 years becomes more apparent.

The following description of common model variables again, follows a seasonal narrative. All variables evaluated in the following account can be found in Table 5.6. and Table 5.19.

6.1.5.1 Winter and the Transition to Spring

Two of the most northerly sites had links to lower snow depths indicating high snow depths may be a limiting growth factor in the north. Cold Marches were a commonly shared variable for southern New Brunswick sites on the north side of the Caledonia Uplands, possibly signifying a positive reaction to less snow melting in that month. The most commonly selected variable among the ten models was a positive relationship to cold Aprils. Since this time period is before the start of photosynthetic capabilities of the trees, positive relationships to cold conditions at this time seem counterintuitive. Warmer conditions in April would be expected to lead to an earlier bud burst in May, and therefore a longer growing season. Due to the wide influence of cold April temperatures on sugar maple trees outside of the photosynthetic season, it

seems that this is a crucial time period, and may in fact indicate that thaw/refreeze is occurring at this time of year. A thaw occurring in this month could lead to a higher recorded average temperature, resulting in April average temperatures being a potential general indicator of an injurious thaw/refreeze event.

Sites away from the Bay of Fundy had positive associations with wet Aprils. Since April is the month of greatest snow melt across the majority of sites, this linkage could be related to snow melting or increased availability of soil moisture.

6.1.5.2 Spring

In May, many positive links to dry conditions occur. Rather than a relationship to precipitation, this variable may be associated with the lack of cloud cover in the drier month of May, resulting in warmer day time temperatures and increased photosynthetic activity for newly formed leaves, and ultimately more energy gained for ring formation in the growth year. This is somewhat counter to arguments of May conditions by Tardif et al. (2001), who suggest high amounts of precipitation in the month of May would lead to excessive soil moisture, lowering radial growth as sugar maple prefers well drained soils.

Numerous positive links to cool Junes were made at four sites away from the Bay of Fundy, but with a more southern geographic position. Conversely, many positive connections to wet Junes were found at five sites distributed in northern areas. It seems that sufficient soil moisture levels are required before the initiation of radial growth during the warm part of the growing season begins (July, August). Sites at different latitudes then have alternate preferences for how they achieve this moisture. Lower June evapotranspiration rates in warmer regions of

the study area and higher levels of June rainfall for cooler areas appear to be important drivers of this process.

6.1.5.3 Summer and Fall

Summer temperature and precipitation associations are at times conflicting. Sites at southern latitudes prefer cool Julys and Augusts, while central areas have no selected preferences and northern areas link to a combination of warmer and cooler Julys and Augusts. These geographic patterns suggest high summer temperatures are limiting to sugar maple in the southern most portions of the study area while low summer temperatures can be limiting in northern portions of the study area in certain circumstances. Links to summer precipitation variables from numerous sites were selected, but they illustrated no discernable geographic pattern. Some connections to warmer Septembers were found, but no spatial pattern was evident. Sites near the Bay of Fundy preferred dry Septembers, while northern sites were more often linked to wet Septembers. Due to a relatively high number of fog days and a large amount of cool air coming off of the Bay of Fundy in summer, it seems sensible sugar maple would favor a sunny September in these locations. Sites near the Bay of Fundy and Grand Lake linked to warmer Octobers, while sites with exposure to the waters connected to the Gulf of St. Lawrence preferred cool falls.

6.1.5.4 Regional and Subregional Summary

April temperatures are important to sugar maple radial growth at most sites, and warm temperatures in that month have caused decreased radial growth in the past. Dry Mays, with their associated clear skies, result in greater radial growth for sugar maple throughout the study areas. Analysis suggests northern sites have grown better in the past when snow depths have

been lower, and Junes have been wetter. Sites near the Bay of Fundy have shown increased radial growth rates when Junes are wet, Septembers are dry, and Octobers are warm. Southern sites have grown better in the past when late spring and summer have been cooler.

6.1.6 Possible Future Climate in Relation to Model Forecasts

A review of the radial growth forecasts produced from the regression models illustrates a general negative trend for trees in southern areas, while more northern sites are forecast to mainly continue in a stable growth pattern. The CGCM3 SRES A1b summary provides some explanation for these trends. Although growing season length and temperature levels are both forecast to increase, precipitation should remain moderately stable. The climatic variables most responsible for this negative forecast are future April temperatures. Increases from 1.5°C averages in the year 2000 to 7°C averages by the year 2100 for southern latitudes cause most models to respond poorly, producing negative forecasts. With relevance to the models, and to the general ecological response of forests, is the projection of a 70% reduction in snow depths within the southern latitudes in the Maritimes by the end of the 21st century. While the north is predicted to maintain comparable levels of snow in future years, and suffer smaller increases in April temperatures, sugar maple is projected to take advantage of the longer growing season or at least maintain relatively stable radial growth rates as forecast for that area.

Southern sites in comparison will have less protective snow cover exposing them to more potentially damaging temperature swings during their transition from winter to spring. Although April temperatures should be substantially warmer, it is probable that more variable temperature fluctuations will occur earlier in the season and more often in March as the year 2100 approaches. The problematic component of forecast assessments for southern sites is with the

CGCM3 model's inaccurate projection of temperature swings in late winter and early spring (Fig. 5.4). Without dependable forecasts of late winter temperatures, and an accurate definition of an injurious climatic event, it is not possible to give a quantifiable estimate of sugar maple radial growth response to future late winter snow and temperature conditions. Therefore, at least a similar frequency of winter thaw/refreeze events as have been experienced in the past should be expected for the future. Based on the sugar maple common response to past climate conditions for southern areas, it appears that hotter July and August conditions combined with an 11% reduction in summer precipitation may result in more frequent drought conditions causing decreased radial growth. Due to its preference for well-drained soils, sugar maple has been shown to be sensitive to mid-summer drought (Payette et al. 1996, Tardif et al. 2001). Increases in growing season length may therefore be counterbalanced by increasing evapotranspiration and decreasing summer time precipitation rates.

6.1.7 Daily Compiled Temperature Variables

The DCT variables were found to be partially successful at identifying past events of relevance to sugar maple. Although the TRF Surficial and the RtFr variables were found to be ineffective in analyses, the Fredericton OP2 model was an example of a successful use of the explanatory power of the TRF Deep variable (Fig. 5.25). Most other locations illustrate a TRF Deep variable of limited functionality. There may be several reasons for this limitation including; (i) substantial distances and elevation between sample sites and climate stations; (ii) an overly simplified definition of a complex event; (iii) climate station data containing inaccurate information due to infilling of missing data or human error; and, or (iv) radial growth depressions due to other climatic events such as ice storms, drought events or possible insect outbreaks. Despite precautions taken to assure a close fit of sampling sites to climate stations, even short

distances and elevations can have large impacts on climatic elements such as snow depth. In relation to the TRF Deep variable, a thaw/refreeze event may have occurred at the climate station but not affected adjacent trees in an upland area due to a partially remaining snow pack.

Also, by only measuring fluctuations in air temperatures to identify when an injurious thaw/refreeze event occurred, part of the potentially complex process may have been overlooked. Both Sperry et al. (1988) and Robitaille et al. (1995) suggest unfrozen soil moisture levels play a large role in the spring time recovery from winter induced xylem embolism. Better measures of tree dehardening and soil moisture may be needed to accurately describe injurious freezing events than just fluctuations in air temperature.

A key point in this analysis is that the DCT/TMP variable set failed to explain a significant amount of radial growth variance. This drawback, in combination with the inability to forecast future climate scenarios (Fig. 5.2), resulted in this variable set not being used. Although the TRF Deep variable and the AMO index do not currently have future forecasts available to allow future projections of radial growth to be better estimated, their inclusion and successful calibration in the Fredericton OP3 model (Fig. 5.26) illustrate the need to take such climatic influence into account. The AMO index and the TRF Deep variables aided the model in achieving an increased descriptive capacity regarding the radial growth suppression periods which was not evident in the original Fredericton OP1 model. Moreover, the AMO index allows the model to be regressed over the entire period as it supplies the necessary information to model periods of divergent radial growth response to climate such as the 1900-1930 period. Due to the very strong correlation between the AMO and sugar maple radial growth in Fredericton OP (r -value = 0.481; $p < 0.01$, and r -value (10-mavg) = 0.713; $p < 0.01$), the AMO's inclusion in this model behaves in a similar manner as a one year lag of radial growth used in previous radial

growth modeling studies (*c.f.*, Laroque and Smith 2003, Goldblum and Rigg 2005, Phillips and Laroque 2007, 2008, Girardin et al. 2008). In this instance the AMO is the best tool to aid the model in explaining radial growth over the divergent periods at this site. Fredericton OP was chosen as it had a long climate record (1878-2005) over which the longer-term GCOAI data could be tested. It is likely that other sites, if long-term climate data was available (1800's-2000), could be best modeled using either the AMO, the NAO or a combination of the two depending on past radial growth response to climate. Ideally it would be most beneficial if the AMO and NAO climate influence could be defined for use in the models rather than using the GCOAI index values. Improvements in the definition and forecasting of these variables will result in large improvements for future radial growth modeling efforts. Ultimately future models incorporating well defined measures of climate stress will be able to more accurately model radial growth responses to more extreme events that may occur in the future due to climatic changes.

6.2 Model Limitations

Many levels of uncertainty exist in the models produced in this study. Five significant areas of error exist and the exact measure of uncertainty is very difficult to quantify. The five general categories are related to; landscape variability, statistical modeling error, climate change uncertainty, biological thresholds and future non-climatic disturbance. The first two categories have been covered in chapter four and explanation of the final three levels of model limitations are discussed below.

6.2.1 Uncertainty of Global Climate Models

The accuracy of the forecast models created in this study are limited by the predictive accuracy of the CGCM3 data. New data suggest global climate models may encounter reduced capability to predict future climate over the North Atlantic Ocean due to problems associated with the prediction of the NAO (Goodkin et al. 2008). Oscillations of ocean conditions may have the potential to erratically influence the progression of climate change, temporarily weakening the effects of regional warming (Keenlyside 2008). Probable inconsistencies of warming trends are likely to affect radial growth in ways the forecast models in this study cannot predict.

The very level of greenhouse gas provoked warming realized over time is also an obstacle in this radial growth modeling exercise. Due to the current highly unpredictable nature of the anthropogenic emissions of green house gases, it is very uncertain which SRES scenario will best characterize the future levels of climate change we will experience. We are presently accelerating our greenhouse gas emission direction above all current IPCC SRES scenarios

(Raupach et. al 2007). If this trajectory continues, the forecasts produced in this paper may happen in a fraction of the century-long time frame specified in the initial SRES scenarios used.

6.2.2 *Prospective Biological Thresholds*

Another limitation of the forecast models of this study is the availability of past climatic situations that are analogous to future climatic scenarios. The forecast models in this study are based on approximately the past 75 years of radial tree growth in comparison with the past 75 years of historical climate data. During this 75 year period, there has been much climatic variability, but there are also potentially future forecast climatic extremes that are outside of the range of past climates. A prime example of this would be future winter precipitation falling as rain instead of snow, drastically changing factors relating to growth (Laroque and Smith 2003, Goldblum and Rigg 2005). The models are therefore limited in their capacity to provide a prediction of radial growth under a forecasted climatic range that is outside of what they experienced in the past.

Important ecological thresholds that relate to a tree's response to temperature or precipitation in a particular month or season may not have been reached in the past 75 years and would therefore be neglected in these forecast models. This is likely the case with the models produced in this study. Due to the period 1900-1930 being omitted from the regression analysis, a certain amount of unknown climatic extremes were also excluded. This exclusion or shortened time period of model calibration has limited the interval over which sugar maple radial growth response could be analyzed and accounted for. Also as the climate changes, new extreme climate conditions will occur that have never been experienced over the instrumental record. Consequently, as the models work their way into more extreme climate change scenarios, it is

expected that their predictive capability will begin to fail, which is why more extreme SRES scenarios (A1F1, A2) are not modeled here.

The potential for a particular species to incorporate specific climatic factors differently into its radial growth pattern as it reaches climatic thresholds remains unknown. We do know that some climate-growth relationships are age dependent (Carrer and Urbinati 2004). The degree to which physiological changes in the studied tree species have altered their response to climate inputs over the timeframe investigated is obscured by the process. How much future physiological changes will impact the radial growth response to future climates is not known and could play a large role in keeping a particular species competitive or contributing to its demise. Due to the very mature trees sampled for this study and the subsequent analysis which examined only mature growth of sugar maple, the hope was this limitation to forecasting would be minimized.

6.2.3 *Nonclimatic Disturbance*

It should also be kept in mind that these models are only predicting radial growth response to the future climatic inputs and do not account for radial growth reductions inflicted by insect outbreaks or other pathogens. As the climate warms, trees will not be the only species to shift ranges in response to the new conditions. Other species will also have a migrational response that could differ substantially in geographical and temporal scales. Both alien and native pest and pathogen disturbance is expected to increase on the poleward margins of temperate forests as bioclimatic barriers are moved through rapid climate changes (IUFRO 2009). Therefore, it should be anticipated that future radial growth of sugar maple could be significantly affected by the influences of pests and pathogens more commonly associated with

southern portions of the sugar maple range. This fact, and the fact that the trees are currently rooted in place compared to the ability of insects to more readily disperse, cannot be taken into account in these radial growth model forecasts.

Although there are many potential external and internal sources of error in these biologically based, deterministic models, I believed that they present the most useful picture of future radial growth rates of sugar maple to date in the Maritimes.

6.3 Hypotheses Insights

Two hypotheses were initially set forth. The first was that;

- 1) Thaw/refreeze late winter conditions are injuring sugar maple trees and these events are occurring more frequently in the southern portions of southern New Brunswick and central areas of Nova Scotia than in more northern portions of the provinces.

Although this hypothesis could not be specifically quantified, several veins of evidence are available to help evaluate this hypothesis. The first and most convincing piece of evidence relates to the identified thaw/refreeze events produced in the TRF Deep variable. Excluding the two closest sites to the Bay of Fundy, there was a persuasive increase in the frequency and severity of thaw/refreeze events from north to south (data not shown). The two most distant sites, Charlo in the north and Collegeville in the south, experienced 4 and 21 events over 65 and 86 years respectively. To qualitatively describe the difference in winter climate between the north and the south, the north experiences a “reliable and persistent” snow cover lasting an average of 160 days, while the south experiences an often deep snow cover that may melt and re-accumulate three or more times a season (Phillips, 1990). Although these climatic events were

far more frequent in southern areas, it should be kept in mind that it does not necessarily translate into tree injury.

Secondly, the average mean sensitivity (AMS) values calculated for each site increase along a transect heading from north to south. Higher AMS values were produced in southern sites indicating more variability and greater amplitude between annual tree-rings (Table 4.1). This does not confirm tree injury by thaw/refreeze but it does indicate that trees at lower latitudes do experience more extreme events that lead to severe reductions in radial growth values. Based on the lower frequency of potential thaw/refreeze events, the lower variability in the tree-ring chronologies, and the protective snow cover in the north, it is unlikely trees with more northern locations would be injured as often by thaw/refreeze events. Only an anomalous winter would provide the conditions necessary for injury in the north.

The second hypothesis put forth stated;

- 2) Late winter thaw/refreeze events are likely to affect trees more often in northern areas of New Brunswick as future climatic changes advance.

Firstly, average winter snow depth by the year 2100 in the SRES A1b scenario is only predicted to decrease by 25cm leaving a substantial protective snow pack in northern regions. Secondly, the growing season is projected to increase in growing degree days by 44%, potentially offsetting any increased frequency of injury. Finally, higher elevations in northern regions will act as a buffer as climate change will not only have to increase temperatures across a latitudinal gradient to warm the north, but it will also need to increase temperatures up the higher elevational gradients. The best quantitative method to assess this hypothesis would have been through the CGCM3 future forecast using the newly constructed thaw/refreeze variable. As was

stated earlier in this thesis, the TRF Deep variable constructed to identify future thaw/refreeze events does not operate flawlessly for several reasons listed in section 6.1.6. Furthermore, the CGCM3 future data produced questionable values as compared with those actually experienced over the last nine years, making the forecasted daily values for late winter unreliable (Figure 5.4). This left only the more general CGCM3 climate summary data on which to base assumptions for this hypothesis.

Evidence used to substantiate both of the stated hypotheses is somewhat arbitrary, however in lieu of an assessment of daily climate data from other coupled global climate models, this evidence must stand as the only response.

6.4 Atlantic Multidecadal Oscillation Influence

The geographic distribution of correlation values between tree-ring chronologies and the AMO produced a fairly random effect with a clumping of poor relationships near the Bay of Fundy. It is possible that the cool waters of the Bay of Fundy have some moderating effect on the influence of the AMO. Although the correlation analysis illustrates less than half of the sampled sugar maple sites having weaker relationships to the AMO, and the remaining sites having a strong relationship, there is still reason to believe that all sites are affected considerably by the AMO. The primary reason for a weak relationship with the majority of the sites to the AMO appears to be the variability in frequency and magnitude of injurious climatic events between sites, possibly a result of NAO influence. This assumption suggests the positive phase of the AMO is related to increased radial growth of all sugar maple sites in the Maritimes although some variability exists due to the numerous marine influences such as the Bay of Fundy.

Positive phases of the AMO correspond to decreased precipitation and increased temperatures during summer months over central North America (Sutton and Hudson 2005). It is uncertain whether these conditions extend over the Canadian Maritimes however. Preliminary results indicate a moderate relationship to September temperature and November precipitation (data not shown). Influence of the AMO is significant in fall months at lower latitudes, but it is unclear how far north the effects could reach (Sutton and Hudson 2007). According to the research of Sutton and Hudson (2007), the AMO projects its influence during the summer months of the growing season and potentially into the fall, lengthening the growing season over the Maritimes during positive phases, and shortening the growing season in negative phases.

It is generally recognized that the last time the AMO shifted phases was in 1994-95. This shift was to a positive phase, which has generally resulted in increased sugar maple growth in the past. It is possible however, that a shift back to a negative phase could happen earlier than anticipated due to an Atlantic thermohaline circulation slow down (Sutton and Hudson 2005). The Meridional Overturning Circulation (MOC) is largely responsible for the transport of heat via ocean currents from equatorial regions of the Atlantic towards northerly regions (Msadek and Frankignoul 2008). Most global coupled climate models suggest a weakening of the MOC in climate change scenarios, although debate still surrounds the processes involved (Guemas and Salas-Me'lía 2008). If MOC slowdowns induced by global warming did occur in the near future, we should expect a phase reversal of the AMO and lower sugar maple radial growth. Perhaps of greater use, given the current debate regarding the future of the MOC influence, is the probabilistic projection of future AMO phase changes based on long-term tree-ring reconstructions. Based on a 424 year AMO reconstruction from tree-rings completed by Gray et al. (2004), Enfield and Cid-Serrano (2005) produced a study of projected risk of future AMO

phase shifting. Their results suggest we should expect a 33% chance of a phase reversal in the next 5 years, a 59% chance of reversal in 10 years, a 78% chance of reversal in 15 years, a 92% chance of reversal in the next 20 years, and finally there is near certainty of a phase reversal of the AMO within 25 years based on past activity (Enfield and Cid-Serrano 2005).

6.5 North Atlantic Oscillation Influence

The winter (DJFM) measurement of NAO in its positive phase shows a negative relationship to radial growth in sugar maple of the Maritimes. Preliminary analysis of temperature and precipitation monthly values with the NAO shows that the greatest correlation and the most negative relationship is with April temperatures (Data not shown). This would also suggest that the NAO may play a role in growth reductions associated with winter thaw/refreeze events. Positive phases of the NAO cause arctic air flow to carry colder winter air into more southerly areas along the eastern Canadian seaboard (Hurrell et al. 2003). Fluctuations of these cold air masses may be associated with reduced sugar maple radial growth increments, but more research is required to better establish the link.

Despite much debate and theoretical positioning regarding the processes which drive the NAO, several studies have linked rising green house gas concentrations with more positive phase trends in the NAO (Hurrell et al. 2003). In contrast to these results are two long-term NAO reconstructions. The first is a well-verified, multiproxy tree-ring reconstruction reaching back to 1400 A.D. by Cook and D'Arrigo (2002). The second is a 218 year long NAO reconstruction from winter coral strontium-to-calcium ratio sampled near Bermuda by Goodkin et al. (2008). Both sets of authors show that the NAO performance is linked to hemispheric mean temperature and the magnitude of the NAO waxes and wanes as the climate warms and cools. It is proposed

green house gas emissions are forcing more extreme NAO phases and they also suggest increasing global temperatures will force a continuation of extended multidecadal NAO phase activity (Cook and D'Arrigo 2002, Goodkin et al. 2008). This they propose, will make climate forecasting more difficult for the North Atlantic region and undermine the predictability of anthropogenic warming (Goodkin et al. 2008).

An implication from their studies for sugar maple radial growth is that it will include both periods of rapid and slow growth. As we are currently ending an extended period of extreme positive phase of the NAO, sugar maple growth should respond favorably, especially considering we are in a warm phase of the AMO. However, if future extended positive phases of the NAO occur simultaneously with negative phases of the AMO, sugar maple could experience extended periods of stress leading to other disturbances such as insect or disease outbreaks and ultimately increased mortality.

6.6 Synthesis: Maritime Sugar Maple Stress Forecasts

Synthesis maps of future stress on sugar maple are presented in Figures 6.1 and 6.2. The definition of time periods, geographic boundaries, and climate stress expectations were substantiated through four categories of evidence. They include: radial growth to climate responses derived from the most commonly occurring regression model forecast variables, the future climatic trends for the Maritimes extracted from the CGCM3, the current ecological land classification system, and the future probability trends of both the AMO and NAO oceanic forcing mechanisms. Geographic boundaries were subjectively chosen using the model forecast variable distribution, the CGCM3 future trends and the ecological land classification system.

Temporal stress periods were defined using the CGCM3 future trends and the GCOAI potential phase reversals.

The period ranging from 2010 to 2024 is assigned a relatively low expectation for climatic induced stress (Fig. 6.1). The northern high elevation region of New Brunswick is assigned low stress levels while the southern portion of New Brunswick, the northern portion of Nova Scotia and the area surrounding the Bay of Fundy is assigned a low-medium stress level for the 2010-2024 period. The most important factor exerting influence over this period will most likely be the AMO. Even though the AMO is a non-stationary process, the probabilistic projection of phase reversal from its current positive phase does not reach over 50% until 2020 and does not reach high values (78%) until 2025 (Enfield and Cid-Serrano 2005). The positive phase of the AMO is historically associated with greater sugar maple radial growth, therefore the longer the current positive phase persists, the longer sugar maple should continue to thrive.

The next principal climatic force on the radial growth success of sugar maple is the multidecadal NAO phase. The projection of the NAO into longer and more extreme intervals (Cook and D'Arrigo 2002, Goodkin et al. 2008), suggests that the current downward trending positive phase of the NAO, should soon flip to a negative phase, which has historically been associated with increased sugar maple radial growth. Although no agreed upon long-term time scale of NAO variability is apparent (Hurrell 2003), recent multidecadal phases have experienced reduced low frequency variance, which should result in an extended negative phase (Goodkin et al. 2008). This assumption bears no probabilistic projections, but if the coming negative phase persists half as long as the current positive phase already has, it should easily extend beyond 2025.

Neither of the forecast summaries from the CGCM3 data, nor the sugar maple radial growth models, indicate any substantial changes in climate or in radial growth rates over the next 15 years. However, background climate fluctuation must not be dismissed and it should be assumed a certain low level of climate induced injury will occur in the absence of other major climatic events. Although the GCOAIs go through low frequency fluctuations, annual and sub-annual spikes occur repeatedly. If these assumptions hold true, then northern regions should be able to avoid much of the normal climatic induced injury due to its more consistent snow cover, while southern regions will likely encounter infrequent climate stress resulting in short radial growth depressions.

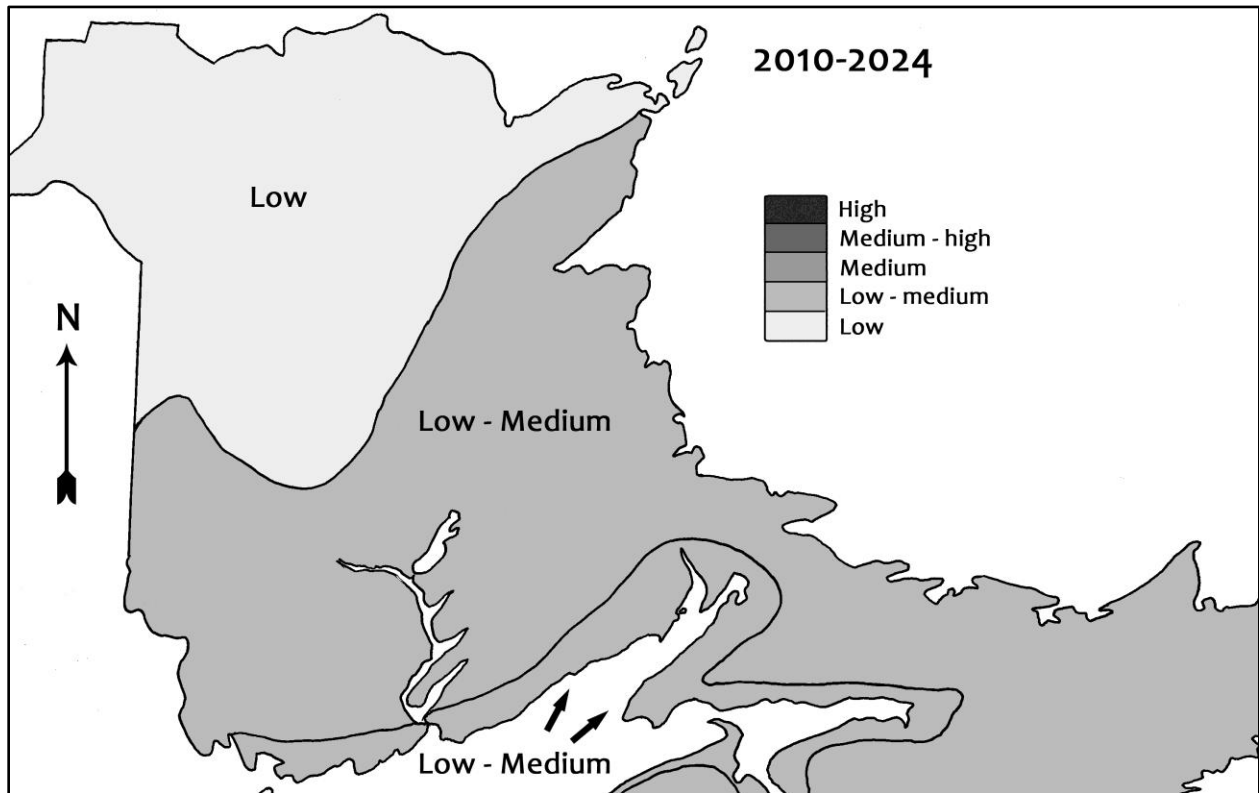


Figure 6.1. A climatic induced stress map for sugar maple from 2010 – 2024 over the provinces of New Brunswick and Nova Scotia.

The period from 2025 to 2050 is assigned relatively high expectations for climate induced stress (Fig. 6.2). The northern high elevation region of New Brunswick is assigned medium stress levels while the southern portion of New Brunswick and the northern portion of Nova Scotia are assigned high stress levels for the 2010-2024 period. The most important factor exerting influence over this period should be the AMO. The probabilistic projection of phase reversal from its current positive phase is 92% in 20 years and reaches near certainty by 2035 (Enfield and Cid-Serrano 2005). The negative phase of the AMO is historically associated with reduced sugar maple radial growth; therefore the transition to a negative phase should result not only in lower radial growth rates, but a diminished ability of sugar maple to recover from biotic or abiotic injury.

The second most important factor influencing sugar maple radial growth for this period is the NAO. If the reduced low frequency variance of the multidecadal phases of the NAO continues as it has over the past 60 years, another extreme positive phase should be entered sometime during the 2025-2050 period. This assumption is highly speculative and the phase change could come much sooner than the 2025 date. During the 1980s and 1990s a negative phase of the AMO and a positive phase of the NAO coincided with radial growth suppression of sugar maple across all sites sampled in this study. The Bay of Fundy area has shown some resistance to AMO influence in the past and has been given a lower potential of climate stress of medium-high for this reason. Although no probability estimate exists, a synchronous period of a negative phase of the AMO and a positive phase of the NAO is most likely to repeat in the 2025-2050 time period.

Both the forecast summaries from the CGCM3 and the sugar maple radial growth models indicate substantial changes in climate and growth rates by the 2025-2050 period. Significant changes in southern snow depth and increases in the length and temperature of the growing season should be evident by this period. Anthropogenic climate forcing will be the main driver of these trends, and the results of this will likely be experienced in the form of increasing thaw/refreeze damage in southern areas due to a lower snow pack, and/or increasing drought frequency in rain shadow areas such as the Miramichi and hotter areas of southern latitudes. Although Payette et al. (1996) identified that drought impacts on sugar maple east of Quebec City were rare in the past 100 years, sugar maple populations in the dryer and more fire prone areas of New Brunswick and Nova Scotia will likely become more susceptible to drought under these new future climatic regimes.

With increasing temperatures, especially in winter months, bioclimatic boundaries of pests and pathogens associated with sugar maple could disappear or move northward, causing an escalation in biotic disturbances (IUFRO 2009). Increasing levels of these normal background stressors of sugar maple in combination with intersecting detrimental phases of the AMO and NAO could overcome weaker individual trees of this normally disturbance resilient species. Significant amounts of mortality could be possible in this scenario. Variability in microclimate, site conditions, and maturity level of the trees may also play a large role in climatic injury and radial growth rates of sugar maple.

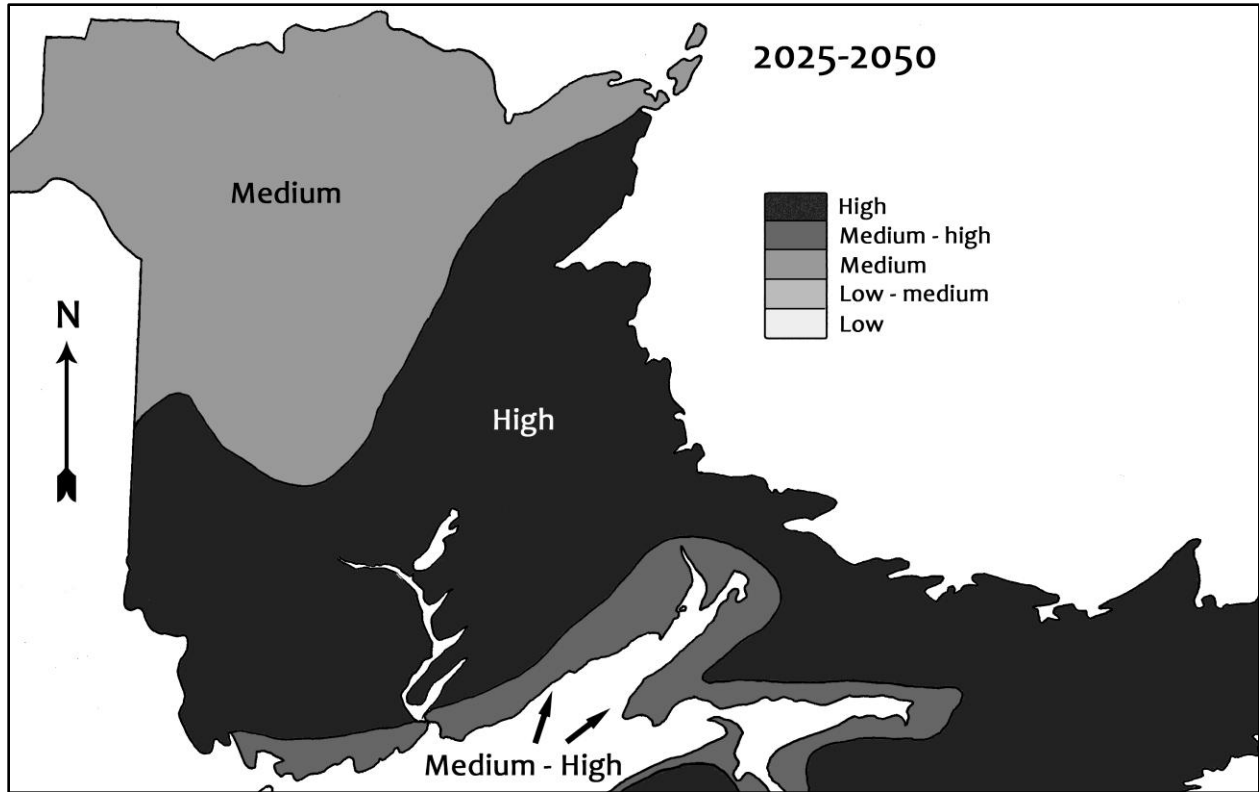


Figure 6.2. A climatic induced stress map for sugar maple from 2025 – 2050 over the provinces of New Brunswick and Nova Scotia.

Chapter 7

7.0 Conclusions

7.1 Further Research

Beyond improvements in global climate models and the ability to better forecast future phase activity in the multidecadal GCOAIs, this study has identified several areas of further research that would greatly aid in understanding the future health of sugar maple trees in the Maritimes. These areas include: investigating the role of soil moisture levels in an attempt to more closely define a thaw/refreeze index, using multiple GCMs to estimate future thaw/refreeze frequency and severity, and an exploration of the influence of various GCOAIs to specific climatic conditions in the Maritimes.

Unfrozen soil moisture was flagged as a potential contributor to sugar maple recovery from winter time freezing damage by Sperry et al. (1988) and Robitaille et al. (1995). Research identifying the process of this potential effect and a way to gauge its past occurrence using archived climate data could vastly increase the identification of both past and potential future sugar maple injury events. Further exploration of the specific conditions necessary to dehardens trees to a level where they are susceptible to injurious freezing at the end of winter may also resolve issues of event identification.

The CGCM3 produced unreliable results concerning potential thaw/refreeze events over the rest of this century (Fig. 5.4). Employment of a range of GCMs could produce a range of potentially more accurate thaw/refreeze values and provide more certainty regarding the future occurrence of such events.

Despite the identification of relationships with two major GCOAIs, the comprehension of their specific climatic influences on radial growth remains obscure. Recognition of specific climatic conditions associated with these GCOAIs on the local or regional scale could result in large increases in the understanding of future radial growth responses.

7.2 Conclusion

Undeterred by an unstable radial growth to climate relationship and the associated difficulties in model building, this study has illustrated that the radial growth of sugar maple tree-rings in the Maritimes is sensitive to climatic stressors. Verification of climatic terms across the ten radial growth models has helped address the statistical issues concerning shortened model calibration periods. Sugar maple has displayed a strong link to the Atlantic Multidecadal Oscillation (AMO) and the North Atlantic Oscillation (NAO) as well as a connection to late winter temperatures and potential thaw/refreeze events. Future climates have been forecast to have lower snow depths in the Southern Maritimes, accompanied with forecasted warmer conditions that could lead to water deficits in the growing season for some areas. These climatic changes alone could result in overall radial growth reductions.

Warming temperatures will also result in pest and pathogen migration on the poleward side of the sugar maple range (IUFRO 2009). Combining these abiotic and biotic shifts with potential multidecadal phase synchrony of the AMO and NAO could result in substantial stress for the sugar maple population, especially in southern areas of their range. The future health of sugar maple trees may affect the number of trees and volume of sap available for future maple syrup production. Potential mortality and crown dieback may also affect the aesthetic

characteristics of the future sugar maple population, as well as the ecological services provided by the sugar maple population.

The magnitude of climate change and the possible phase synchrony of the AMO and NAO currently have low levels of associated certainty. An extended period of beneficial climatic conditions should provide the time necessary to complete further research on a more precise understanding of the reaction of sugar maple radial growth to various climatic conditions. This period will also provide the time for coupled global climate models and other predictive climate models to become more robust and improve their accuracy. These activities could provide the information necessary to develop mitigation strategies for the avoidance of climate stress on sugar maple.

Sugar maple has proven difficult to model, but portions of its complex climatic relationship have been illuminated. Regardless of the current uncertainty, this study has raised important concerns for sugar maple trees based on scientific evidence. Application of the lessons from this study to other tree species of the Maritimes will hopefully provide similar useful information relating to new understandings of adaptation to our current climatic changes.

References

- Auclair, A. N. D., Martin, H. C., and Walker, S. L., 1990. A Case Study of Forest Decline in Western Canada and the Adjacent United States. *Water, Air and Soil Pollution* 53:13-31.
- Auclair, A. N. D., 1993a. Extreme Climatic Fluctuations as a Cause of Forest Dieback in the Pacific Rim. *Water, Air, and Soil Pollution* 66: 207-229.
- Auclair, A. N. D., 1993b in Luisis, N., Lerario, P., and Vannini, A. (eds.), Recent Advances in Studies on Oak Decline, pp. 139-148. Proc, IUFRO Conference, September 1992, Seva di Fasano, Italy.
- Auclair, A. N. D., Lill, J. T., and Revenga, C., 1996. The Role of Climate Variability and Global Warming in the Dieback of Northern Hardwoods. *Water, Air, and Soil Pollution* 91: 163-186.
- Auclair, A. N. D., 2005. Patterns and General Characteristics of Severe Forest Dieback from 1950 to 1995 in the Northeastern United States. *Canadian Journal of Forest Research* 35: 1342-1355.
- Arbaugh, J.M., and Peterson, L.D., 1989. Variable Selection in Dendroclimatology: An Example Using Simulated Tree-Ring Series. *Forest Science* 35(2):294-302.
- Bauce, E., and Allen, D. C., 1991. Etiology of a Sugar Maple Decline. *Canadian Journal of Forest Research* 21:686-693.

- Beier, C. M., Sink, S. E., Hennon, P. E., D'Amore, D. V., and Juday, G. P., 2008. Twentieth-Century Warming and the Dendroclimatology of Declining Yellow-Cedar Forests in Southeastern Alaska. *Canadian Journal of Forest Research* 38: 1319-1334.
- Bergeron, N., and Sedjo, R., 1999. The Impact of El Niño on Northeastern Forests: A Case Study on Maple Syrup Production. *Discussion Paper Rff:99-43*.
- Bourque, C. P.-A., Cox, R. M., Allen, D. J., Arp, P. A., and Meng, F. R., 2005. Spatial Extent of Winter Thaw Events in Eastern North America: Historical Weather Records in Relation to Yellow Birch Decline. *Global Change Biology* 11: 1477-1492.
- Brown, D. R., and Braaten, O. R., 1998. Spatial and Temporal Variability of Canadian Monthly Snow Depths, 1946-1995. *Atmosphere-Ocean* 36:37-54.
- Burnham, K. P., and D. R. Anderson. 1998. *Model Selection and Inference: A Practical Information-Theoretic Approach*. Springer-Verlag, New York, New York, USA.
- Burnham, P., K., 2002. *Model Selection and Multi-Model Inference: A Practical Information-Theoretic Approach* (2nd Edition). Secaucus, NJ, USA: Springer-Verlag New York, Inc.
- Burns, Russell M., and Barbara H. Honkala, tech. coords. 1990. *Silvics of North America*: 1. Conifers; 2. Hardwoods. Agriculture Handbook 654. U.S. Department of Agriculture, Forest Service, Washington, DC. vol.2, 877 p.
- Carrer, M., and Urbinati, C., 2004. Age-Dependent Tree-Ring Growth Responses to Climate in *Larix decidua* and *Pinus cembra*. *Ecology* 85(3):730-740.

- Campbell, J. L., Mitchell, M. J., Groffman, P. M., Christenson, L. M., and Hardy, J. P., 2005. Winter in Northeastern North America: a Critical Period for Ecological Processes. *Frontiers in Ecology and the Environment* 3(6):314-322.
- Clayden, S. R., 2000. History, Physical Setting, and Regional Variation of the Flora. In Hinds, H. R., *Flora of New Brunswick* (pp 35-73). Fredericton, NB: Biology Department, University of New Brunswick.
- Cook, E. R., 1985. A Time Series Analysis Approach to Tree-Ring Standardization. Ph.D. dissertation. The University of Arizona, Tucson, Arizona, USA.
- Cook, E. R. and D'Arrigo, R. D., 2002. A Well-Verified, Multiproxy Reconstruction of the Winter North Atlantic Oscillation Index since A.D. 1400. *Journal of Climate* 15(13):1754-1764.
- Cox, M., R., and Zhu, B., X., 2003. Effects of Simulated Thaw on Xylem Cavitation, Residual Embolism, Spring Dieback and Shoot Growth in Yellow Birch. *Tree Physiology* 23:615-624.
- Diaz-Nieto, J., and Wilby, L., R., 2005. A Comparison of Statistical Downscaling and Climate Change Factor Methods: Impacts on Low Flows in the River Thames, United Kingdom. *Climatic Change* 69: 245–268.
- Enfield, D.B., Mestas-Nuñez, A.M., and Trimble, P.J., 2001. The Atlantic Multidecadal Oscillation and its Relation to Rainfall and River Flows in the Continental U.S. *Geophysical Research Letters* 28:2077-2080.

- Enfield, D. B., and Cid-Serrano, L., 2005. The Probabilistic Projection of Climate Risk. *US Clivar* 3(3):10, 12-1.
- Farrar, J. L., 1995. *Trees of the Northern United States and Canada*. Markham, Ontario, Fitzhenry & Whiteside Ltd., and Ottawa, Ontario, Canadian Forest Service, Natural Resources Canada.
- Fritts, H.C., 1976. *Tree Rings and Climate*. Academic Press, London.
- Girardin, P., M., Raulier, F., Bernier, Y., P., and Tardiff, C., J., 2008. Response of Tree Growth to a Changing Climate in Boreal Central Canada: A Comparison of Empirical, Process-Based, and Hybrid Modeling Approaches. *Ecological Modeling* 213:209-228.
- Goldblum, D., and Rigg, L., S., 2005. Tree Growth Response to Climate Change at the Deciduous-Boreal Forest Ecotone, Ontario, Canada. *Canadian Journal of Forest Research* 35:2709-2718.
- Goodkin, N. F., Huguen, K. A., Doney, S. C., and Curry, W. B., 2008. Increased Multidecadal Variability of the North Atlantic Oscillation since 1781. *Nature Geoscience* 1:844-848.
- Graumlich, L. J., 1993. Response of Tree Growth to Climatic Variation in the mixed Conifer and Deciduous Forests of the Upper Great Lakes Region. *Canadian Journal of Forest Research* 23:133-143.
- Gray, S. T., Graumlich, L. J., Betancourt, J. L., and Pederson, G. T., 2004. A Tree-Ring Based Reconstruction of the Atlantic Multidecadal Oscillation since 1567 A.D. *Geophysical Research Letters* 31:L12205.

- Grissino-Mayer, H. D., 2001. Evaluating Crossdating Accuracy: A Manual and Tutorial for the Computer Program COFECHA. *Tree-Ring Research* 57:205-221.
- Guemas, V., and Salas-Me'lia, D., 2008. Simulation of the Atlantic Meridional Overturning Circulation in an Atmosphere-Ocean Global Coupled Model. Part II: Weakening in a Climate Change Experiment: A Feedback Mechanism. *Climate Dynamics* 30-831-844.
- Hacke, U. G., and Sauter, J. J., 1996. Xylem Dysfunction During Winter and Recovery of Hydraulic Conductivity in Diffuse-Porous and Ring-Porous Trees. *Oecologia* 105: 435-439.
- Hacke, U. G., and Sperry, J. S., 2001. Functional and Ecological Xylem Anatomy. *Perspectives in Plant Ecology, Evolution and Systematics* 4(2): 97-115.
- Hartmann, H., and Messier C., 2008. The Role of Forest Tent Caterpillar Defoliations and Partial Harvest in the Decline and Death of Sugar Maple. *Annals of Botany* 102:377-387.
- Holmes, R. L., 1992. Dendrochronology Program Library, Version 1992-1 Edition. *Laboratory of Tree-Ring Research, University of Arizona, Tucson*.
- Hurrell, J., Kushnir, Y., Ottersen, G., and Visbeck, M., 2003. An Overview of the North Atlantic Oscillation. The North Atlantic Oscillation: Climatic Significance and Environmental Impact. *Geophysical Monograph* 134 35p.

[IPCC] International Panel on Climate Change, 2007. Summary for Policymakers. In: *Climate Change 2007: The Physical Science Basis. Contribution of Working Group I to the Fourth Assessment Report of the Intergovernmental Panel on Climate Change* [Solomon, S., D. Qin, M. Manning, Z. Chen, M. Marquis, K.B. Averyt, M. Tignor and H.L. Miller (eds.)]. Cambridge University Press, Cambridge, United Kingdom and New York, NY, USA.

[IUFRO] International Union of Forest Research Organizations, 2009. Adaptation of Forests and People to Climate Change. A Global Assessment Report. Seppälä, R., Buck, A., and Katila, P., (eds.). IUFRO World Series Volume 22. Helsinki. 224 p.

Iverson, L. R., Prasad, A. M., Matthews, S. N., and Peters, M., 2008. Estimating Potential Habitat for 134 Eastern US Tree Species Under Six Climate Scenarios. *Forest Ecology and Management*. 254:390-406.

Kaplan, A., Crane, M., Kushnir, Y., Clemetn, A., Blumenthal, B., and Rajagopalan, B., 1998. Analyses of Global Sea Surface Temperature 1856-1991. *Journal of Geophysical Research* 103:18567-18589.

Keenlyside, N. S., Latif, M., Jungclaus, J., Kornblueh, L., and Roeckner, E., 2008. Advancing Decadal-Scale Climate Prediction in the North Atlantic Sector. *Nature* 453:84-88.

Lane, C. J., Reed, D. D., Mroz, G. D., and Liechty, H. O., 1993. Width of Sugar Maple (*Acer saccharum*) Tree Rings as Affected by Climate. *Canadian Journal of Forest Research* 23:2370-2375.

- Laroque, C.P. and Smith, D.J. 2003. Radial-Growth Forecasts for Five High-Elevation Conifer Species on Vancouver Island, British Columbia. *Forest Ecology and Management* 183:313-325.
- Livingstone, D. A., 1968. Some Interstadial and Post-Glacial Pollen Diagrams from Eastern Canada. *Ecological Monographs* 38(2):87-126.
- Loo, J., and Ives, N., 2003. The Acadian Forest: Historical Condition and Human Impacts. *The Forestry Chronicle* 79(3):462-474.
- Lutz, S.G., 1997. *Pre-European Settlement and Present Forest Composition in Kings County, New Brunswick, Canada*. Masters Thesis. Faculty of Forestry and Environmental Management, University of New Brunswick. Fredericton, N.B.
- Mantua, N.J., Hare, S.R., Zhang, Y., Wallace, J.M., and Francis, R.C., 1997. A Pacific Interdecadal Climate Oscillation with Impacts on Salmon Production. *Bulletin of the American Meteorological Society* 78:1069-1079.
- McKenney, D. W., Pedlar, J. H., Lawrence, K., Campbell, K., and Hutchinson, M. F., 2007. Potential Impacts of Climate Change on the Distribution of North American Trees. *Bioscience* 57(11):939-948.
- Millers, I., Shriner, D. S., and Rizzo, D., 1989. History of Hardwood Decline in the Eastern United States. *General Technical Report NE-126*. U.S. Department of Agriculture, Forest Service, Northeastern Forest Experiment Station, Radnor, Pennsylvania, U.S.A., 75 p.

- Mosseler, A., Lynds, J. A., Major, J. E., 2003. Old-Growth Forests of the Acadian Forest Region. *Environmental Review* 11:S47-S77.
- Mott, R. J., 1975. Palynological Studies of Lake Sediment Profiles from Southwestern New Brunswick. *Canadian Journal of Earth Science* 12:273-288.
- Msadek, R. and Frankignoul, C., 2008. Atlantic Multidecadal Oceanic Variability and its Influence on the Atmosphere in a Climate Model. *Climate Dynamics*, published online August 08
- Neily, P., D., Quigley, E., Benjamin, L., Stewart, B., and Duke, T., 2003. Ecological Land Classification for Nova Scotia. Volume 1 - Mapping Nova Scotia's Terrestrial Ecosystems. Nova Scotia Department of Natural Resources. Renewable Resources Branch.
- Payette, S., Fortin, M-J., and Morneau, C., 1996. The Recent Sugar Maple Decline in Southern Quebec: Probable Causes Deduced from Tree Rings. *Canadian Journal of Forest Research* 26:1069-1078.
- Pitelka, L. E., and Raynal, D. J., 1989. Forest Decline and Acidic Deposition. *Ecology* 70(1):2-10.
- Phillips David, 1990. The Climates of Canada. Environment Canada. Canadian Government Publishing Centre (Ottawa).

- Phillips, B. E., and Laroque, C. P., 2007. Future Radial Growth Forecast for Six Coniferous Species In Southeastern New Brunswick. MAD Lab Report 2007-02. Available at <http://www.mta.ca/madlab/2007-02.pdf>
- Phillips, B. E., and Laroque, C. P., 2008. Expanding on Radial Growth Forecasting: The Potential Future Response of Three Southeastern New Brunswick Tree Species. MAD Lab Report 2008-04. Available at <http://www.mta.ca/madlab/2008-04.pdf>
- Raupach, R. M., Marland, G., Ciais, P., Le Quéré, C., Canadell, G. J., Klepper, G., and Field, B. C., 2007. Global and Regional Drivers of Accelerating CO₂ Emissions. *PNAS* *104(24):10288-10293*.
- Richardson, A. D., Bailey, A. S., Denny, E. G., Martin, C. W., and O'Keefes, J., 2006. Phenology of a Northern Hardwood Forest Canopy. *Global Change Biology* *12:1174-1188*.
- Ritchie, G. A., 1959. Trees of Knowledge: A Handbook of Maritime Trees. Canadian Forest Service, Natural Resources Canada, Fredericton, New Brunswick.
- Robitaille, G., Boutin, R., and Lachance, D., 1995. Effects of Soil Freezing Stress on Sap Flow and Sugar Content of Mature Sugar Maples (*Acer saccharum*). *Canadian Journal of Forest Research* *25:577-587*.
- Smith, K. T., and Shortle, W. C., 2003. Radial Growth of Hardwoods Following the 1998 Ice Storm in New Hampshire and Maine. *Canadian Journal of Forest Research* *33:325-329*.

- Sperry, J. S., Donnelly, J. R., and Tyree, M. T., 1988. Seasonal Occurrence of Xylem Embolism in Sugar Maple (*Acer saccharum*). *American Journal of Botany* 75(8):1212-1218.
- Stokes, M. A., and Smiley, T. L., 1968. An Introduction to Tree-Ring Dating. University of Arizona Press, Tucson.
- St.Clair, S. B., Sharpe, W. E., and Lynch, J. P., 2008. Key Interactions between Nutrient Limitation and Climatic Factors in Temperate Forests: a Synthesis of the Sugar Maple Literature. *Canadian Journal of Forest Research* 38:401-414.
- Sutton, R. T., and Hodson, D. L. R., 2005. Atlantic Ocean forcing of North American and European summer climate. *Science* 309:115–118.
- Sutton, R. T., and Hodson, D. L. R., 2007. Climate Response to Basin-Scale Warming and Cooling of the North Atlantic Ocean. *Journal of Climate*. 20:891-907.
- Tardif, J., Brisson, J., and Bergeron, Y., 2001. Dendroclimatic Analysis of *Acer saccharum*, *Fagus grandifolia*, and *Tsuga canadensis* from an Old-growth Forest, Southwestern Quebec. *Canadian Journal of Forest Research* 31:1491-1501.
- Walker, S. L., Auclair, A. N. D., and Marin, H. C., 1990. History of Crown Dieback and Deterioration Symptoms of Hardwoods in Eastern Canada, Parts I, II and III. *Environment Canada, Atmospheric Environment Service, Federal LRTAP Liaison Office. Downsview, Ontario, Canada, 561 p.*

- Williams, C.N., Jr., Menne, M.J., Vose, R.S., and Easterling, D.R., 2006. United States Historical Climatology Network Daily Temperature, Precipitation, and Snow Data. ORNL/CDIAC-118, NDP-070. Available on-line [<http://cdiac.ornl.gov/epubs/ndp/ushcn/usa.html>] from the Carbon Dioxide Information Analysis Center, Oak Ridge National Laboratory, U.S. Department of Energy, Oak Ridge, Tennessee.
- Woodley, S., Forbes, G., and Skibicki, A., 1998. *State of the Greater Fundy Ecosystem*. Greater Fundy Ecosystem Research Project. UNB Faculty of Forestry and Environmental Management.
- van Mantgem, P.J., Stephenson, N.L., Byrne, J.C., Daniels, L.D., Franklin, J.F., Fulé, P.Z., Harmon, M.E., Larson, A.J., Smith, J.M., Taylor, A.H., and Veblen T.T., 2009. Widespread Increase of Tree Mortality Rates in the Western United States. *Science* 323:521-524.
- Vasseur, L., and Catto, N., 2008. Atlantic Canada; *in* From Impacts to Adaptation: Canada in a Changing Climate 2007. Edited by D.S. Lemmen, F.J. Warren, J. Lacroiz and E. Bush; Government of Canada, Ottawa, ON, p. 119-170.
- Vincent, L.A., and Gullett, D.W., 1999. Canadian Historical and Homogeneous Temperature datasets for climate change analyses. *International Journal of Climatology* 19:1375-1388.
- Vincent, L.A., and Gullett, D.W., 2002. Homogenization of Daily Temperatures over Canada. *Journal of climate* 15:1322-1334.

- Yin, X., and Arp, P. A., 1994. Tree-Ring Based Growth Analysis for a Sugar Maple Stand: Relations to Local Climate and Transient Soil Properties. *Canadian Journal of Forestry Research* 24:1567-1574.
- Zelazny, V. F., Martin, G. L., Toner, M., Gorman, M., Colpitts, M., Veen, H., Godin, B., McInnis, B., Steeves, C., Wuest, L., and Roberts, M. R., 2003. Out Landscape Heritage: the Story of Ecological Land Classification in New Brunswick. *Ecosystem Classification Working Group. New Brunswick Dept. of Natural Resources.*
- Zhu, X. B., Cox, R. M., Bourque, C.-P. A., and Arp, P. A., 2002. Thaw Effects on Cold-Hardiness Parameters in Yellow Birch. *Canadian Journal of Botany* 80: 390-398.